DOT/FAA/CT-82/93

DEGRADATION AND CHARACTERIZATION OF ANTIMISTING KEROSENE (AMK)

R. J. Mannheimer

Southwest Research Institute
6220Culebra Road
San Antonio, Texas 78284

December 1982

Final Report

U.S. Department of Transportation
Federal Aviation Administration
Technical Center
Atlantic City Airport, N.J. 08405

NOTICE

This document is disseminated under the sponsorship of the Department of Transportation in the interest of information exchange. The United States Government assumes no liability for the contents or use thereof.

The United States Government does not endorse products or manufacturers. Trade or manufacturer's names appear herein solely because they are considered essential to the object of this report.

TECHNICAL REPORT STANDARD TITLE PAGE

1. Report No.	2. Government Accession No.	3. Recipient's Catalog No.
DOT/FAA/CT-82/93		

4. Title and Subtitle	5. Report Date
DEGRADATION AND CHARACTERIZATION OF ANTIMISTING KEROSENE (AMK)	December 1982
	6. Performing Organization Code

7. Author(s)	8. Performing Organization Report No.
R.J. Mannheimer	MED132

9. Performing Organization Name and Address	10. Work Unit No.
Southwest Research Institute Mobile Energy Division P.O. Drawer 28510 San Antonio, Texas 78284	11. Contract or Grant No. DOT-FA79WA-4310
12. Sponsoring Agency Name and Address	13. Type of Report and Period Covered
U.S. Department of Transportation Federal Aviation Administration FAA Technical Center Atlantic City Airport, New Jersey 08405	July 1980-November 1981 Final Report
	14. Sponsoring Agency Code ACT 310

15. Supplementary Notes

16. Abstract

Experiments are described which demonstrate the feasibility of degrading AMK in a single pass with a system consisting of a hydraulic fuel pump from a TF30 engine and several types of flow restrictors such as packed tubes or needle valves. The performance of the degraded AMK was evaluated with full-scale aircraft filters (JT8D and CF6), a T63 combustor and laboratory scale tests including filtration, ignition, and gel permeation chromatography.

Rheological experiments indicated that while the shear viscosity of AMK increases above a critical shear rate, the magnitude of the shear viscosity is not large enough to explain the effectiveness of the FM-9 additive. However, it has been shown that, associated with the critical shear rate, AMK exhibits strong viscoelastic effects that are not evident at low shear rates or in flow through an orifice.

17. Key Words	18. Distribution Statement
Fire Safety - Rheology - Polymers Surfactants - Polymer Degradation	Document is available to the U.S. public through the National Technical Information Service, Springfield, Virginia 22161

19. Security Classif. (of this report)	20. Security Classif. (of this page)	21. No. of Pages	22. Price
UNCLASSIFIED	UNCLASSIFIED	77	

Form DOT F 1700.7 (8-69)

METRIC CONVERSION FACTORS

Approximate Conversions to Metric Measures

Symbol	When You Know	Multiply by	To Find	Symbol
	LENGTH			
in	inches	*2.5	centimeters	cm
ft	feet	30	centimeters	cm
yd	yards	0.9	meters	m
mi	miles	1.6	kilometers	km
	AREA			
in^2	square inches	6.5	square centimeters	cm^2
ft^2	square feet	0.09	square meters	m^2
yd^2	square yards	0.8	square meters	m^2
mi^2	square miles	2.6	square kilometers	km^2
	acres	0.4	hectares	ha
	MASS (weight)			
oz	ounces	28	grams	g
lb	pounds	0.45	kilograms	kg
	short tons (2000 lb)	0.9	tonnes	t
	VOLUME			
tsp	teaspoons	5	milliliters	ml
Tbsp	tablespoons	15	milliliters	ml
fl oz	fluid ounces	30	milliliters	ml
c	cups	0.24	liters	l
pt	pints	0.47	liters	l
qt	quarts	0.95	liters	l
gal	gallons	3.8	liters	l
ft^3	cubic feet	0.03	cubic meters	m^3
yd^3	cubic yards	0.76	cubic meters	m^3
	TEMPERATURE (exact)			
°F	Fahrenheit temperature	5/9 (after subtracting 32)	Celsius temperature	°C

*1 in = 2.54 (exactly). For other exact conversions and more detailed tables, see NBS Misc. Publ. 286, Units of Weights and Measures, Price $2.25, SD Catalog No. C13.10:286.

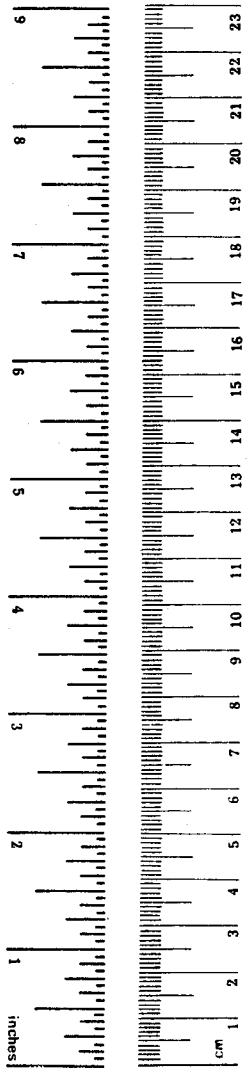

Approximate Conversions from Metric Measures

Symbol	When You Know	Multiply by	To Find	Symbol
	LENGTH			
mm	millimeters	0.04	inches	in
cm	centimeters	0.4	inches	in
m	meters	3.3	feet	ft
m	meters	1.1	yards	yd
km	kilometers	0.6	miles	mi
	AREA			
cm^2	square centimeters	0.16	square inches	in^2
m^2	square meters	1.2	square yards	yd^2
km^2	square kilometers	0.4	square miles	mi^2
ha	hectares (10,000 m^2)	2.5	acres	
	MASS (weight)			
g	grams	0.035	ounces	oz
kg	kilograms	2.2	pounds	lb
t	tonnes (1000 kg)	1.1	short tons	
	VOLUME			
ml	milliliters	0.03	fluid ounces	fl oz
l	liters	2.1	pints	pt
l	liters	1.06	quarts	qt
l	liters	0.26	gallons	gal
m^3	cubic meters	35	cubic feet	ft^3
m^3	cubic meters	1.3	cubic yards	yd^3
	TEMPERATURE (exact)			
°C	Celsius temperature	9/5 (then add 32)	Fahrenheit temperature	°F

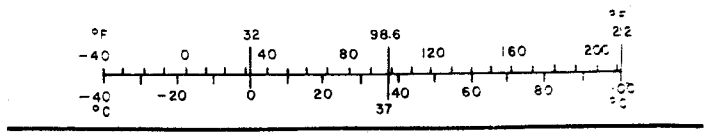

ACKNOWLEDGMENTS

This program was funded by the Department of Transportation under DOT-FA79WA-4310. The work was performed for the Federal Aviation Administration (FAA) under the management of Mr. A. Ferrara, Federal Aviation Administration Technical Center. Messrs. J.L. Jungman and P.J. Gutierrez of Southwest Research Institute (SwRI) performed the experimental portion of this program. Ms. K.B. Kohl and Mr. K.B. Jones also of SwRI were responsible for the developments of the test methods for determining the glycol and amine content of AMK. Finally, I wish to express my appreciation to Ms. G. Tate, who typed and helped edit this manuscript.

TABLE OF CONTENTS

TABLE OF CONTENTS (CONT'D)

LIST OF ILLUSTRATIONS

LIST OF ILLUSTRATIONS (CONT'D)

LIST OF TABLES

LIST OF SYMBOLS AND ABBREVIATIONS

Abbreviations

A	-	area normal to flow
AMK	-	Antimisting Kerosene
CFV	-	Critical Filtration Velocity
D	-	diameter of tube
d_p	-	diameter of particle (packed tube)
FCTA	-	Flammability Comparison Test Apparatus
FM-9	-	proprietary polymer provided by ICI Americas, Inc.
FR	-	Filtration Ratio (flow time of AMK relative to Jet A through a standard 16-18 μm Dutch Weave Screen at 25°C unless specified otherwise)
GPC	-	Gel Permeation Chromatography
h	-	fluid head (Orifice Cup Test)
L	-	length of tube
M	-	molecular weight
m	-	flow coefficient for kinetic energy correction
n	-	flow index defined by $R\Delta P/2L = K\ (8V/D)^n$
OF	-	orifice flow cup measurements
PS	-	polystyrene (GPC Standard)
Q	-	flow rate
R	-	radius of tube
Re	-	Reynolds number
RAE	-	Royal Aircraft Establishment
r	-	radial position in tube
T	-	measured thrust
U	-	local velocity
V	-	average velocity (Q/A)
VR	-	Viscosity Ratio (viscosity of AMK relative to Jet A at low shear rates)

Symbols

ΔP	-	pressure drop
η_a	-	apparent shear viscosity
$[\eta]$	-	intrinsic velocity
θ	-	relaxation time (property of viscoelastic liquid)
ρ	-	density
$P_{11}-P_{22}$	-	normal stress difference
P_{12}	-	shear stress

EXECUTIVE SUMMARY

Single pass degradation of Antimisting Kerosene (AMK) has been accomplished with a system consisting of a fuel pump from a TF30 engine and three different types of flow restrictors (packed tubes, static mixing tubes, and needle valve). The relatively simple needle valve has the advantage of being able to accommodate a wide range of fuel flow rates at a fixed power level and is less susceptible to plugging by fuel contaminants.

The quality of AMK degraded by the needle valve method was assessed in terms of full-scale fuel system component performance (JT8D and CF6 engine fuel filters and a T63 combustor) and small-scale filtration and ignition tests. Results of these experiments showed that the degradation system returned AMK to Jet A performance standards. Flow rates over the range of idle to cruise appeared to have little or no effect on the specific power required to obtain a fuel that would filter and ignite like Jet A; however, fuel temperature was found to be very important. For example, at ambient temperature (24°C) satisfactory filtration was achieved at a specific power as low as 14 kWs/ℓ; but at -12°C twice the power (28-30 kWs/ℓ) was necessary. The specific power requirement (in terms of mist flammability) for fuels degraded at temperatures from 24° to 50°C was not significantly lower than 14 kWs/ℓ.

AMK, blended from a slurry of FM-9 powder in carrier fluid and degraded within one hour, had a high filtration ratio (generally associated with poorly degraded AMK) even at a specific power of 23-26 kWs/ℓ. However, viscosity and mist flammability measurements indicated that a relatively high level of degradation had been achieved. Furthermore, Gel Permeation Chromatography (GPC) results showed that AMK blended from a slurry and degraded within one hour had a much lower molecular size than AMK blended and degraded in the conventional manner. This apparent conflict is thought to be due to a very small amount of poorly solubilized (i.e., poorly swollen) FM-9 powder that has little or no effect on viscosity, GPC, or mist flammability but which can readily plug a filter. Since small-scale flammability tests indicate the carrier fluid increases the antimisting effectiveness of FM-9, infrared and chemiluminescence methods have been developed to measure the glycol and amine content of AMK.

A laboratory test (Pump Filtration Test) has been developed that measures the filter plugging characteristics of intentionally degraded AMK. In this procedure, the pressure drop across a small section of a paper filter or a metal screen is measured as a function of time (up to two minutes) for different superficial velocities (flow rate/filter area). Below a critical velocity, the pressure drop across the filter is independent of time; however, at higher velocities the pressure increases with time. Filter properties (paper versus metal and pore size) and fuel temperature have been shown to influence the critical filtration velocity of intentionally degraded AMK. With some samples, the critical filtration velocity was found to decrease with time following degradation. This

phenomenon was not evident in other physical property measurements such as the filtration ratio, viscosity ratio, and mist flammability. The reason for this anomalous behavior is not known, but it is suspected to be related to the slow agglomeration of degradation products.

Rheological experiments with capillary tubes have documented that the viscosity of AMK increases when a critical shear rate ($\sim$2500 s^{-1} at 25°C) is exceeded. However, the magnitude of the viscosity is not large enough to explain the effectiveness of AMK. On the other hand, very large viscoelastic effects were evident in the swelling and recoil of jets of AMK at high shear rates. This *shear induced viscoelasticity* is a major difference between the FM-9 polymer and conventional viscoelastic polymers such as polyisobutylene. For example, when the L/D of the capillary tube was below a certain value, little or no shearing occurred and viscoelastic effects were not developed with AMK. This observation explains why previous attempts to measure elongational viscosity were unable to distinguish between AMK and ordinary jet fuel. In addition to providing insight as to the rheological mechanism of AMK, these observations suggest that normal stresses, which were not evident in earlier experiments with orifices, could be readily determined from jet thrust measurements with capillary tubes. While it is more difficult to obtain and properly interpret jet thrust experiments than flow experiments, a quality control test, based on normal stress measurements, would have a much stronger theoretical basis than one that measures shear viscosity.

I. INTRODUCTION

When a high molecular weight polymer (FM-9)* is blended into aviation kerosene, the fuel resists the formation of small droplets under impact dispersion conditions and thus has been identified as antimisting kerosene (AMK) fuel. Simulated crash tests(1,2)** have demonstrated this improved fire safety, however, this attribute creates significant fuel filtration problems and the fuel atomization characteristics preclude direct use in aircraft turbine engines. Therefore, AMK fuel is unacceptable until methods are developed by which the antimisting characteristics can be eliminated just prior to the fuel entering the main engine fuel control system. Such restoration or degradation of the fuel is the goal of this project.

While both shear and elongational effects can contribute to polymer degradation, it is expected that elongational flows will be more destructive than shear flows.(3) Some insight into this expectation can be provided by considering the differences between these two types of flows. The familiar shear flow that is commonly produced in a long capillary tube is characterized by a velocity gradient that is normal to the direction of flow. As a dilute polymer solution flows through the capillary, polymer molecules tend to be stretched along the principal axis of stress. However, shear flows are rotational. Because of this rotational motion, polymer molecules cannot stay oriented in the stress field; consequently, very little polymer deformation occurs with a low viscosity solvent even at high rates of shear.(3) Elongational flows occur in many practical situations, such as in the entrance region to a capillary tube, in flow through an orifice, and in porous media. In all of these examples, the velocity gradient is in the direction of flow. Since this type of flow is irrotational, a polymer molecule would be expected to stay oriented in the stress field longer; therefore, larger polymer deformations should occur.

Because of the presence of solid boundaries, most flows are a combination of both shear and elongation; however, by an appropriate choice of geometry, one type of flow can be made to dominate. For example, laminar flow in a long capillary tube is primarily a shear flow except for the entrance region. On the other hand, in a very short tube (L/D<1) or for a tube filled with beads, the flow is predominantly elongational.(4)

Since elongational flow is expected to be more effective in producing polymer degradation than shear flow, the primary objective of this work is to determine the effect of the sudden acceleration produced by flow into valves, the pores of metal screens, or tubes paced with beads on the mist ignition and filtration properties of AMK. However, relatively few standard

---

*This is a proprietary polymer that was provided by ICI Americas, Inc.
**Underscored numbers in parentheses refer to the References at the end of this report.

tests have been found to be useful in measuring the performance characteristics of AMK; therefore, a second but equally important part of this work is the development of test methods that relate to mist flammability and rheological properties of AMK.

II. DEGRADER TESTS

A. DESCRIPTION OF APPARATUS AND EXPERIMENTAL PROCEDURE

The essential components of the degrader are shown in Figure 1. A hydraulic pump from a TF30 engine is driven by a 50-HP electric motor with a magnetic coupling device. A flow restrictor (needle valve or packed tube) is located immediately downstream of the pump so that the high pressure produced by the pump is dissipated within a very short distance. At the beginning of each test, a closed loop of Jet A is used to set the flow rate and pressure drop across the flow restrictor. The latter is measured with a guage and a transducer attached to a strip-chart recorder. After the pump speed and pressure have stabilized, a pair of three-way valves switch the flow from Jet A to a drum of AMK that is under a head of nitrogen (55 kPa)*. The flow rate of AMK is obtained by weighing the sample and recording the time. Flow rates were varied at a fixed pump speed by changing pump displacement. Because of the speed limitations of the electric motor, maximum flow rates were in the range of 1500 Kg/hr. This is equivalent to cruise conditions for the JT8D engine. However, only minor modifications would be required to increase the capacity of the degrader to full take-off flow rates (4600 Kg/hr). Experiments at temperatures other than ambient were conducted by cooling or heating a drum of fuel. Temperatures in the drum of fuel, the feedline to the pump, and to the fuel filters were measured with thermocouples.

The filtration characteristics of degraded AMK were evaluated with full-scale fuel filter components placed immediately downstream of the needle valve as shown in Figure 2. The fuel filters shown in Figure 2 include the main fuel filter and the fuel control wash-filter for the JT8D engine. A low pressure (0 to 5 psi) transducer was placed upstream of these filters to monitor the pressure drop as a function of test time. Valves, located on the fuel control filter housing, were used to vary the amount of through-flow (i.e., flow to the engine) and wash-flow (i.e., flow to the fuel controller). The main fuel filter used in the CF6 engine (not shown in Fig. 2) was also evaluated.

B. EXPERIMENTAL RESULTS

1. Full-Scale Filtration Tests

Typical pressure-time traces for successful degradation and filtration of AMK are shown in Figure 3. The transducer that measures the high

---

*1.0 psi = 6.895 kPa.

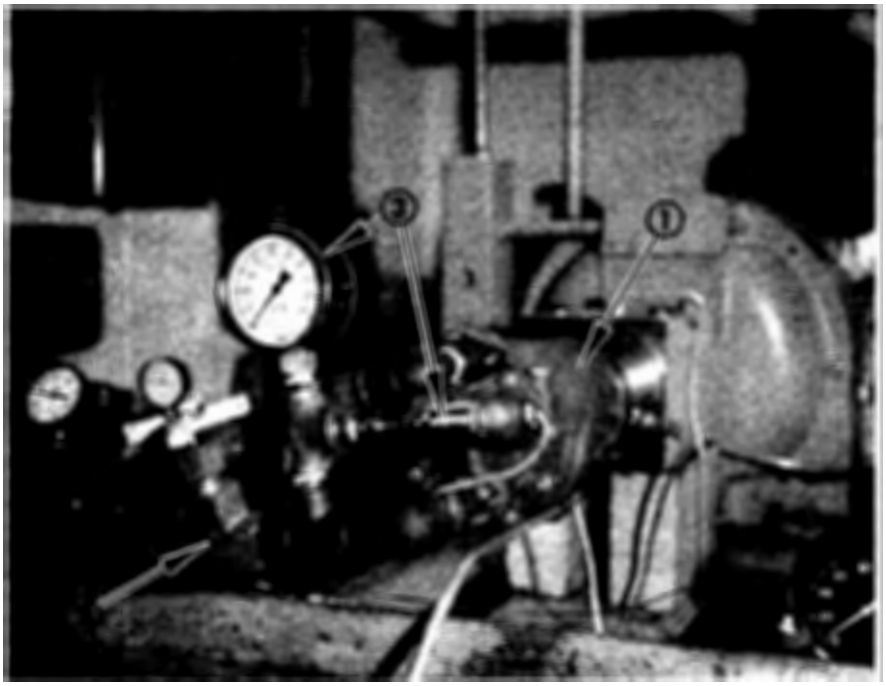

① TF 30 HYDRAULIC PUMP

② 3/4-IN. NEEDLE VALVE

③ PRESSURE GAUGE AND TRANSDUCER (0-5000 psi)

FIGURE 1. AMK DEGRADER

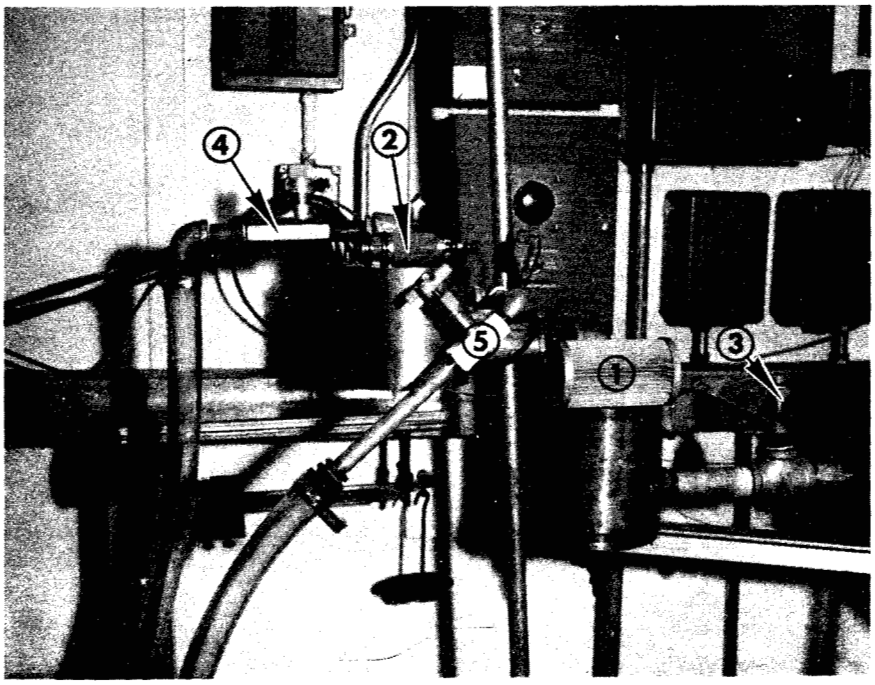

① MAIN FUEL FILTER (40 μm PAPER)

② FUEL CONTROL WASH FILTER (METAL)

③ PRESSURE TRANSDUCER (0-10 psi)

④ THROUGH FLOW (TO ENGINE)

⑤ WASH FLOW (TO FUEL CONTROLLER)

FIGURE 2. JT8D FUEL FILTERS

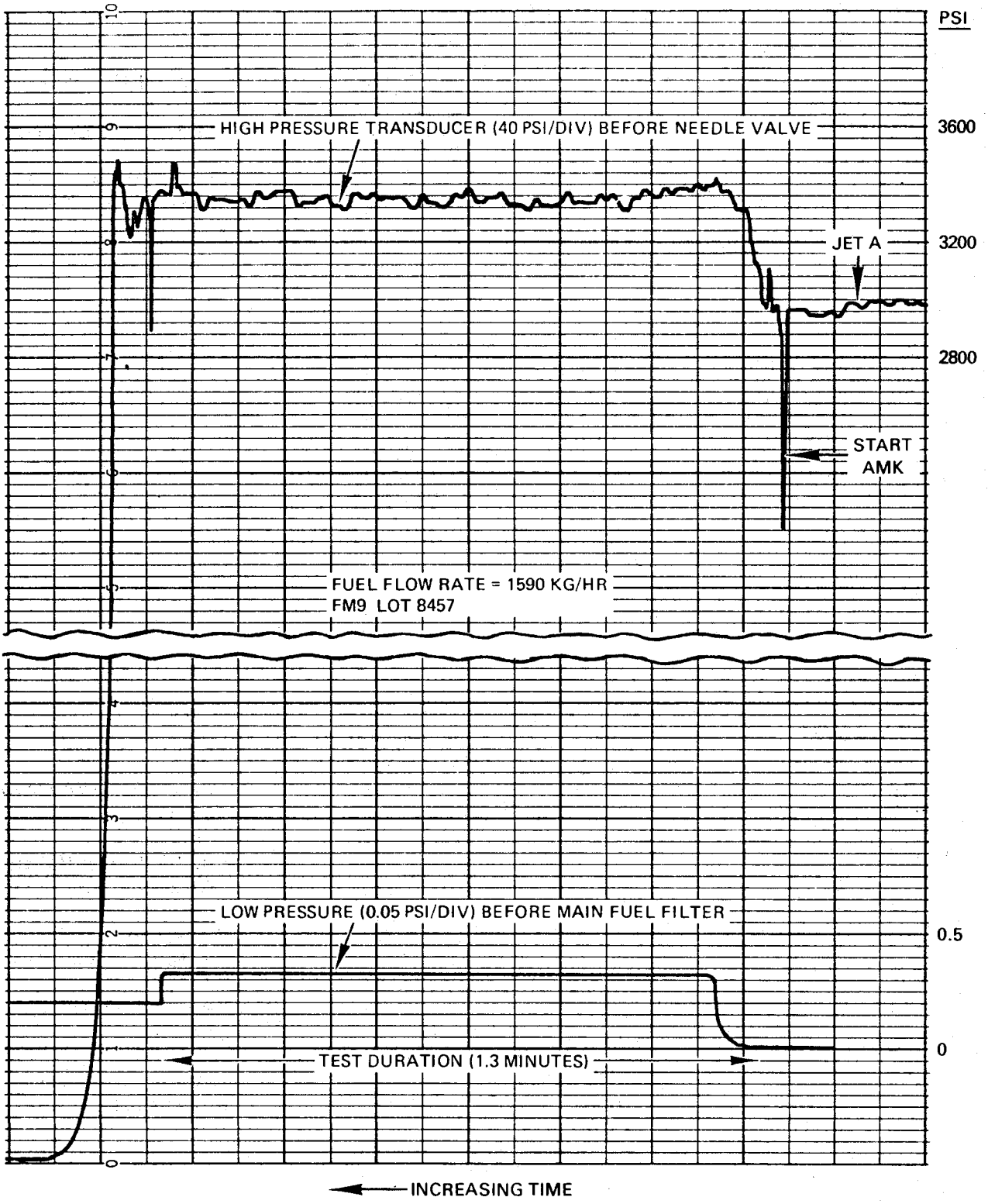

FIGURE 3. PRESSURE-TIME TRACE FOR AMK WITH NEEDLE VALVE AND MAIN FUEL FILTER (JT8D)

pressure upstream of the needle valve increased from 3000 psi (20.7 kWs/ℓ) to 3300 psi (22.7 kWs/ℓ) when the three-way valves were switched from Jet A to AMK. However, this higher pressure was maintained during the duration of the test (1.3 minutes) without any adjustment of the needle valve. The transducer that measured the low pressure upstream of the main fuel filter also remained constant for the duration of the test. Because the filter holder was originally empty, but was full of fuel at the end of the test, the transducer did not return to the original baseline.

The results in Table 1 summarize experiments with the JT8D and CF6 engine fuel filters and AMK degraded at ambient temperatures. These results indicate that degraded AMK (21 kWs/ℓ) can flow through these aircraft filters at flow rates equivalent to cruise conditions (1500 Kg/hr) for the JT8D engine and at pressures close to those produced by Jet A. A reduction in degrader power from 21 to 14 kWs/ℓ gave essentially identical performance; however, at 7 kWs/ℓ almost instantaneous filter plugging occurred (i.e., $\Delta P \rightarrow \infty$).

The results in Table 2 summarize tests in which both the JT8D main fuel filter and fuel control filter were used. The latter is a "last-chance" filter that is intended to prevent large metal particles from entering the fuel controller. The small area of the wash-screen (10 cm^2 compared to 3900 cm^2 for the main filter) would be prone to plugging. Therefore, all tests on the fuel control filter also included the main fuel filter as it would be used in the JT8D fuel system. The terms "through-flow" and "wash-flow" refer to the fuel streams that go to the engine and fuel controller, respectively. The relative amounts of these two streams were controlled by partially closing valves on the discharge side of the wash-filter housing (Fig. 2).

In the first series of tests, the wash-flow valve was closed so that all of the fuel (1440 Kg/hr) flowed through a relatively coarse (50 mesh) screen. The pressure drop across the two filters reached its maximum value within 10 to 12 seconds and remained essentially constant for the duration of the test. The pressure level (56 kPa) was much higher than that observed for the main filter alone (1.7 kPa), and this was probably caused by the higher flow resistance of the fuel control filter housing and the smaller screen area. Nevertheless, the pressure drop for AMK was only slightly higher than for Jet A. Furthermore, the pressure did not increase with time over the duration of the test (1.5 minutes).

In tests in which the wash-flow valve was partially opened, it was observed that there was a slower build-up of pressure with degraded AMK than with Jet A (see Figs. 4 and 5). Similar results were reported with fuel that was degraded by three passes through a JT8D fuel pump, and it was concluded that the degraded AMK resulted in unsatisfactory performance due to filter plugging.(5) Since the steady-state pressure drop in Figure 4 was only slightly higher for AMK (2.6 psi or 17.9 kPa) in Figure 4 than for Jet A (2.1 psi or 14.5 kPa) in Figure 5. This observed time dependency does not appear to be due to filter plugging. However, these results suggest that longer duration tests should be made.

TABLE 1. FLOW OF JET A AND DEGRADED AMK THROUGH JT8D AND CF6 MAIN FUEL FILTERS AT AMBIENT TEMPERATURE

Fuel Sample	Specific Power, kWs/ℓ	Filter Type	Fuel Flow Rate, Kg/hr	Filter ΔP, kPa	Test Duration, minutes	Fuel Temp
Jet A	21	CF6[1]	550	0.8	3.3	22 to 24°C
AMK	22	CF6[1]	580	0.7	14.5	22 to 24°C
AMK	21	CF6[1]	1510	1.7	1.2	22 to 24°C
AMK	23	JT8D[2]	1580	0.8	1.3	22 to 24°C
AMK	14	JT8D[2]	1510	1.4	1.2	22 to 24°C
AMK	7	JT8D[2]	1460	∞	0.8	22 to 24°C

1 - Main fuel filter, wire mesh, 74 micron absolute, 3000 cm^2.
2 - Main fuel filter, paper, 40 micron, 3900 cm^2.

TABLE 2. FLOW OF JET A AND DEGRADED AMK THROUGH JT8D MAIN FUEL FILTER AND FUEL CONTROL FILTER AT AMBIENT TEMPERATURE

Fuel Sample	Fuel Flow Rate (Kg/hr)			Filter ΔP, kPa	Test Duration, minutes	Fuel Temp
	Main Filter[1]	Fuel Control Filter[2]				
		Through Flow	Wash Flow			
Jet A	1440	1440	0	43	1.4	22 to 24°C
AMK[3]	1440	1440	0	56	1.5	22 to 24°C
AMK[3]	1510	1150	360	30	1.7	22 to 24°C
AMK[3]	1510	1190	320	36	3.5	22 to 24°C
AMK[3]	1330	680	650	33	1.8	22 to 24°C

1 - Main fuel filter, paper, 40 micron, 3900 cm^2.
2 - Fuel control filter, through-flow screen (50 mesh, 63 cm^2), wash-flow screen (325 mesh, 10 cm^2).
3 - Specific power, 21-24 kWs/ℓ.

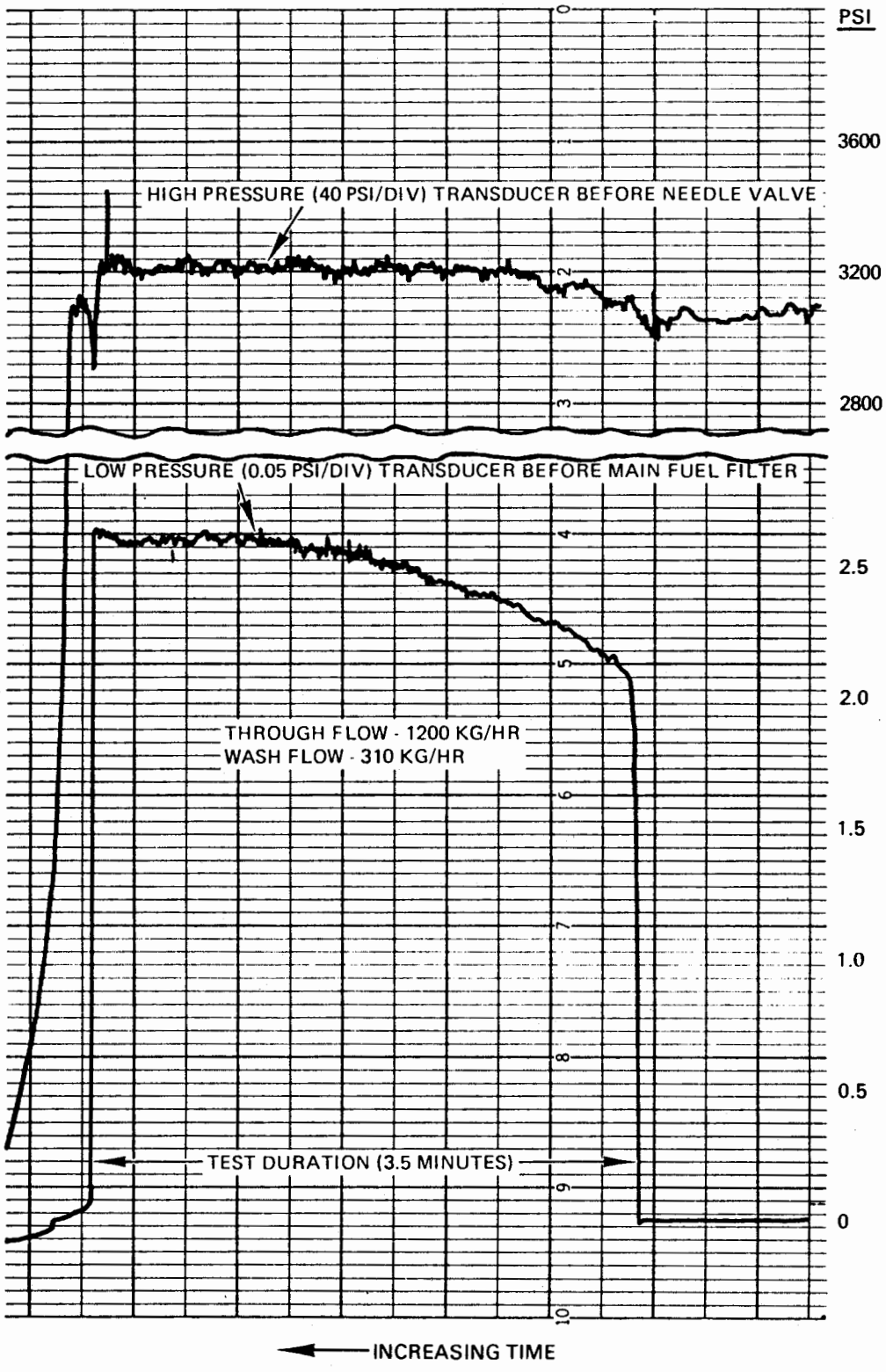

FIGURE 4. PRESSURE-TIME TRACE FOR AMK WITH NEEDLE VALVE, MAIN FUEL FILTER AND FUEL CONTROL FILTER (JT8D)

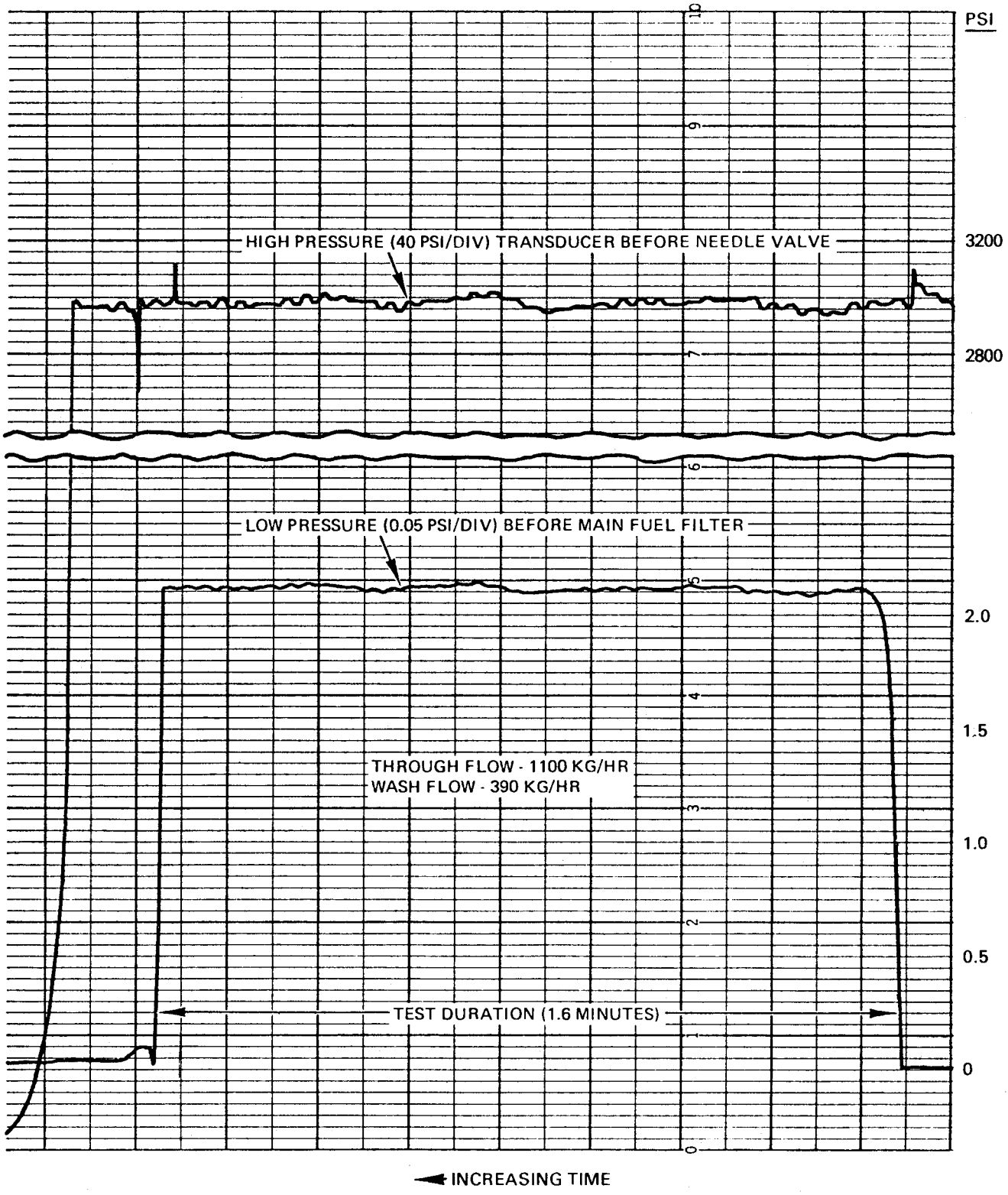

FIGURE 5. PRESSURE-TIME TRACE FOR JET A WITH NEEDLE VALVE, MAIN FUEL FILTER AND FUEL CONTROL FILTER (JT8D)

The results in Table 3 summarize attempts to filter AMK that was degraded at low temperatures. At a power level of 23 kWs/ℓ and a fuel temperature (pump inlet) of -14°C, the JT8D main fuel filter (40 μm paper) plugged immediately. Experiments with the CF6 main fuel filter (74 μm metal) produced almost identical results on the first attempt. In the second experiment, the pressure increased only slightly; however, it is felt that plugging would have occurred if the test had continued. *Due to the increased resistance of amk to mechanical degradation at low temperatures, satisfactory filter performance could be obtained only by increasing the specific degrader power to 29 kWs/ℓ.*

Because of the strong effect of low temperature on specific power, experiments were conducted at elevated temperatures (50°C). Preliminary results indicated that AMK could be filtered at a lower specific power (7 kWs/ℓ) than fuel degraded at room temperature. However, closer examination revealed that the improved filter performance was due only to the elevated fuel temperature and that the level of degradation was essentially the same as fuel degraded at ambient temperatures. This fact will be evident in mist ignition tests.

2. Mist Ignition Tests

Ignition tests of AMK degraded at ambient temperature were conducted with a T63 combustion rig. In Figure 6, the ignition delay, as determined from the time of rapid temperature rise, is plotted as a function of the fuel flow rate for a fixed air flow rate. These data are averages of three runs and, because of the statistical nature of the ignition process, show a fair degree of scatter. Nevertheless, these data indicate no significant difference in the ignition delay of degraded AMK (25 kWs/ℓ) and Jet A. This result is in good agreement with the Spinning Disc Test and the Flammability Comparison Test Apparatus (see Section V) which also showed no significant difference between these samples of degraded AMK and Jet A.

The results in Figure 7 show the effect of fuel temperature (at the inlet of the degrader) and specific power on mist ignition as determined by the Spinning Disc Test*. For fuels degraded at ambient temperatures, there is a measurable difference between Jet A and AMK at a specific power of 7 kWs/ℓ. However, at 14 kWs/ℓ AMK is indistinguishable from Jet A. The increased resistance to degradation at low temperature is illustrated by the fact that at least 29 kWs/ℓ is required to produce a fuel that ignites like Jet A. The absence of high temperature effects (at least up to 50°C) on specific power is clearly evident in the similar antimisting characteristics of AMK degraded at 22°C and 50°C and at a specific power level of 7 kWs/ℓ.

The RAE has reported that AMK blended from a slurry of FM-9 powder in carrier fluid is more difficult to degrade (at least for several hours) than AMK blended in the conventional manner.(6) This conclusion is based on the observation that the filtration ratio (FR)** remained relatively high (10-20) even after exposure to a high specific degrader power (70 kWs/ℓ).

---

*This test method is described in Appendix A.
**This test method has been described in Reference 10.

TABLE 3. FLOW OF JET A AND AMK DEGRADED THROUGH MAIN FUEL FILTERS AT LOW TEMPERATURE

Fuel Sample	Specific Power, kWs/ℓ	Filter Type	Fuel Flow Rate, Kg/hr	Filter ΔP, kPa	Test Duration, minutes	Fuel Temp
Jet A	21	JT8D[2]	1590	1.5	4.3	-16°C
AMK	23	JT8D[2]	1540	∞	0.3	-14°C
AMK	24	CF6[1]	1540	∞	1.2	-12°C
AMK	23	CF6[1]	1610	2.4	1.0	-14°C
AMK	29	CF6[1]	1460	1.0	1.1	-17°C
AMK	29	JT8D[2]	1740	0.9	1.0	0°C

1 - Main fuel filter, wire mesh, 74 micron absolute, 3000 cm^2.
2 - Main fuel filter, paper, 40 micron, 3900 cm^2.

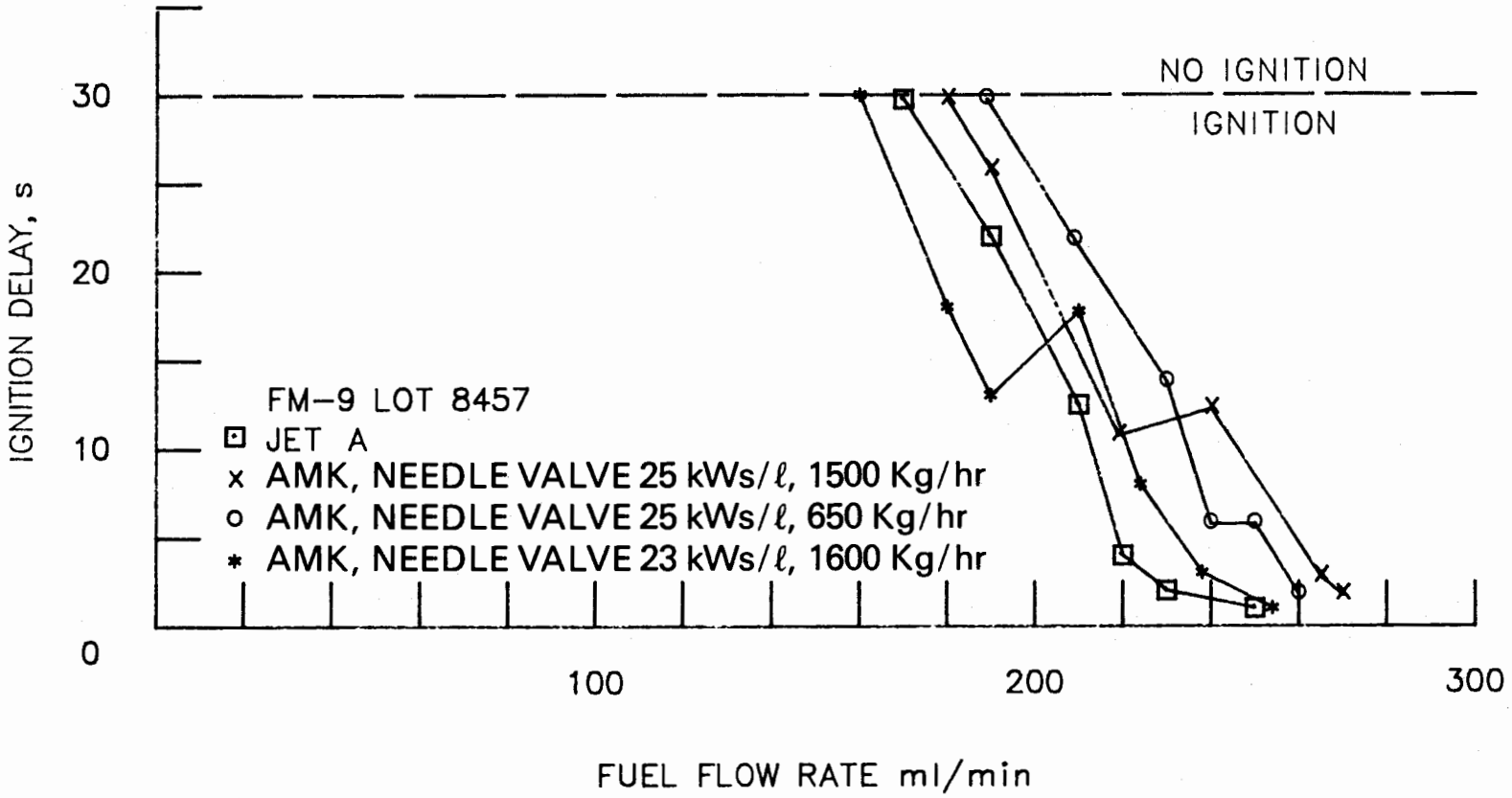

AIR INLET TEMPERATURE (29 °C), INLET PRESSURE (138 kPa),
AIR FLOW RATE (0.18 Kg/s).

FIGURE 6. IGNITION OF JET A AND DEGRADED AMK (T 63 COMBUSTOR)

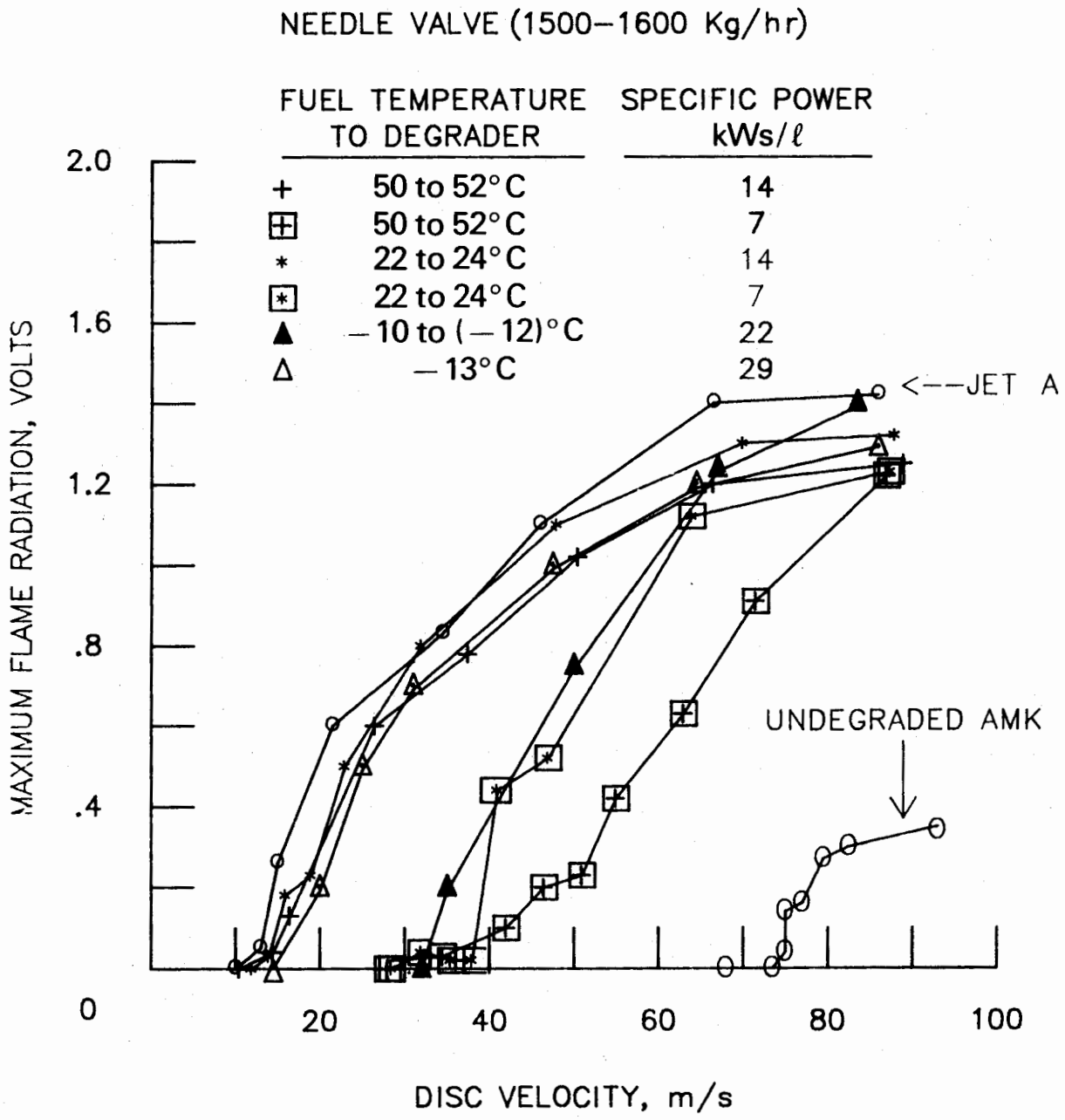

FIGURE 7. EFFECT OF FUEL TEMPERATURE TO DEGRADER AND DEGRADER POWER ON MIST FLAMMABILITY OF AMK

While the RAE used an in-line blending device that was specifically designed to disperse the extremely viscous ($\sim 10^6$ poise) slurry, it was found possible to disperse the slurry with an ordinary air driven mixer if the FM-9 powder was added to the carrier fluid and the resulting slurry was added to the fuel before it had time to harden. In several instances, the resulting AMK blend cleared in approximately 15 minutes; however, in other instances, as long as one hour was required for the solution to clear. Furthermore, the physical properties of AMK blended in this manner exhibited a much wider range of values than AMK made by the conventional blending procedure. For example, the orifice flow (OF)* varied from a high of 3.3 (Fig. 8) to a low of 2.3 (Fig. 10), while the filtration ratio varied from a low of 31 (Fig. 8) to a high of 47 (Fig. 10). Despite these wide ranges of physical properties, the mist ignition characteristics were not measurably different (see Figs. 8 through 10). *Furthermore, these results indicate that despite the fact that the FR remains relatively high, AMK blended from slurry can be degraded to a level that appears to be equivalent to Jet A in terms of mist flammability.* In only one case (Fig. 10) did the degraded AMK appear to have a slightly higher resistance to misting than Jet A following degradation. The fact that the FR of the degraded sample was only slightly lower (27 compared to 47) than the undegraded sample suggests that a poorly dissolved (i.e., poorly solvated) polymer is present that is ineffective as an antimisting agent but that readily plugs a filter.

3. Small-Scale Filtration Tests

In small-scale filtration tests (Pump Filtration Test)** with degraded AMK, the pressure drop across a section of filter material was observed as a function of time (up to two minutes) at increasing flow rates. Because of the low dirt holding capacity of the small (0.1-0.4 cm^2) filter area, samples were gravity filtered through a number 41 Whatman® paper filter prior to their use in this test. The critical filtration velocity (CFV) was determined by the highest superficial velocity (flow rate divided by filter area) at which AMK could flow through a particular filter without resulting in a significant pressure increase in a two-minute period.

The filtration characteristics of AMK degraded at ambient conditions (23 kWs/ℓ) are shown in Figure 11. The filter materials in these tests correspond to those used in the full-scale filter tests (Tables 1 and 2). With the 40 μm paper filter, there was a rapid increase in the rate of plugging at velocities above 0.5 cm/s. The absence of any measurable pressure rise with time at velocities below 0.5 cm/s is in agreement with the full-scale experiments in which satisfactory performance was obtained at 1500 Kg/hr (0.16 cm/s).

The rate of plugging with the 40 μm metal screen (wash-flow screen) was barely discernible up to velocities near 10 cm/s; therefore, the critical velocity is estimated to be approximately 10 cm/s. Since the full-scale

*British Standard 1733.
**This test method is described in Appendix B.

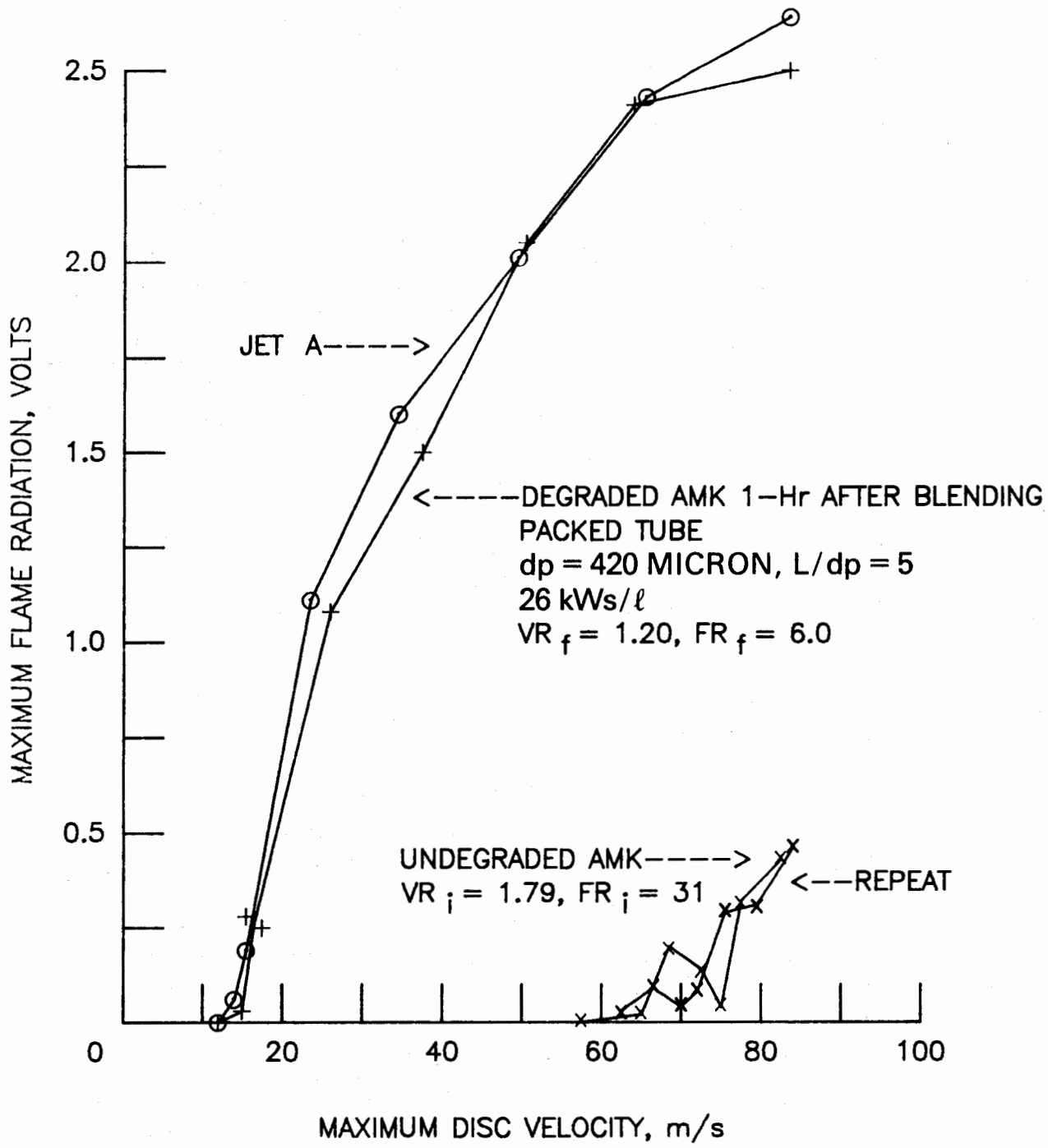

FIGURE 8. MIST IGNITION CHARACTERISTICS OF DEGRADED (PACKED TUBE) AND UNDEGRADED AMK BLENDED FROM SLURRY (OF = 3.3)

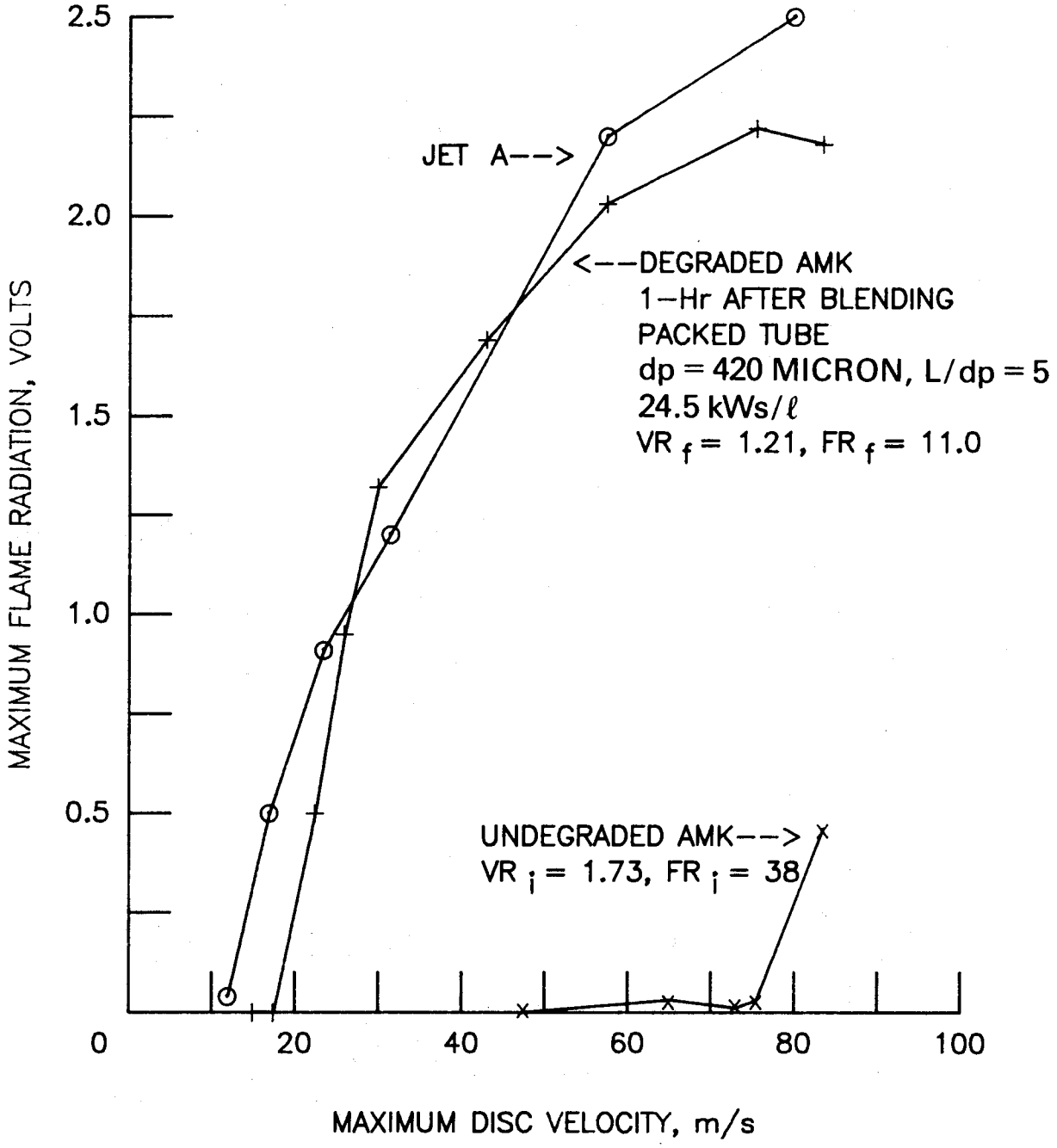

FIGURE 9. MIST IGNITION CHARACTERISTICS OF DEGRADED (PACKED TUBE) AND UNDEGRADED AMK BLENDED FROM SLURRY (OF = 2.8)

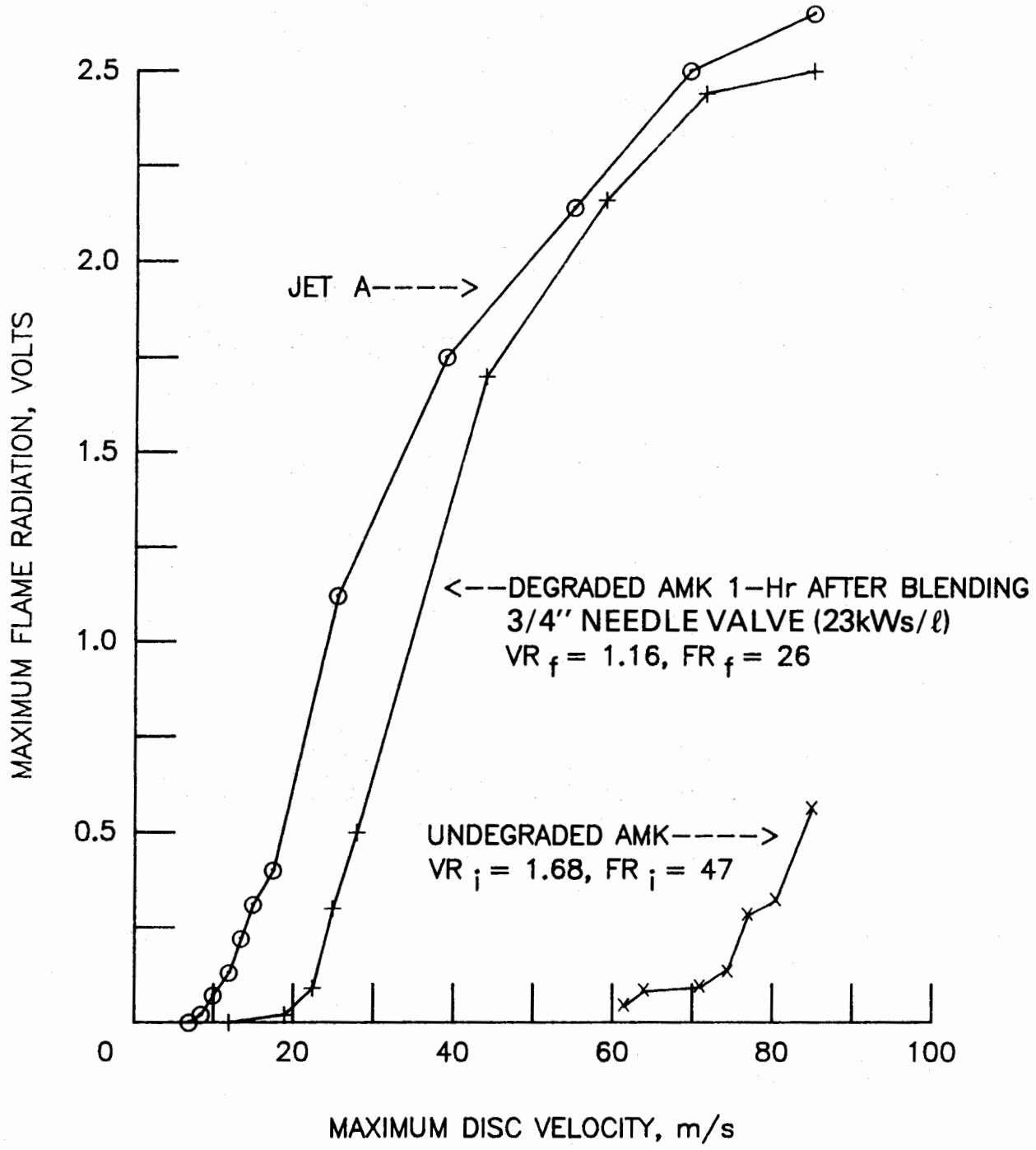

FIGURE 10. MIST IGNITION CHARACTERISTICS OF DEGRADED (NEEDLE VALVE) AND UNDEGRADED AMK BLENDED FROM SLURRY (OF = 2.3)

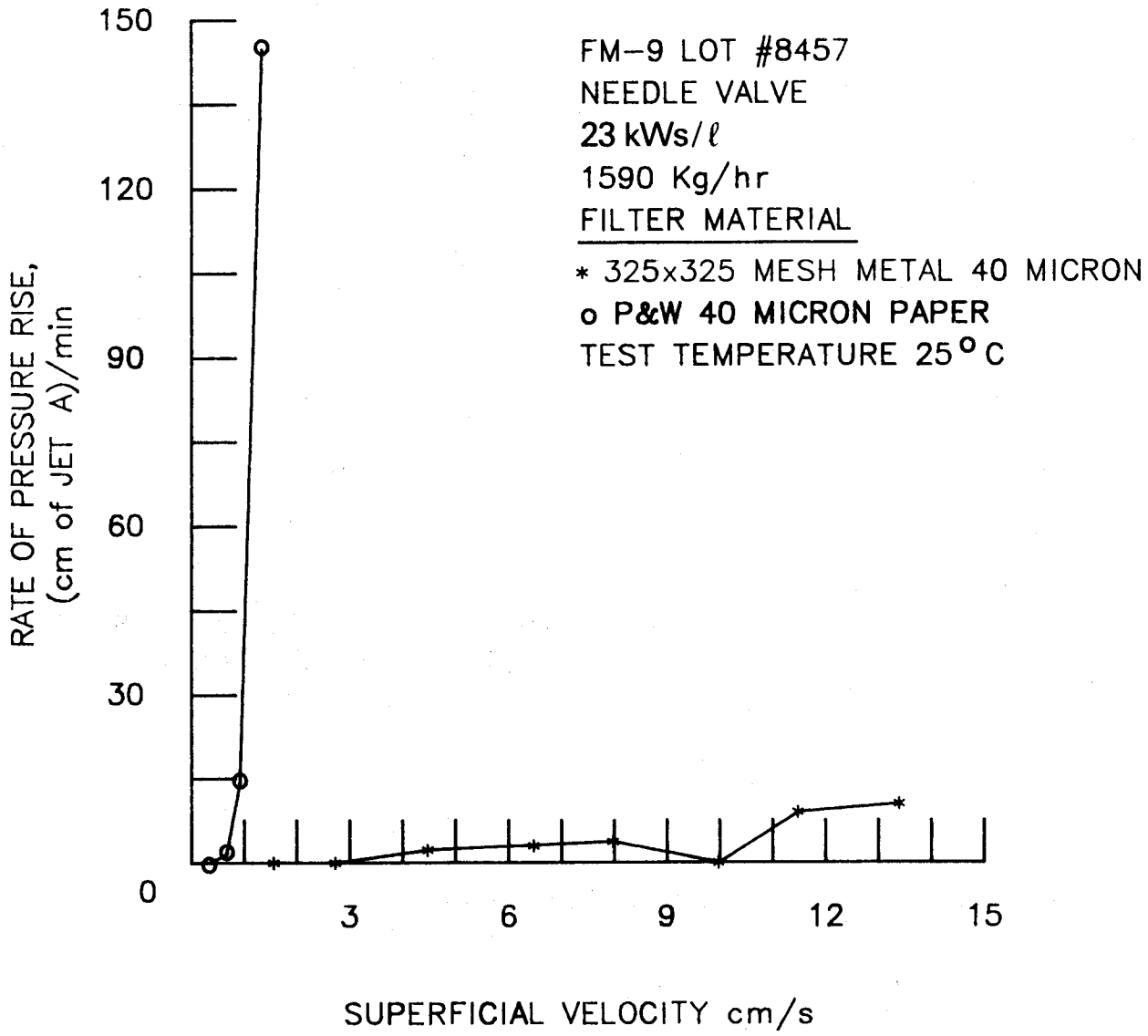

FIGURE 11. PUMP FILTRATION DATA FOR DEGRADED AMK WITH DIFFERENT FILTER MATERIALS

filtration experiments involved very high velocities through the wash-flow screen (11 cm/s at 320 Kg/hr and 22 cm/s at 650 Kg/hr), the results in Figure 11 indicate that filter plugging would be expected. The fact that none was observed suggests that the duration of the test might have been too short. However, it is also possible that the conditions in the full-scale test (particularly the wash-flow action) were not simulated by the small-scale test and that these conditions may be important to filter plugging.

A second comparison between the full-scale and small-scale filtration tests is provided by the data in Figure 12. The AMK samples in these experiments were degraded with a needle valve at a fixed flow rate and different specific powers (21, 14, and 7 kWs/ℓ, see Table 1). Because of the effect of temperature on filtration, the small-scale experiments were conducted at slightly different temperatures (38°, 35°, and 32°C) which corresponded to the temperatures of the degraded fuel as it flowed through the filter in the full-scale tests. The CFV for fuels degraded at 21 and 14 kWs/ℓ were not significantly different (∿0.4 cm/s). However, at 7 kWs/ℓ the CFV was between 0.2 cm/s and 0.3 cm/s. It should be noted that rapid plugging was produced in the JT8D fuel filter with degraded AMK (7 kWs/ℓ) at a velocity of 0.15 cm/s (Table 1).

Beginning around January 1981, anomalous results were observed in which the CFV of AMK was found to decrease with time following degradation (Fig. 13). This effect could not be detected in the standard filtration ratio test. For example, a particularly odd sample had filtration ratios of 1.11 (1.10)* for a 16-18 μm metal screen and 1.64 (1.50) for 40 μm paper immediately after degradation. Approximately six weeks later, the filtration ratios were 1.11 (1.10) and 1.51 (1.47) for the metal and paper filters, respectively. *In light of these results, it is difficult to understand how this degraded sample (24 kWs/ℓ) could have poorer filtration characteristics than undegraded AMK in which filtration ratios are typically 40-50 with 16-18 μm metal screens and 200-250 with 40 μm paper.* Nevertheless, it was observed that this degraded sample could not be filtered prior to its use in the Pump Filtration Test. A brief description of this experiment is given in the following paragraph.

Two separatory flasks, one containing 1.5 liters of degraded AMK and the other an identical quantity of undegraded AMK, were allowed to slowly drip into two funnels that were lined with number 41 Whatman filter papers. Once the filtration rate for the undegraded AMK was established, no further adjustment was necessary. However, the filtration rate of the degraded sample decreased with time so that the rate of flow into the funnel had to be continually decreased to prevent overflow. After approximately three hours, the entire 1.5 liters of undegraded AMK had been filtered, but less than one liter of the degraded sample had been collected in 12 hours!

---

* The number in parenthesis is the result of a duplicate experiment.

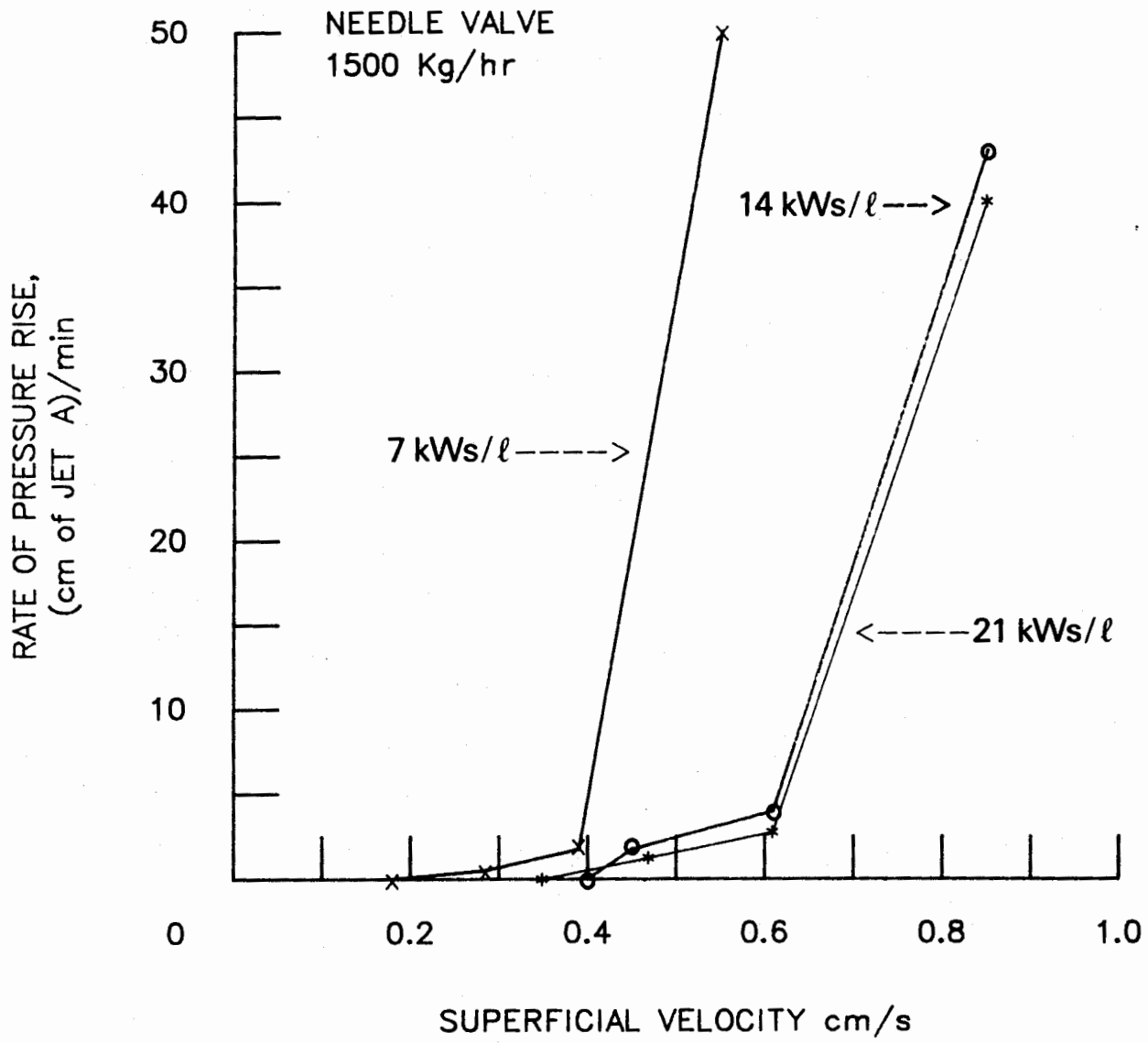

FIGURE 12. PUMP FILTRATION DATA FOR AMK DEGRADED AT DIFFERENT SPECIFIC POWERS (22-24°C)

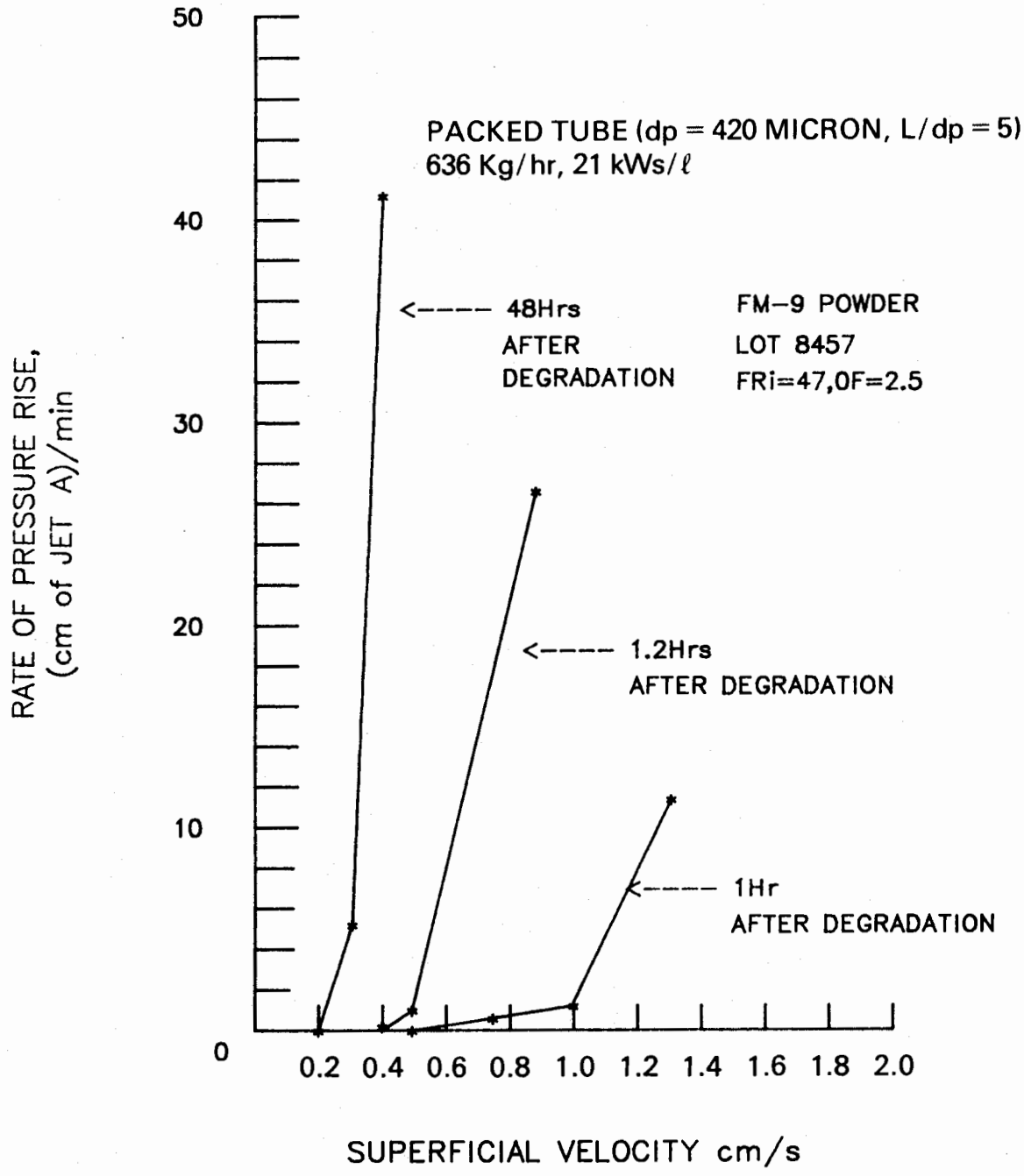

FIGURE 13. PUMP FILTRATION DATA FOR DEGRADED AMK WITH A 40 MICRON PAPER FILTER (JT8D)

This result suggested that the filtration ratios were incorrect due to the relatively short flow time (4-5 seconds) for the standard filtration ratio test. Consequently, experiments were conducted in which the flow time in the filtration ratio test was increased by decreasing the cross-sectional area of the filter. This was achieved by placing the filter paper between two discs with a hole of the desired size in the center. Data were obtained for areas from 5.0 cm^2 (standard filtration ratio test) to 0.2 cm^2. The flowtime was first measured for Jet A and then degraded AMK, and each filtration ratio was obtained with a new filter. The time for the flow of 96 mℓ of Jet A increased inversely with the filter area, so that the average velocity (V = Q/A) remained essentially constant. On the other hand, the velocity of degraded AMK samples generally decreased with increasing flow time or decreasing area. For example, the results in Figure 14 show the effect of flow time on the degraded AMK sample that exhibited the poor filtration characteristics which were previously discussed. *These results demonstrate that filtration ratios, as measured by the current test, can be in serious error.*

In addition to the dependency of the CFV on the elapsed time following degradation, a comparison with earlier experiments (Fig. 15) indicated that recent blends were harder to degrade. The only obvious difference between these experiments was that the FM-9 powder was from different lots. A second batch of this same lot (8406) was obtained from ICI Americas and a fresh AMK blend was made with this new material. Filtration data for a degraded sample (packed tube, 840 μm, L/D_p = 6, 25 kWs/ℓ) are compared with an earlier experiment in Figure 16. These results indicated almost an order of magnitude difference in the CFV. Of the various physical properties for these two samples, only the undegraded filtration ratios (FR_i) were significantly different. In particular, the more recent blend of Lot 8406 had a higher FR_i (51 compared to 37) and was harder to degrade.

It is unlikely that these observations can be explained solely by differences in the FM-9 powder, and it is suspected that the addition of the amine in the blending of AMK may also be a factor. Earlier experiments showed that if the amine were added before complete dissolution of the powder in the glycol, very high filtration ratios (100-200) could occur. However, within a few days these high values decreased and eventually resulted in normal filtration ratios that were of the order of 40-45. At present, there is no prescribed way of determining how long to wait before addition of the amine, and it is possible that this time can vary from one batch of FM-9 powder to the next. While these results may be an artifact of small-scale filtration experiments, it should be noted that all of the full-scale filtration experiments summarized in Tables 1-3 were conducted with recent AMK blends that appeared to be more difficult to degrade in terms of small-scale filtration tests.

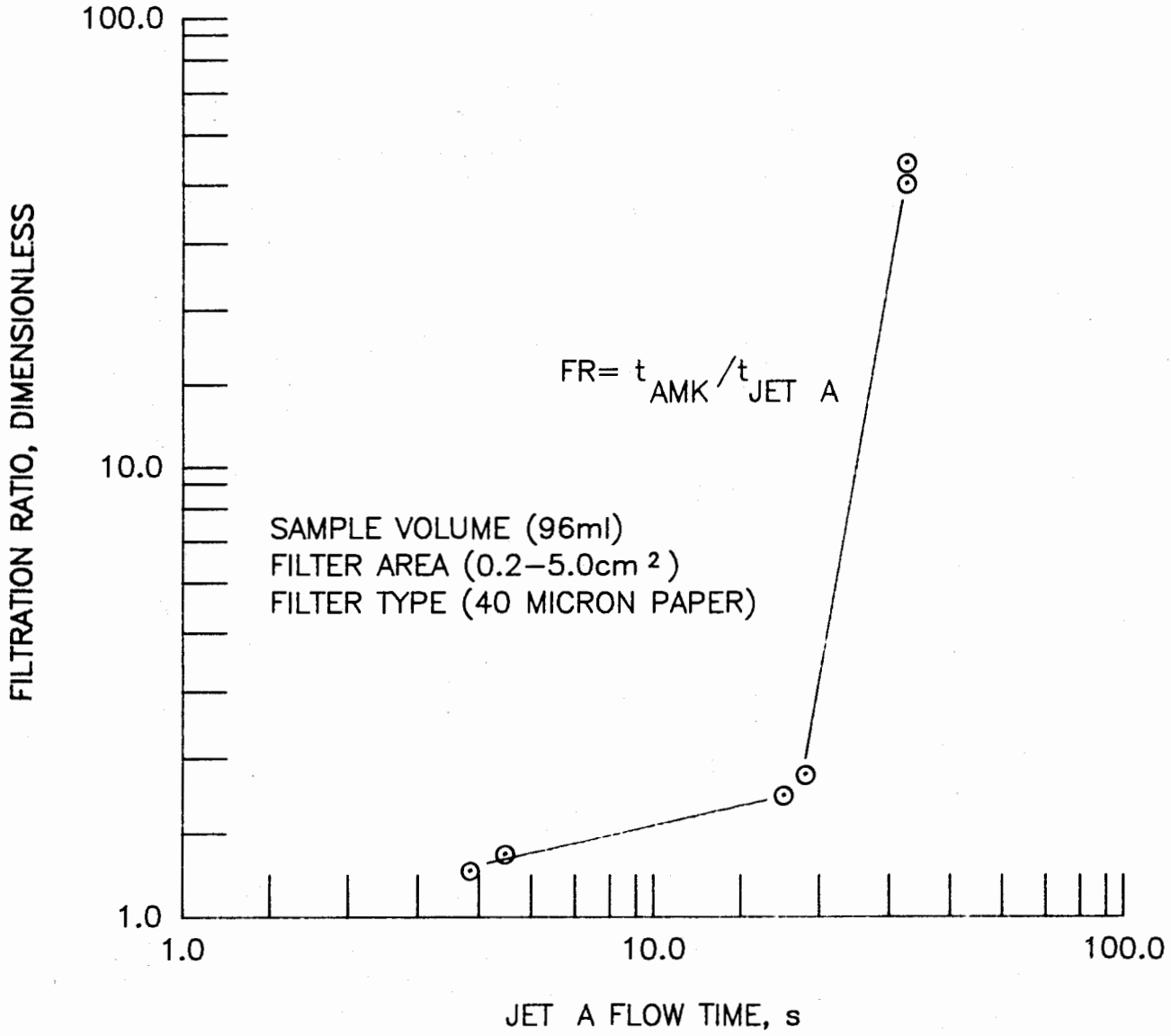

FIGURE 14. EFFECT OF JET A FLOW TIME ON THE FILTRATION RATIOS OF DEGRADED AMK

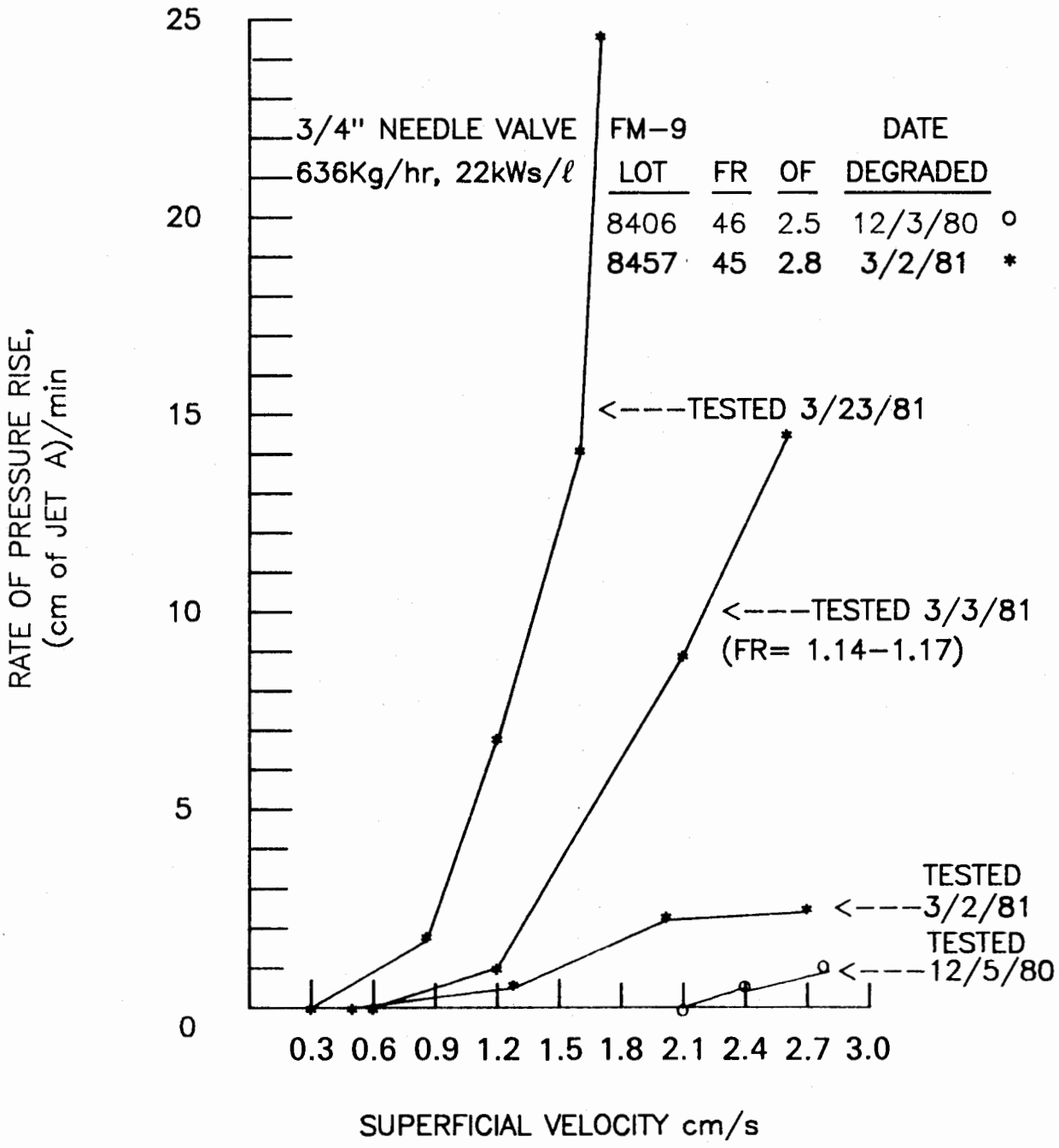

FIGURE 15. PUMP FILTRATION DATA FOR DEGRADED AMK WITH A 16-18 MICRON METAL SCREEN

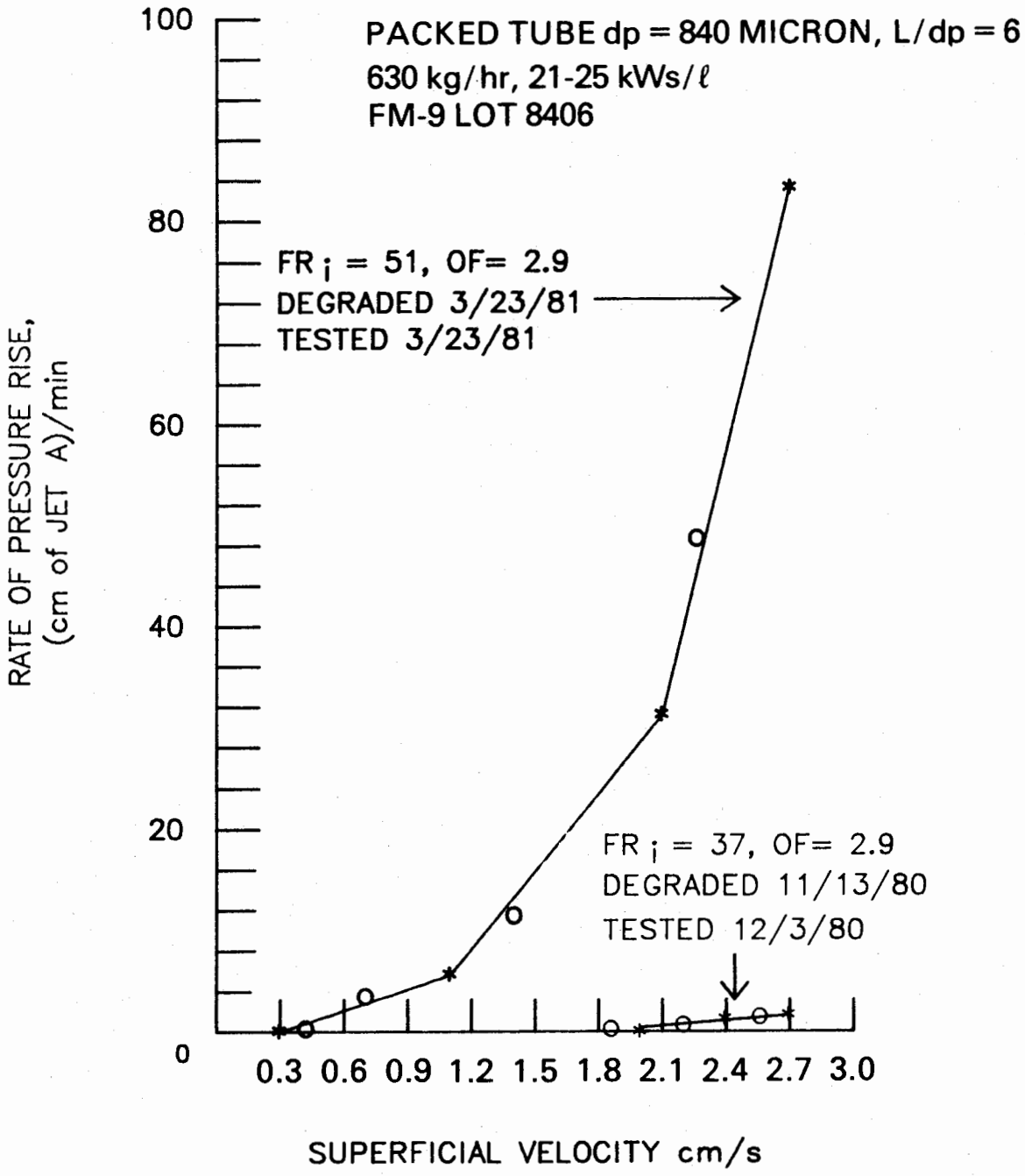

FIGURE 16. PUMP FILTRATION DATA FOR DEGRADED AMK WITH A 16-18 MICRON METAL SCREEN

III. ANALYSIS OF AMK FOR GLYCOL AND AMINE

The measurement of glycol content of AMK can be readily accomplished by the use of infrared spectroscopy*. For example, several runs with the same standard blend (calculated glycol content of 0.5884%) are summarized in the following table. In each case the cell was removed, washed, dried, and then refilled:

Wt % Glycol by Infrared
0.548
0.598
0.590
0.557
0.586
0.590
0.584
0.624
0.617
0.592

$\overline{X}$ = 0.589

σ = 0.023

The results in the next table compare the measured and calculated glycol content of five samples that were sent for analysis and identified only as A, B, C, D, and E. Actually, samples B and C were the same blend as were samples D and E. The measured glycol content was consistently 2 to 4% lower than the calculated values. Sample A was made from slurry in which 0.5 wt % water was added to the glycol (this is less than 50 ppm water in the finished AMK blend) as specified by RAE, all other blends were made without the addition of water.

	Wt % Glycol	
Sample	Measured	Calculated
A	0.59	0.60
B	0.54	0.57
C	0.54	0.57
D	0.56	0.57
E	0.55	0.57

* A description of this test procedure is given in Appendix C.

Measurement of the amine content of AMK has been found to be much more difficult. The relatively low concentration of amine (~150 ppm) requires a very sensitive method such as would be provided by combustion and nitrogen detection with chemiluminescence (sensitivity ~ a few parts per billion nitrogen). However, it has been found that it is difficult to inject AMK into the pyro-reactor (950°C) with small bore needles (5.0 μℓ syringes). This is not due to the gel forming characteristics of the FM-9 but rather to the evaporation of fuel and the formation of solid polymer in the needle tip. An alternate procedure in which the sample is introduced first into a quartz boat which is then pushed into the reactor was tried and also found to be unsatisfactory. For example, the following data show several consecutive runs with the same AMK blend (175 ppm amine).

Measured Amine Content, ppm
126
137
95
121
121
74
126
$\bar{X}$ = 114
σ = 22

The consistently low values measured for the amine is a shortcoming of this technique in which the boat must rapidly cool from 950°C to ambient. A thermocouple placed in the boat indicated that the temperature dropped from 950°C to 60°C within five minutes. However, no further temperature reduction with time was observed. This was probably due to radiation heating of the boat by the furnace. Consequently, there is a good chance of appreciable loss of sample due to evaporation.

Because of the high sensitivity of this technique, it has been found possible to dilute the AMK and reduce plugging of the microsyringe*. The mean and standard deviation (based on five consecutive injections) for three AMK blends received from ICI Americas, Inc., are summarized in the following table:

	RMH-1-129 (0.3% FM-9)	RMH-1-136 (0.27% FM-9)	RMH-1-138 (0.3% FM-9)
$\bar{X}$ =	181 ppm	112 ppm	144 ppm
σ =	5 ppm	6 ppm	11 ppm

*A description of this test method is provided in Appendix D.

Based on the nominal polymer content indicated on these sample containers, the expected amine content (5% of the FM-9 polymer) would be 150 ppm, 135 ppm and 150 ppm for RMH-1-129, RHM-1-136 and RMH-1-138, respectively. Differences between the measured and nominal amine content of two of these samples are greater than the expected experimental error; however, additional data are required before a high degree of confidence can be attributed to this technique.

IV. GEL PERMEATION CHROMATOGRAPHY (GPC)

GPC measurements of undegraded and degraded AMK (both conventional blends and blends made by dispersing a slurry of FM-9 powder and glycol/amine carrier fluid in Jet A) have been made with a Water's ALC 100 unit equipped with differential refractiometer and UV detectors. Microstyrogel was used in 1-foot columns of the following sizes 10^6, 10^5 (2 each), and 10^4 Å. The solvent was tetrahydrofuran (THF) and the flow rate was 1 mℓ/min. In addition, AMK samples were diluted by a factor of 10/1 with THF to minimize flow induced shear thickening of the polymer and then filtered (Whatman #42 paper) to remove insoluble contaminants.

GPC separates polymer solutions according to their molecular size, not necessarily according to their molecular weight. For example, smaller molecules diffuse into the internal pore structure of the microstyrogel. Larger molecules can do this to a lesser degree and the very largest molecules ($M > 10 - 20 \times 10^6$) may be completely excluded. Therefore, the largest molecules flow through the column and emerge first while smaller molecules emerge later. Consequently, a GPC chromatogram contains information regarding the entire spectrum of molecular sizes present in a particular sample. It is not possible to theoretically predict the rate of elution for a particular molecular size. However, this can be established by calibrating the columns with high molecular weight materials whose size have been determined by a more basic measurement technique such as light scattering. While some success has been reported in correlating GPC data in terms of a molecular size parameter ($M[\eta]$)(7), where M is the molecular weight and $[\eta]$ is the intrinsic viscosity, this procedure is quite tedious. The procedure used in this work has been to calibrate the column with high molecular weight polystyrene (PS) standards and to report results in terms of the peak elution volume (PEV) which is representative of the average molecular size.

The data in Table 4 summarize GPC measurements in which dates of experiments are presented to help explain certain pecularities that were observed. The first three entries in Table 4 represent consecutive experiments conducted on the same day with a polystyrene ($M = 3.8 \times 10^6$) standard. These results show that the PEV of the 3.8×10^6 PS was highly repeatable (24.4 mℓ). However, reruns of the standard on different days, particularly following the use of undegraded AMK in the columns, indicated a significant shift in the PEV (e.g., PEV = 25.1 mℓ on 11/7/80). The fact that this shift was not noted after the initial experiments with undegraded AMK (10/29/80 and 11/10/80) suggests that very high molecular weight species (possibly microgel) may temporarily interfere with subsequent GPC experiments.

TABLE 4. EFFECT OF DEGRADER POWER AND DEGRADER TYPE ON PEAK ELUTION VOLUME

Date	Sample	Type of Degrader	Specific Power, kWs/ℓ	Filtration Ratio	Viscosity Ratio	Peak Elution Vol, mℓ
10/28/80	3.8 x 10^6 PS	----	----	----	----	24.4
"	"	----	----	----	----	24.4
"	"	----	----	----	----	24.4
10/29/80	AMK	JT8D Fuel Pump	(3-pass)	1.3-1.5	1.33	25.1
"	3.8 x 10^6 PS	----	----	----	----	24.4
"	AMK	JT8D Fuel Pump	(16-pass)	1.17	1.17	26.1
"	AMK	Packed Tube (d_p=840 μm, L/D=6)	26.0	1.0	1.10	26.1
"	AMK*	Packed Tube (d_p=420 m, L/D=5)	26.0	6.0	1.20	24.4
"	3.8 x 10^6 PS	----	----	----	----	24.4
11/07/80	3.8 x 10^6 PS	----	----	----	----	24.1
"	AMK	None	0	38	1.72	24.4
"	AMK*	None	0	31	1.79	24.7
"	3.8 x 10^6 PS	----	----	----	----	25.1
11/10/80	3.8 x 10^6 PS	----	----	----	----	24.3
"	AMK	Packed Tube (d_p=420 μm, L/D_p=5)	24.0	1.2	1.17	26.4
"	3.8 x 10^6 PS	----	----	----	----	24.2
01/14/81	AMK	None	0	37	1.67	23.0
"	"	Static Mixing Tube (D=3/8", L/D=27)	21.5	3.3	1.29	24.6
"	"	" " " "				
"	"	3/4 in. Needle Valve	22.4	1.16	1.17	26.2
"	"	" " "	13.0	1.60	1.25	25.1
"	"	" " "	12.0	1.57	1.22	25.1
"	"	Packed Tube (d_p=840 μm, L/D_p=6)	20.5	1.17	1.17	25.6
"	"	" " "	9.3	1.80	1.24	24.6
"	"	Packed Tube (d_p=420 μm, L/D_p=5)	20.5	1.17	1.15	26.0
"	"	" " "	10.5	1.22	1.21	24.9
"	AMK*	3/4 in. Needle Valve	23.0	26	1.16	26.9
"	AMK	JT8D Fuel Pump	(16-pass)	1.17	1.17	26.0
"	"	" "	(3-pass)	1.3-1.5	1.32	25.0
"	"	RAE	100	1.2-1.3	1.22	25.2
"	3.8 x 10^6 PS	----	----	----	----	23.6
"	6.7 x 10^5 PS	----	----	----	----	26.1

*Blended from a slurry of FM-9 powder in glycol/amine carrier fluid.

The initial experiments with degraded AMK samples (10/29/80) showed that GPC could detect differences between highly degraded AMK samples (e.g., PEV = 25.1 mℓ for 3-pass and 26.1 mℓ for 16-pass AMK)*. Furthermore, these results indicated that a level of molecular size reduction equivalent to 16 passes through a JT8D fuel pump could be achieved by a single pass through a packed tube at a higher specific power.

Results of degrading a particular AMK blend (OF = 2.9 mℓ/30 sec., VR = 1.67, FR = 37) by different methods and at different specific powers are also presented in Table 4 (01/14/81). The effect of these parameters have been interpreted in terms of a molecular weight ratio (M/M_i, where M_i is the peak molecular weight of undegraded AMK relative to polystyrene) is shown in Figure 17. These results suggest that the packed tubes and needle valve are more efficient (i.e., require less power to produce a specific molecular weight reduction) than the static mixing tube (Komax Systems, Inc.). However, a shorter static mixing tube should be tested before this conclusion is drawn. Since the VR of a dilute polymer solution is related to the intrinsic viscosity, which in turn is related to molecular size, one would expect a reasonably good correlation between peak molecular weight as determined by GPC and the VR. That such a correlation exists for partially degraded AMK is shown by the data in Figure 18.

While these preliminary results were very encouraging, GPC measurements for *a sample of AMK that was blended from a slurry of FM-9 powder in a glycol/amine carrier fluid and then degraded within one hour (Packed tube, d_p = 420 μm, L/d_p = 5, 26 kWs/ℓ) indicated an even higher level of degradation (PEV = 26.4 mℓ) than 16 pass AMK!* Since the RAE reported that AMK blended from slurry is difficult to degrade for several hours following blending, the high level of degradation indicated by the GPC appears to conflict with their results. However, this conflict can be partially explained by the fact that the RAE have based their conclusion on the higher than normal filtration ratios observed for degraded AMK blended from slurry. Similar results are shown for the sample blended from slurry in Table 4 (10/29/80). For example, the FR_i before degradation was 31 (this FR value is lower than typical AMK blends) and was reduced to only 6.0 after flow through a packed tube (d_p = 420 μm, Ld_p = 5) at a specific power of 26 kWs/ℓ. Generally, a FR of 1.0-1.2 would be expected for typical AMK blends. On the other hand, the VR was reduced from 1.79 (this VR value is higher than typical AMK blends) to 1.20. This low VR is indicative of a high level of degradation that has been confirmed by the mist flammability experiments discussed earlier (Fig. 8).

Similar results (PEV = 26.9 mℓ, Table 4, 01/14/81) were obtained with a second AMK sample that was blended by dispersing slurry into Jet A and degrading the blend within one hour with a needle valve (23 kWs/ℓ). The initial FR of this blend was 47 and the initial VR was 1.68. Immediately following, degradation duplicate FR measurements gave values of 12 and 19, respectively, and approximately a week later these values were 26 and 27. However, the VR remained at a very low value of 1.16. Mist flammability experiments, that were discussed earlier, indicated a high degree of

*These samples were received from Pratt & Whitney.

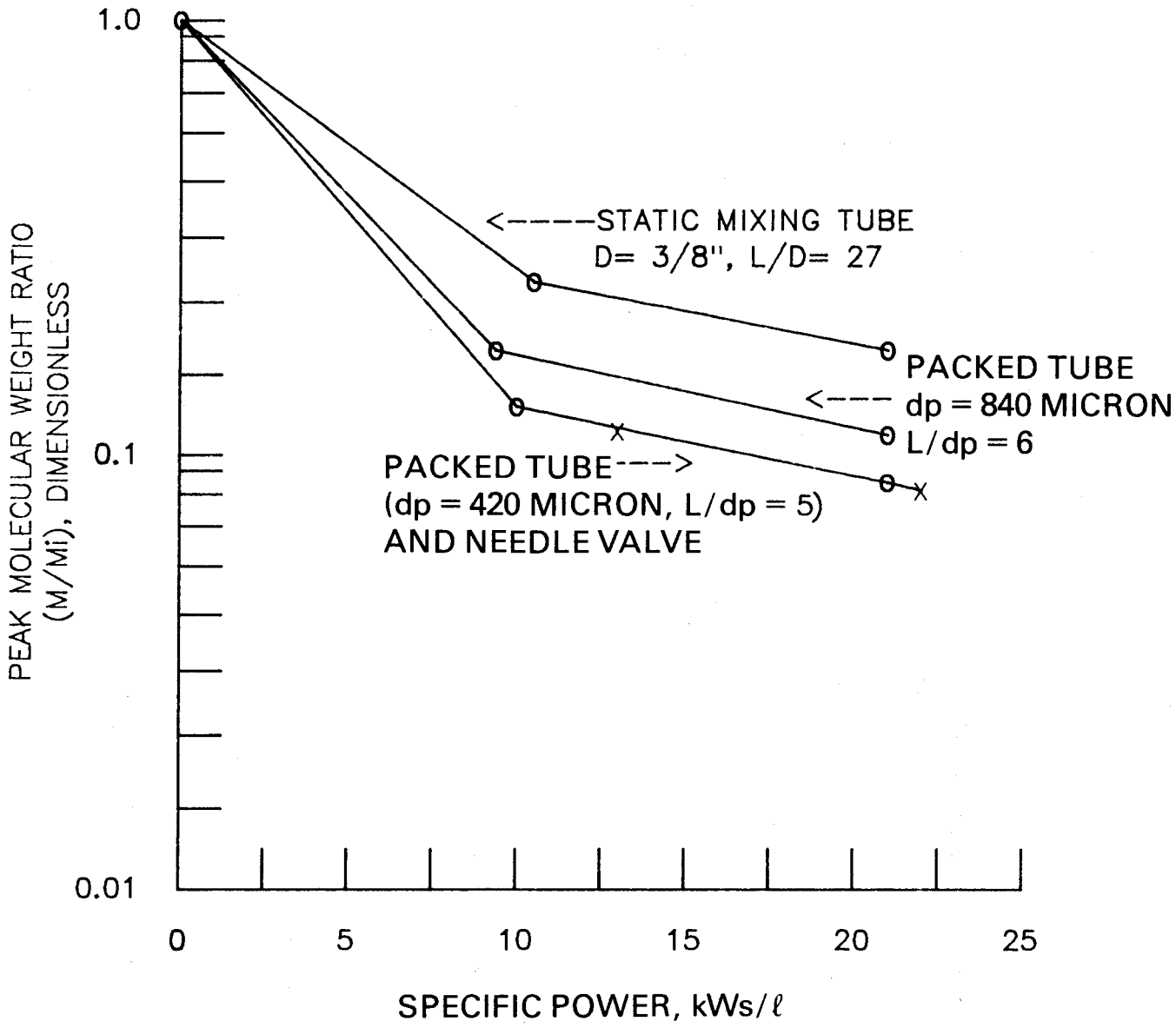

FIGURE 17. EFFECT OF SPECIFIC POWER AND DEGRADER TYPE ON PEAK MOLECULAR WEIGHT OF AMK

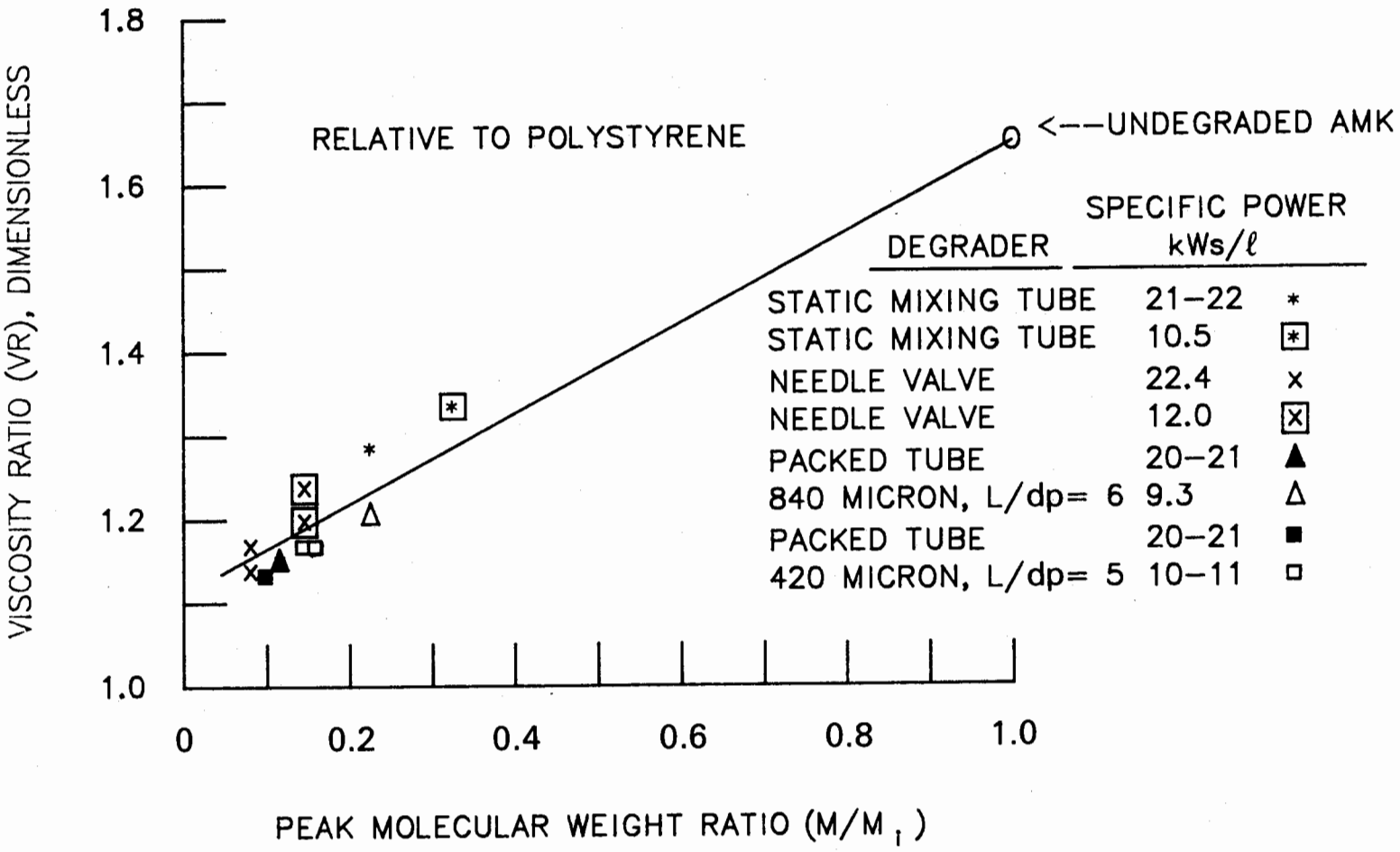

FIGURE 18. CORRELATION BETWEEN VISCOSITY RATIO AND GPC PEAK MOLECULAR WEIGHT

degradation; but this fuel was slightly more difficult to ignite than Jet A (Fig. 10). These findings indicate that the PEV can be used to establish different levels of degradation; however, the PEV may not be able to predict the filterability of degraded AMK if slurry blended fuels are involved. This may be due to small amounts of poorly solubilized (i.e., poorly swollen) polymer that have little effect on VR or PRV but that could readily plug a filter.

V. FLAMMABILITY COMPARISON TEST APPARATUS (FCTA)

Mist ignition characteristics of AMK were measured with a Flammability Comparison Test Apparatus (Unit 5) that was developed at the Federal Aviation Administration Technical Center.(8) Preliminary (non-ignition) experiments indicated a large drop in pressure and a correspondingly large change in air velocity during the fuel dump. For example, with the initial air pressure set at 80 psi, the final pressure was 52 psi. This is equivalent to a drop in air velocity from 71 m/s to 47 m/s, respectively*. Attempts to supplement the air pressure in the tank with shop air resulted in only slightly better results. This uncertainty of the exact pressure or velocity associated with failure of the fuel would make it difficult to compare results with different flammability tests. However, instrumentation of the air reservoir with a pressure transducer and strip-chart recorder showed that the maximum heat release from the resulting mist fire closely coincided with the midpoint of the fuel dump. Therefore, the mean air velocity**, based on the midpoint of the fuel dump, should be an excellent measure of the characteristic air velocity at the time of ignition.

A second problem, that could not be solved as easily, is apparently due to the difficulty of atomizing fuel inside of a pipe with a relatively small diameter (one inch). A pan was placed beneath the diffuser cone and the amount of fuel collected (i.e., run-off) was measured as a function of the initial air pressure in the tank. The results in Figure 19 show that the amounts of Jet A and AMK collected decreased with increasing air pressure. At low pressures, approximately 90% of the AMK was collected as run-off. This would probably be attributed to the relatively high resistance of AMK to atomization that results in the majority of the AMK contacting the wall of the pipe. The reason for the observed crossover at high pressures, in which more Jet A was collected than AMK, is less evident. Nevertheless, the important point is that the fuel run-off (which is a function of air speed and atomization characteristics of the fuel) results in the actual fuel dump rate (i.e., corrected for fuel run-off) being lower than expected. Furthermore, fuel that is trapped on the wall of the pipe cannot readily contribute to the heat release of the mist fire; consequently, heat release rates may be expected to be a function of atomization (which is the desired parameter) and also a function of fuel run-off (which is an artifact of the apparatus).

---

*The equivalent air velocity was calculated from a calibration curve that was provided with the apparatus.

**Calibration curves were also provided in terms of the mean air velocity.

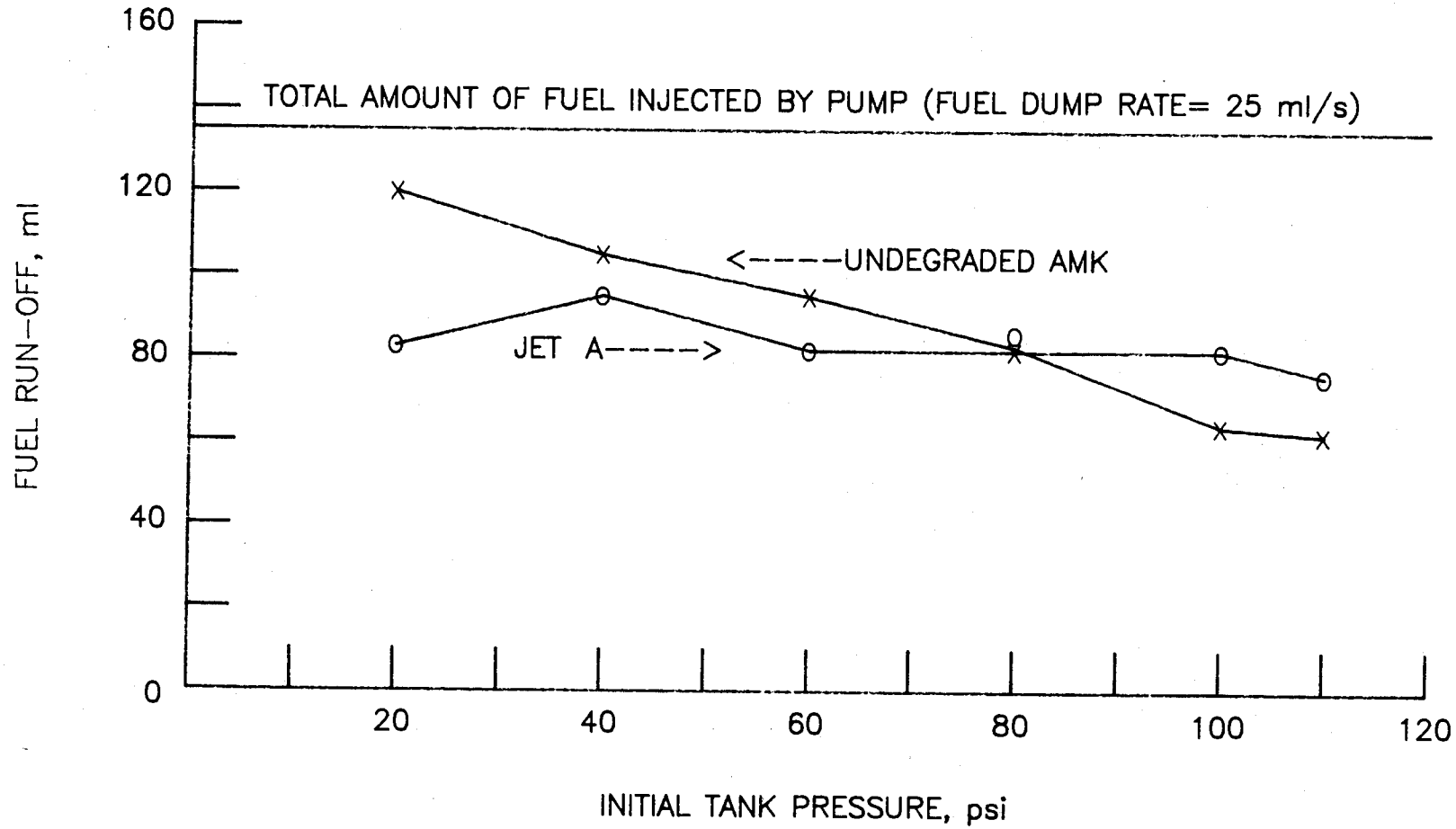

FIGURE 19. EFFECT OF INITIAL TANK PRESSURE ON FUEL RUN-OFF
(FLAMMABILITY COMPARISON TEST APPARATUS)

Since spinning disc experiments indicate that AMK made without the amine component of the carrier fluid is as effective as standard AMK(9,10), the FCTA was used to evaluate the effect of the amine. The data in Figure 20 are for two different AMK blends made without amine and a standard AMK. Both blends without amine start to burn at lower air velocities than standard AMK; however, with one sample, the differences in heat release are barely measurable. Similar sample differences have been observed for AMK in the Spinning Disc Test(10) and the JPL mini-Wing Test.(11) The reason for these differences is not presently known.

A second important observation was that while the maximum heat release for Jet A was of the same order of magnitude as reported earlier(8), the heat release for AMK was significantly lower. Even at the air velocities approaching 90 m/s, the heat release for AMK was well below the pass/marginal value of 0.6 BTU/ft^2-sec. Checks of fuel flow rates and air velocities showed them to be well within their expected values; however, upon closer inspection the fuel dump tube was found to be slightly off-center. Realignment of the fuel dump tube increased the heat release to above 0.6 BTU/ft^2-sec (Fig. 21); however, fail conditions associated with flashback of mist fire into the diffuser cone could not be achieved with freshly blended samples of AMK. A recheck of fuel run-off after realignment of the fuel dump tube has not as yet been made; therefore, it is not known whether or not the increased heat release is due to decreased fuel run-off.

The results in Figure 21 compare the mist flammability of AMK with another modified Jet A (0.3% Gulf AMA-2B). The FCTA indicates that both fuels have similar antimisting properties with the AMK fuel producing slightly lower heat release rates. It is interesting to note that the Spinning Disc Test indicated that the critical velocity of AMK was close to 60 m/s while that of Gulf AMA-2B was only 50 m/s. While this is the same directional effect as observed with the Flammability Comparison Apparatus, the mode of failure appeared to be much more severe with the Gulf additive than with AMK in the Spinning Disc Test (Fig. 22).

VI. RHEOLOGICAL PROPERTIES OF AMK

A. CAPILLARY TUBE EXPERIMENTS

Flow experiments with AMK were conducted with the pump filtration apparatus in which a series of different size capillary tubes replaced the filter elements. The pressure drop was measured as a function of time at different flow rates. Data for undegraded AMK at 25°C are shown in Figure 23 in which the steady-state pressure drop was used to calculate the wall shear stress ($R\Delta P/2L$), and the flow rate was used to calculate the wall shear rate ($8V/D$). These results show that the flow data were independent of both capillary tube length and diameter over the range of variables that were investigated. The absence of an intercept for the data in Figure 24 show that entrance effects are negligible.(12) The invariance of these measurements substantiates that they are representative

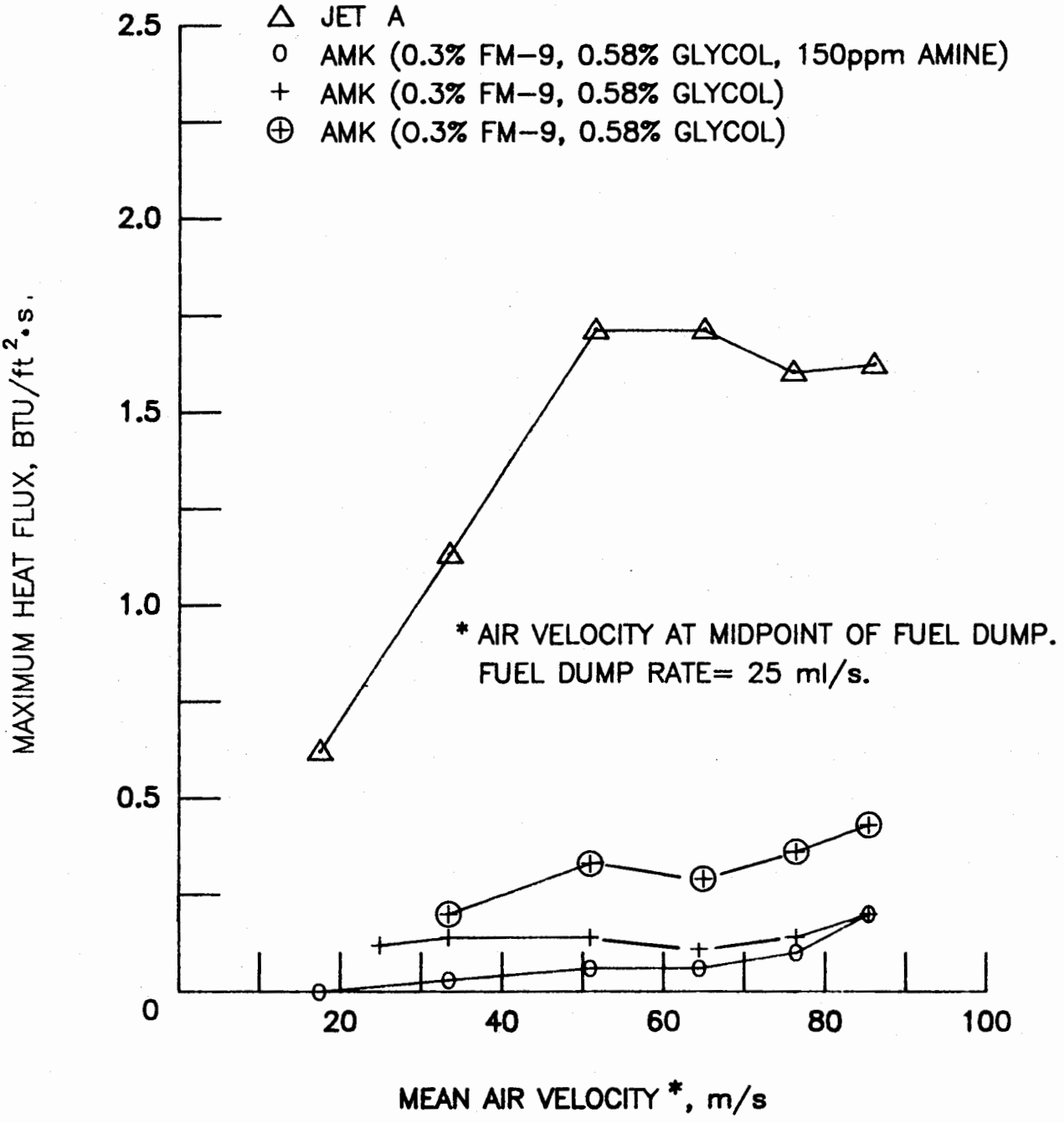

FIGURE 20. EFFECT OF AMINE ON MIST FLAMMABILITY OF AMK
(FLAMMABILITY COMPARISON TEST APPARATUS)

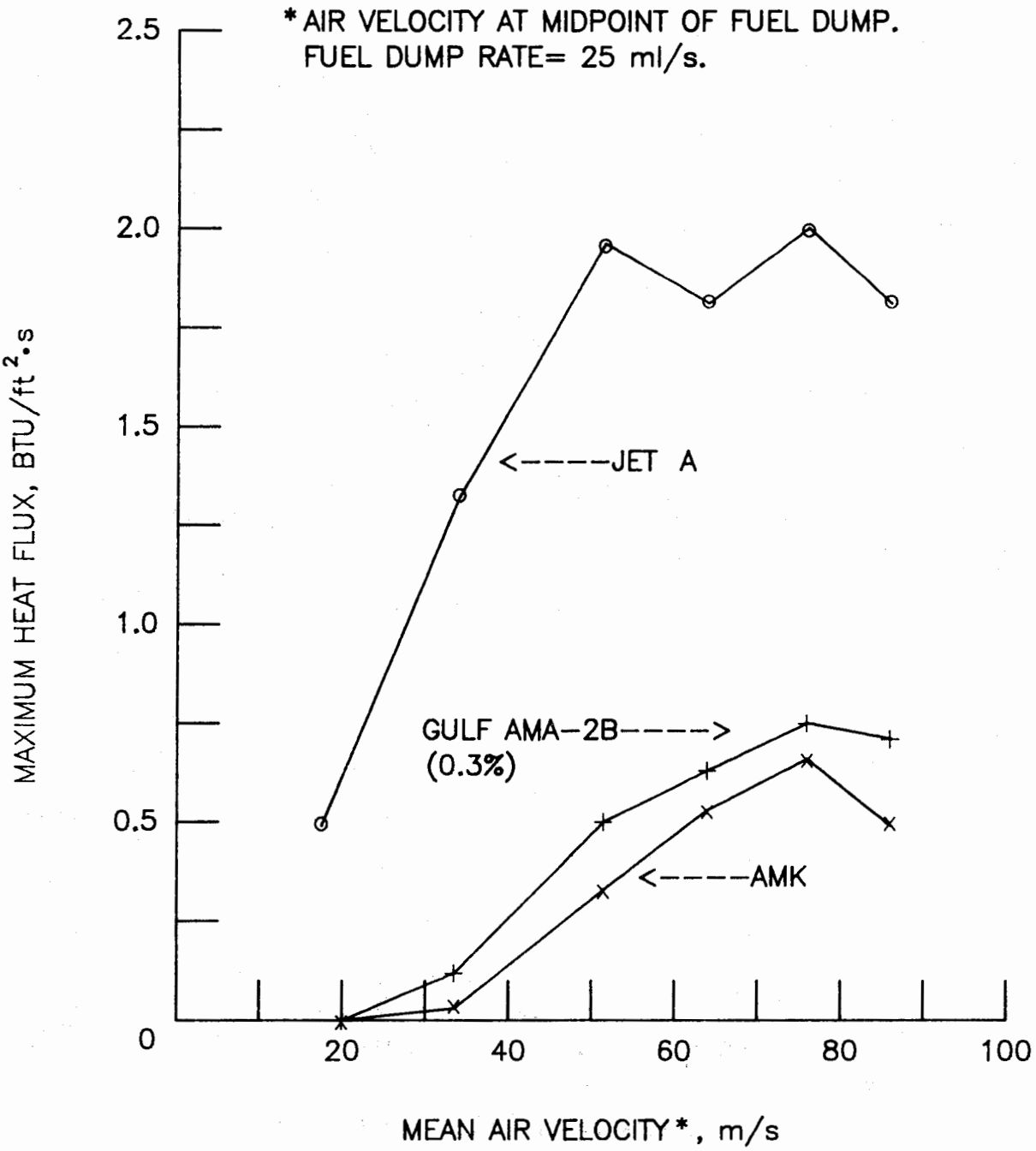

FIGURE 21. MIST FLAMMABILITY OF AMK AND GULF AMA-2B (FLAMMABILITY COMPARISON TEST APPARATUS)

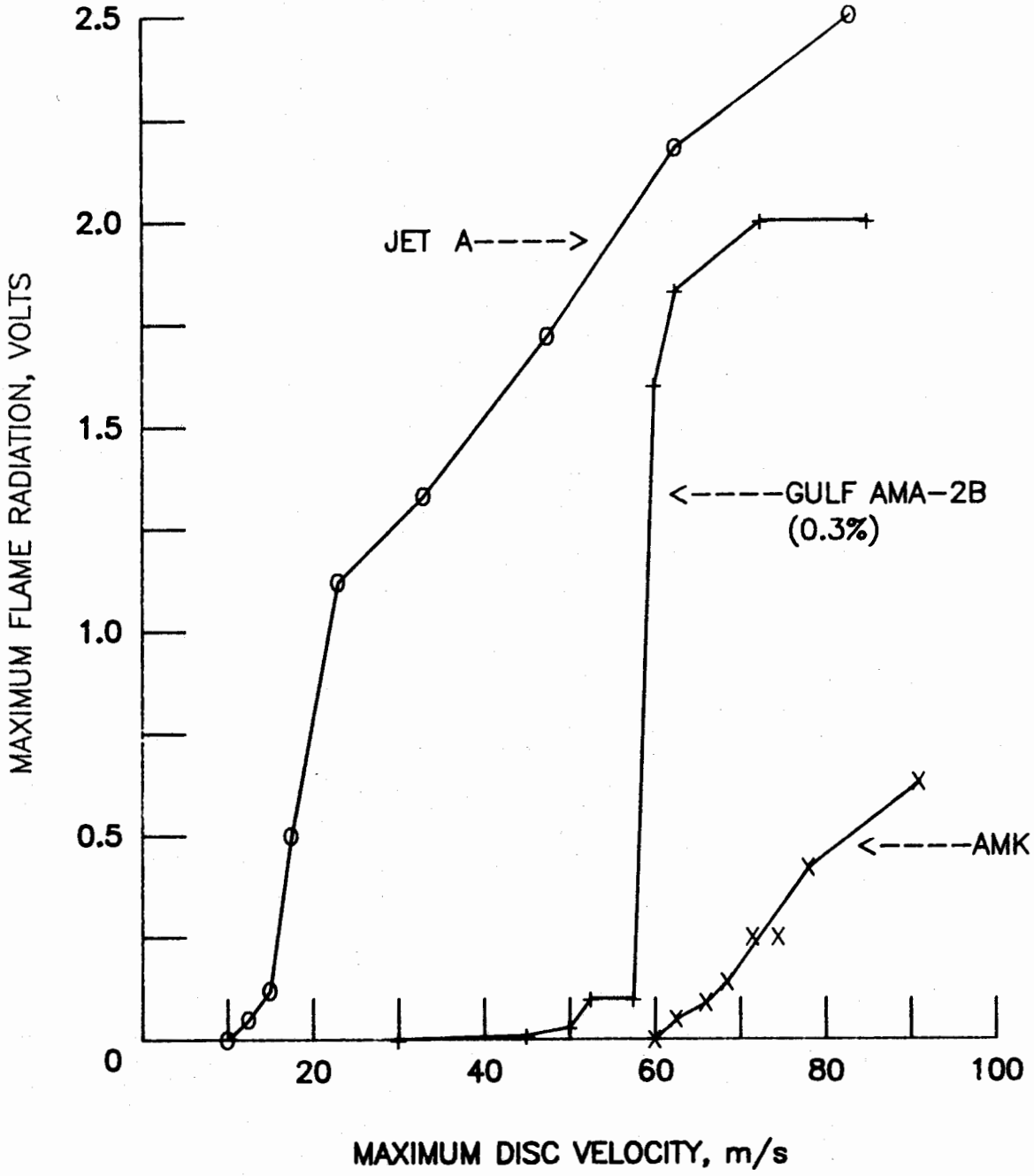

FIGURE 22. MIST FLAMMABILITY OF AMK AND GULF AMA-2B (SPINNING DISK)

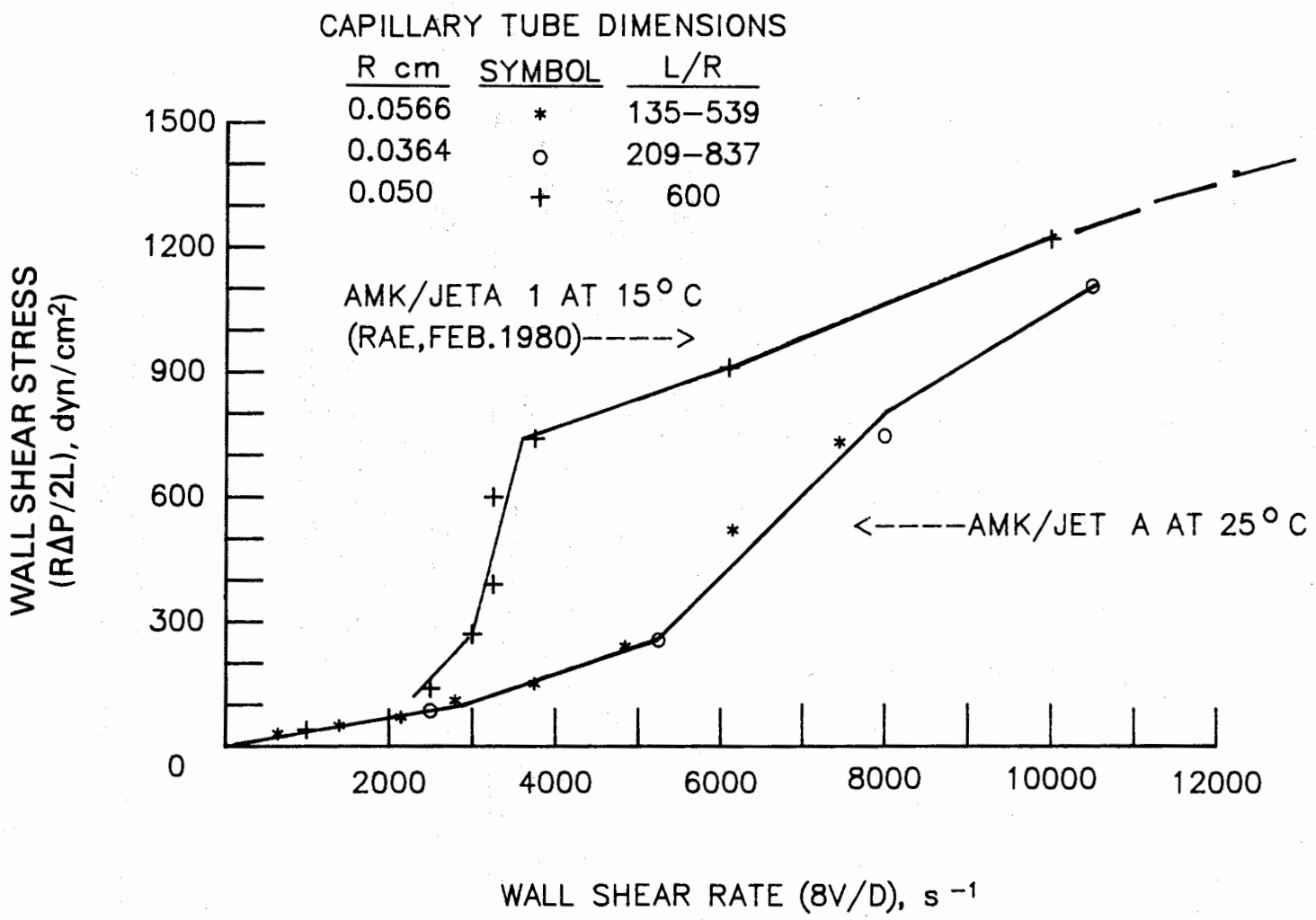

FIGURE 23. SHEAR THICKENING OF AMK IN CAPILLARY TUBES

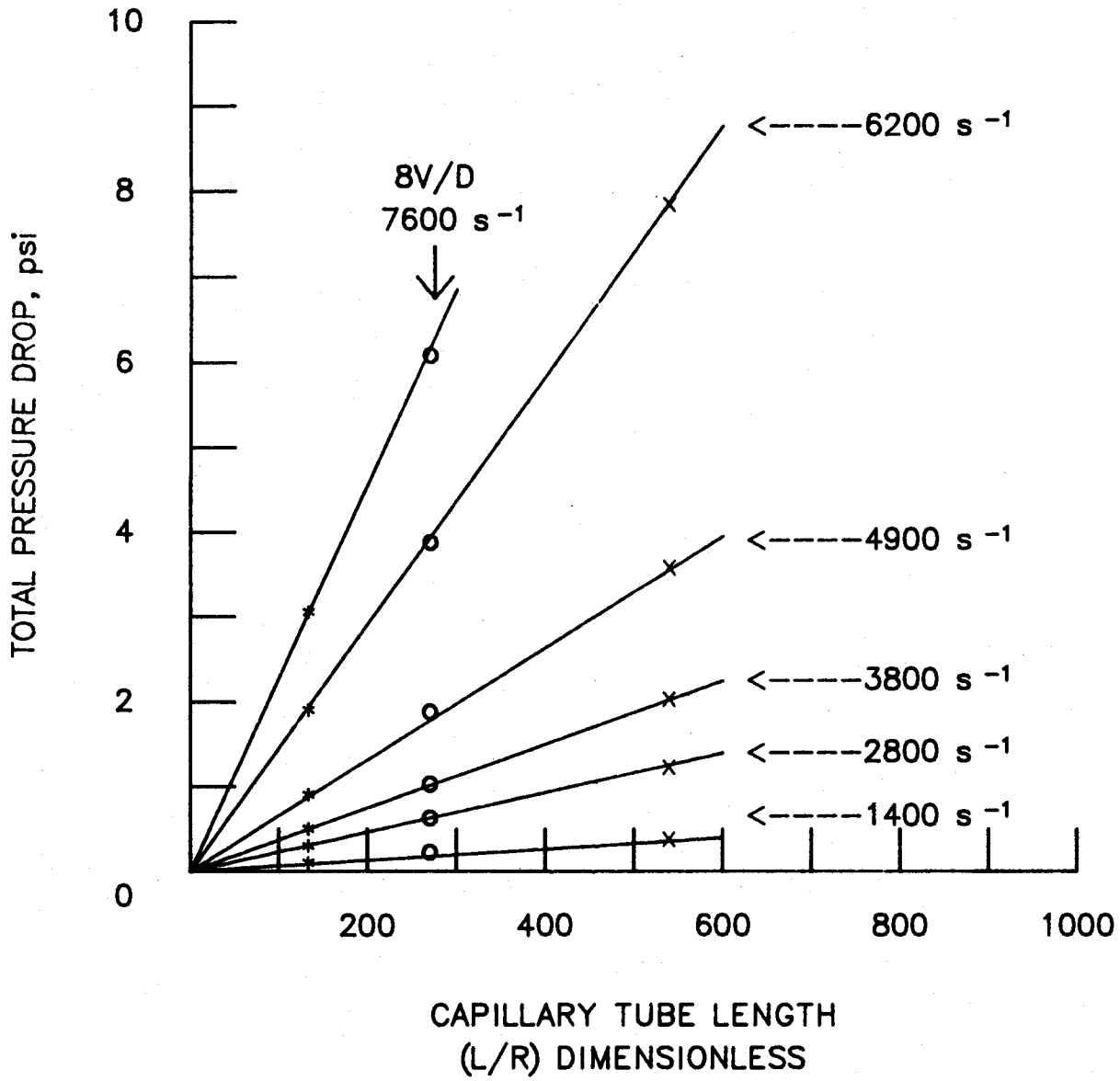

FIGURE 24. VISCOUS RESISTANCE OF AMK IN DIFFERENT LENGTH CAPILLARY TUBES (R = 0.57 mm)

of the shear viscosity of AMK. Therefore, differences between these data and earlier data reported by RAE (Fig. 23) are probably due to differences in the test temperatures.

While the quantity 8V/D is the true shear rate only for a Newtonian liquid, the correction term for the data in Figure 23 is of second order*. Consequently, a reasonable approximation of the apparent shear viscosity can be obtained by taking the ratio of $R\Delta P/2L$ to 8V/D. This quantity, which has been plotted in Figure 25, shows that the shear viscosity of AMK increases when a shear rate of 2500 s^{-1} is exceeded. However, the magnitude of the viscosity appears to reach a maximum value of slightly greater than 10 cP. It is obvious that such a low apparent viscosity cannot account for the effectiveness of AMK. For example, the effect of viscosity on the critical ignition velocity (Fig. 26) is only slightly higher for Jet A thickened with mineral oil (13 cP) than ordinary Jet A (1.5 cP). Moreover, viscosities in excess of 100 cP would be required to provide mist fire protection equivalent to AMK. *It has long been realized that the shear viscosity of viscoelastic polymers such as FM-4, AM-1, and polyisobutylene (PIB) cannot explain their antimisting effectiveness. It is now evident that the same statement holds for FM-9.*

While the important rheological parameter for most antimisting additives is generally thought to be the elongational viscosity, attempts to measure this property for FM-9 indicated that this additive was not viscoelastic.(13) However, the rheological experiments with capillary tubes that were previously described indicated that AMK (FM-9 in Jet A with carrier fluid) became highly viscoelastic when the critical shear rate was exceeded. This fact was readily apparent from the recoil and swelling of jets of AMK as they issued from the tip of a capillary tube. For example, the photographs in Figure 27 cannot be explained by differences in the shear viscosity and must be attributed to the development of normal stresses. It is important to note that if the L/R of the capillary tube is less than a critical value (L/R = 3, Fig. 27), these characteristic viscoelastic effects were not developed with AMK. This *shear induced viscoelasticity* is a major difference between FM-9 and most antimisting polymers.

---

*In particular, for 8V/D = 8000 s^{-1} the true shear rate is estimated from the slope of the lower curve in Figure 23 to be 7700 s^{-1}.

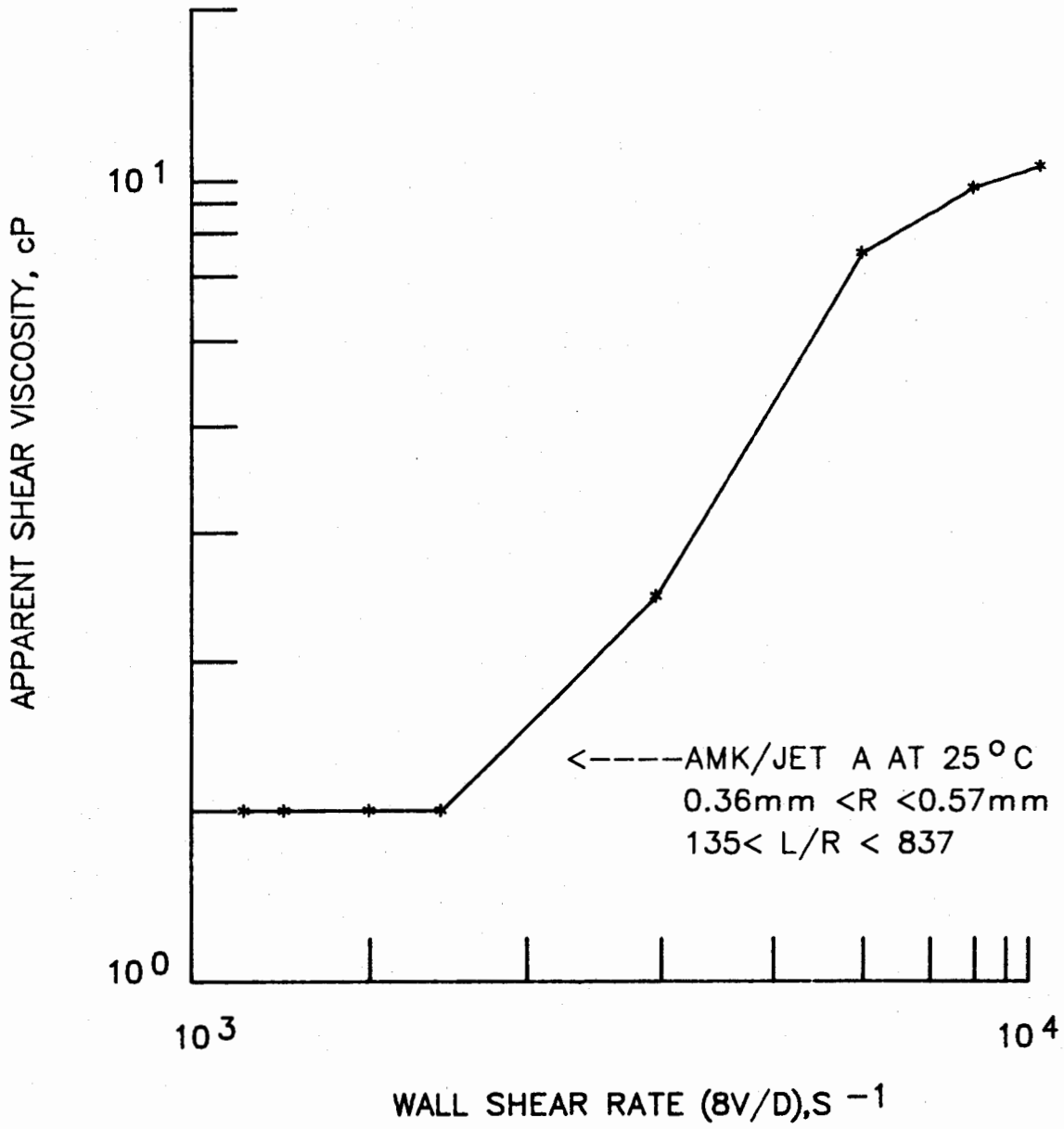

FIGURE 25. EFFECT OF SHEAR RATE ON APPARENT VISCOSITY OF AMK IN CAPILLARY TUBES

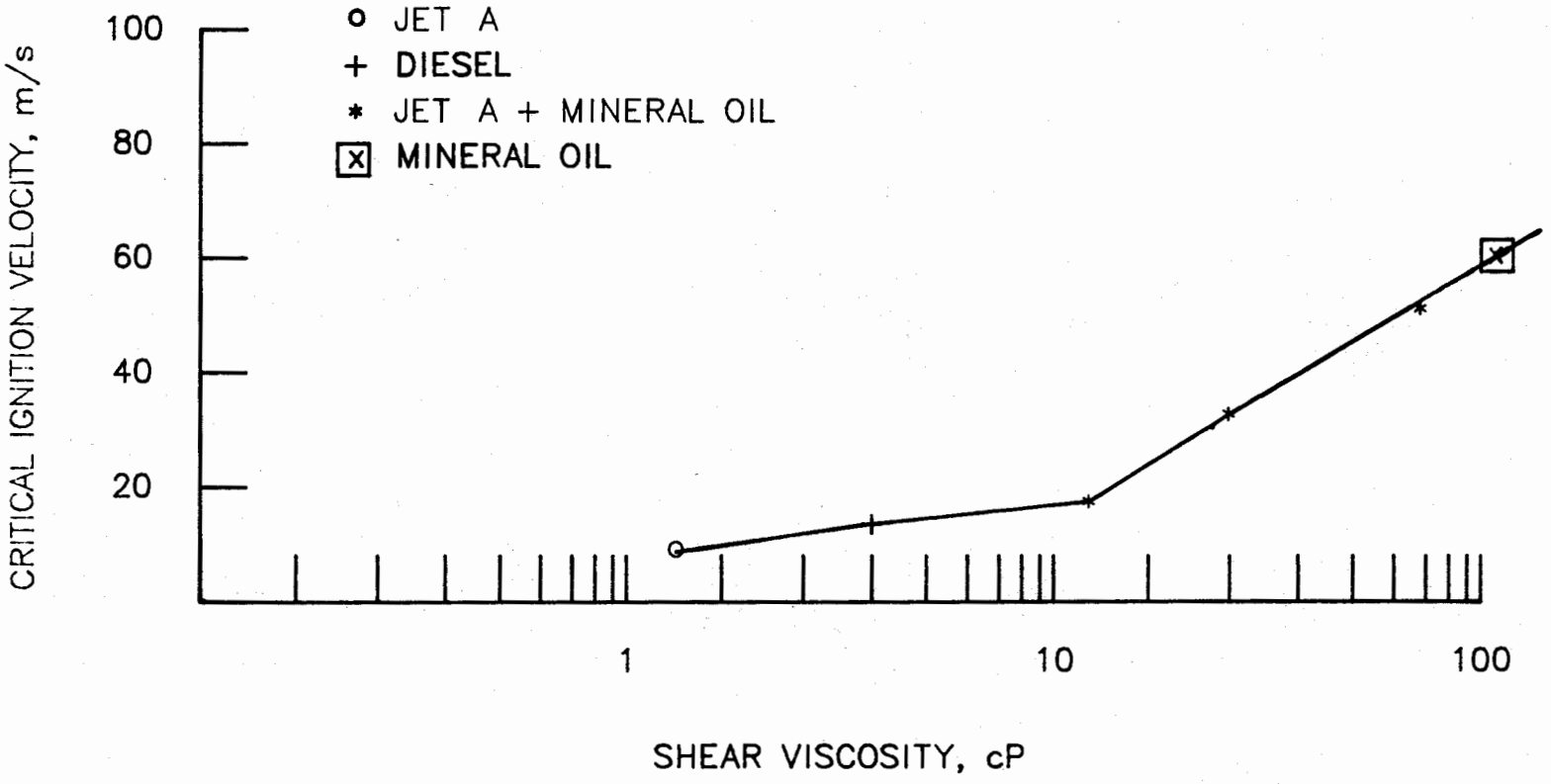

FIGURE 26. EFFECT OF SHEAR VISCOSITY ON CRITICAL IGNITION VELOCITY (SPINNING DISC)

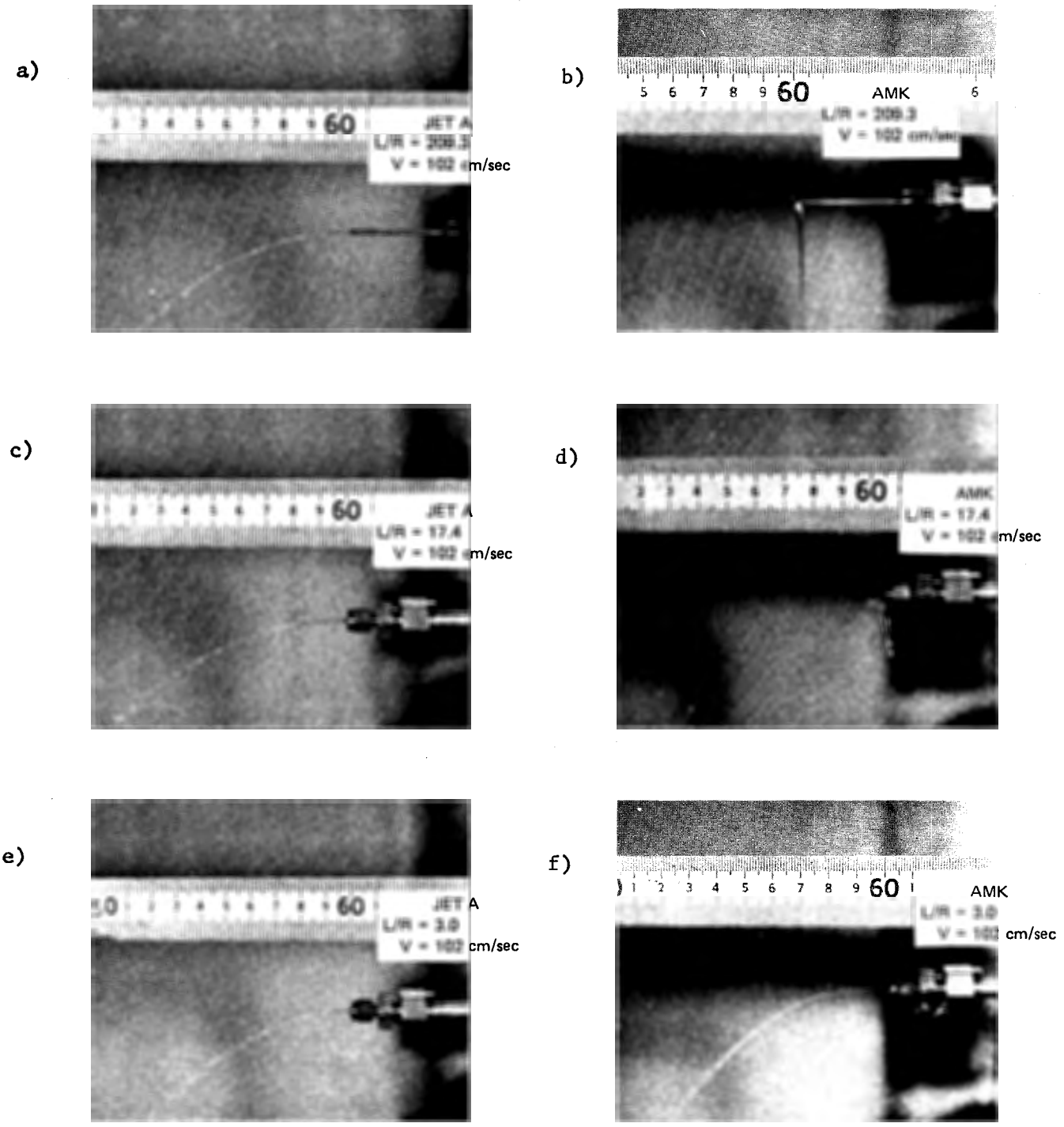

FIGURE 27. JETS OF AMK AND JET A IN DIFFERENT LENGTH CAPILLARY TUBES (8 V/D = 10,600 s^{-1}, R = 0.0364 cm)

In addition to providing insight as to the rheological mechanism of AMK, these observations suggest that normal stresses, which were not evident in earlier experiments with orifices, could readily be determined from jet thrust measurements in capillary tubes. While the jet thrust experiment is more difficult to execute and interpret than flow experiments, a quality control test based on normal stresses would have a much stronger theoretical basis than one that measures shear viscosity. The following equation illustrates some of the difficulties in interpretating jet thrust data:[14]

$$P_{11} - P_{22} = \rho V^2 \left[\frac{3n+1}{n} - 2 \int_0^1 \left(\frac{U}{V}\right)^2 \left(\frac{r}{R}\right) d\left(\frac{r}{R}\right) \right] - \frac{T}{\pi R^2} \left[1 + \frac{1}{2n} \frac{d \ln T}{d \ln (8V/D)} \right]$$

where $P_{11} - P_{22}$ is the normal stress differences,

ρ is the density,

V is the average velocity (Q/A),

U is the local velocity in the tube,

n is a flow index defined by $R\Delta P/2L = K\ (8V/D)^n$,

R is the radius of the capillary tube,

r is any radial position in the tube,

and T is the measured thrust.

Because of the complexity of this equation, it would be inappropriate to obtain jet thrust data relative to Jet A or any other base fuel. In particular, this equation indicates that not only is the thrust at a given shear rate important, but the rate of change of the thrust with shear rate is also important. Therefore, thrust measurements made at only one shear rate could be misleading.

Provided jet thrust data are properly analyzed, the resulting normal stress can be interpreted in terms of a relaxation time:

$$\Theta \equiv \frac{P_{11} - P_{22}}{2P_{12}(8V/D)} = \frac{P_{11} - P_{22}}{2\eta_a\ (8V/D)^2}$$

where P_{12} is the shear stress,

and η_a is the apparent shear viscosity

While it does not appear to be practical to measure the elongational viscosity of AMK at this time, the use of the shear viscosity and the relaxation time with an appropriate rheological model, such as the convected Maxwel Model, would make it possible to calculate the elongational viscosity. Although this degree of rigor may not be required for a quality control test, *it is clear that jet thrust measurements would provide essential rheological information that have not previously been available for AMK.*

B. SIGNIFICANCE OF ORIFICE FLOW CUP MEASUREMENTS

The orifice flow cup is one of the primary quality control tests for the production of an acceptable AMK blend. Since flow through an orifice involves primarily elongational rather than shearing deformations, one would expect the orifice flow cup to measure something other than shear viscosity. However, the dimensions of the orifice cup (L/R = 4.85) suggested that shear effects could be important. Experiments with Newtonian liquids (Jet A, diesel fuel, and Jet A/mineral oil blends) showed that the effect of shear viscosity on the orifice flow rate was significant. In particular, a Newtonian liquid having a shear viscosity of 13.6 cP resulted in an orifice flow rate of 3.2 mℓ/30 sec (Fig. 28). Despite the fact that this value is within the specification limit of 3.5 mℓ/30 seconds, it is evident that this fuel would offer little mist fire protection (Fig. 29). Additional evidence that the orifice flow cup is primarily a viscometer is illustrated by the excellent agreement between the measured and calculated viscosities in Figure 28. The details of these calculations are summarized in Table 5. While the kinetic energy correction ($m\rho v^2$) can usually be neglected with long capillary tubes (L/R > 100), this term is important with the orifice flow cup. Unfortunately, the value of m depends on the Reynolds number and widely different values have been reported by different sources.(15) For the calculations in Table 5, an average value of m = 1.2 was used. The almost perfect agreement between the measured (1.56 cP) and calculated (1.5 cP) viscosities for Jet A would have to be considered to be due to the fortuitous choice of m. Because of the very small L/R of the orifice cup, the 30% differences between measured and calculated viscosities observed for the more viscous liquids would probably be more realistic. While these results indicate that the orifice flow cup primarily measures viscosity, it is important to point out that the calculated shear rate (8V/D) in the orifice test (Table 5) is well above the critical value (2500 s^{-1}) that was established for shear thickening with capillary tubes. Consequently, the magnitude of the shear viscosity measured by the orifice flow cup is much higher than that measured by ASTM D-445 which is used for the VR. Furthermore, the magnitude of the shear viscosity for a sample of AMK with an orifice flow rate of 3.2 mℓ/30 seconds is approximately the same value (13.6 cP) as the shear viscosity measured with long capillary tubes (Fig. 19). Admittedly, these similarities occur at different shear rates (10,000 s^{-1} with capillary tubes and 4000 s^{-1} with the orifice flow cup); nevertheless, the general agreement between these two test methods is quite remarkable and cannot be completely fortuitous. For certain conditions, it is possible that the shear viscosity of AMK (above the critical shear rate) could have a direct bearing on the magnitude of the normal stresses that are developed. However, it is doubtful that such a relationship could be relied on in all instances to accurately predict antimisting effectiveness.

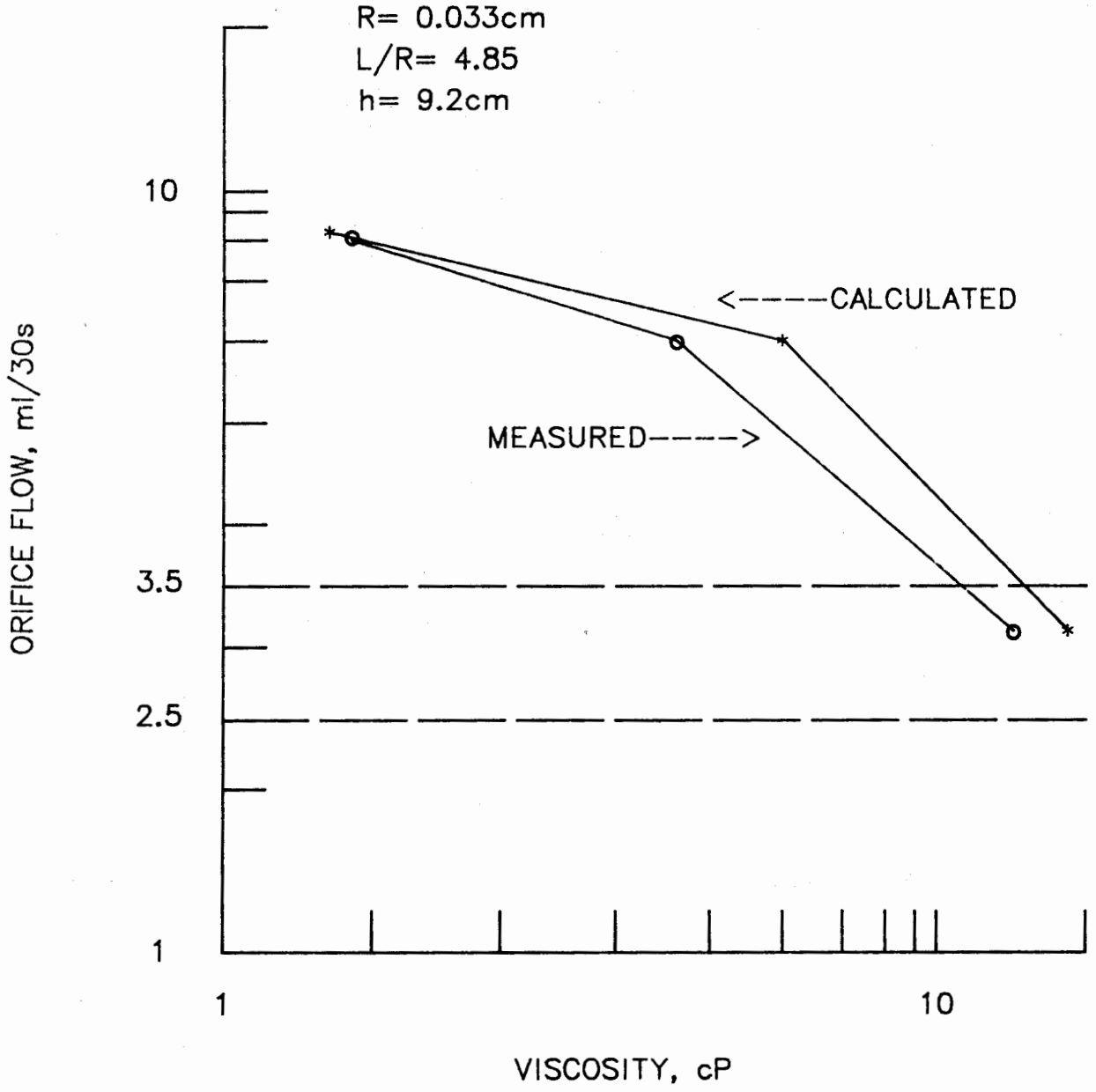

FIGURE 28. EFFECT OF SHEAR VISCOSITY ON ORIFICE FLOW CUP

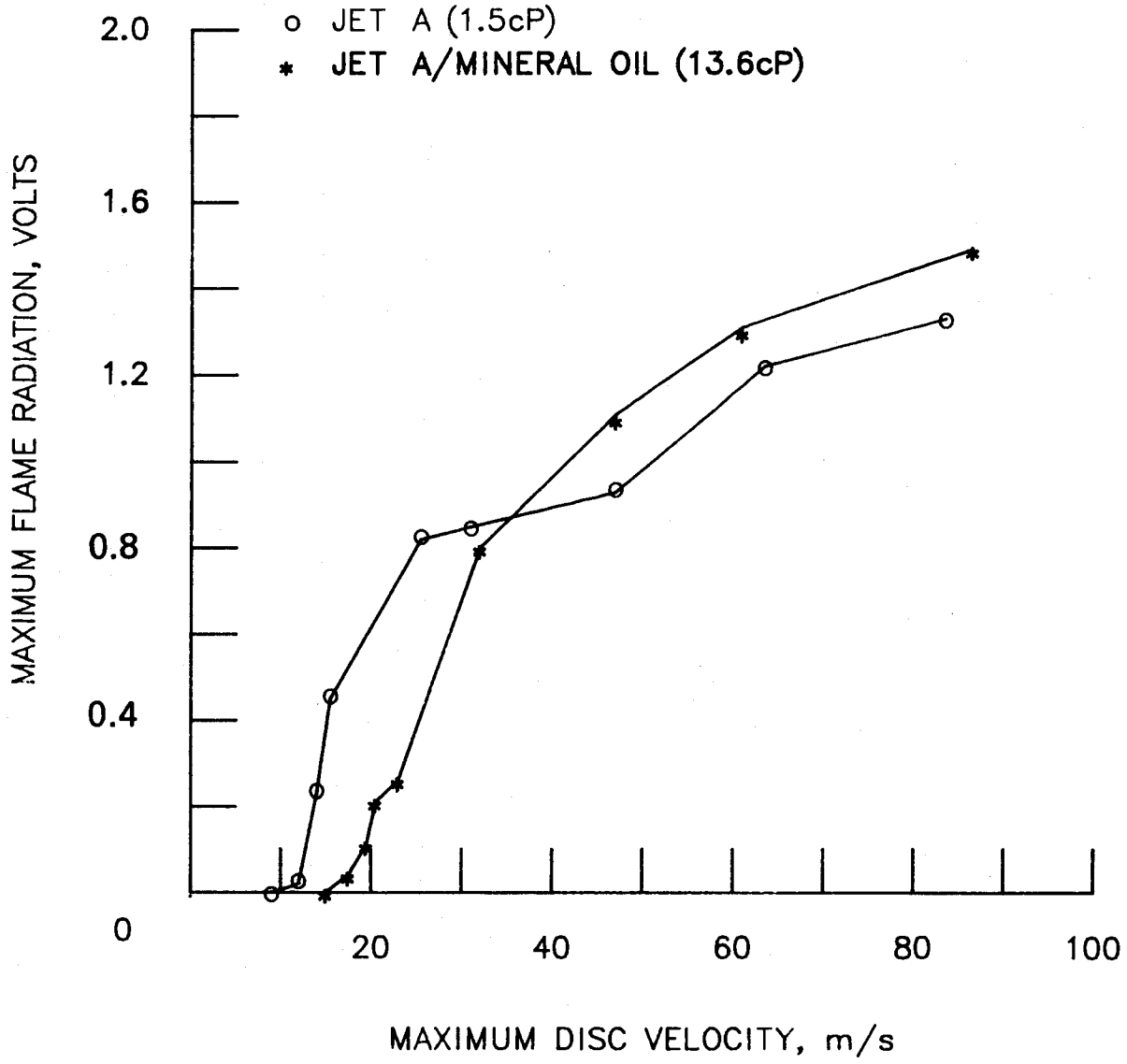

FIGURE 29. MIST FLAMMABILITY CHARACTERISTICS OF JET A AND JET A/MINERAL OIL BLEND

TABLE 5. ESTIMATION OF SHEAR VISCOSITY FROM ORIFICE CUP DATA*

Fuel Sample	Flow Rate, mℓ/30 s	Velocity, cm/s	ΔP_V** dyn/cm^2	$R\Delta P_V/2L$ dyn/cm^2	8V/D s^{-1}	Apparent Viscosity
Jet A 1.56 cP 0.80 gm/mℓ	8.0	78***	1380	142	9450	1.5 cP
Diesel 4.2 cP 0.86 gm/mℓ	6.2	60	4040	416	7270	5.7 cP
Jet A + Mineral Oil 13.6 cP 0.83 gm/mℓ	3.2	31	6530	673	3760	18 cP

*R = 0.033 cm, L/R = 4.85, h = 9.2 cm.

**$\Delta P_V = \rho gh - m\rho V^2$, m = 1.2.

***R_e = 259.

VII. CONCLUSIONS

A. DEGRADER TESTS

1. A hydraulic fuel pump (TF30 engine) is a practical means of producing the high pressure that is required to degrade AMK in a single pass.

2. A simple needle valve or variable area orifice is as effective as a packed tube ($L/d_p = 5$) and is able to provide a specific power level that is essentially independent of the fuel flow rate.

3. At temperatures near ambient and at fuel flow rates from idle to cruise (JT8D engine), it is possible to produce a fuel with filtration and ignition properties similar to those of Jet A for a specific power of (14-21 kWs/ℓ).

4. At temperatures below 0°C, higher specific power (28 kWs/ℓ) is required than at ambient.

5. At temperatures near 50°C, less specific power may be required to meet filtration requirements; however, no reduction in specific power can be expected in terms of mist ignition performance.

B. ANALYSIS OF AMK FOR GLYCOL AND AMINE

1. The glycol content of AMK can be determined by infrared spectroscopy.

2. The amine content of AMK can be determined by combustion and chemiluminescence detection.

C. GEL PERMEATION CHROMATOGRAPHY

1. The peak elution volume (PEV) can be used to characterize AMK blends that have been degraded by different methods and at different specific power levels.

2. There is a correlation between the peak molecular weight (relative to polystyrene) and the viscosity ratio. A similar correlation exists between peak molecular weight and the filtration ratio except for the case of AMK blended from slurry and degraded within one hour.

3. Despite the high filtration ratio associated with AMK blended from slurry and degraded within one hour, a high level of polymer degradation can be achieved. This apparent anomaly is probably due to the presence of relatively small quantities of poorly solubilized (i.e., poorly swollen) FM-9 powder that have little effect on PEV, viscosity or flammability but which can effectively plug a small filter.

D. FLAMMABILITY COMPARISON TEST APPARATUS

1. Because of the difficulty of atomizing fuel inside of a one-inch pipe, the effective fuel dump rate is a function of the air velocity and the atomization resistance of the fuel.

2. This test can distinguish between AMK made without the amine component of the carrier fluid; however, in some instances this difference is very small.

3. Slight misalignment of the fuel dump tube can have a significant effect on test results.

E. RHEOLOGICAL PROPERTIES OF AMK

1. The shear viscosity of AMK at high rates of shear (10,000 s^{-1}) is not large enough to explain the effectiveness of FM-9 as an antimisting agent.

2. At a critical shear rate of approximately 2500 s^{-1}, AMK exhibits large viscoelastic effects that are not apparent at lower shear rates. This shear induced viscoelasticity is probably the primary mechanism for antimisting.

3. The orifice flow cup test is essentially a viscometer that measures the shear viscosity of AMK above the critical shear rate.

4. The flow time in the filtration ratio test is too short to detect filter plugging of highly degraded AMK. This problem can be solved by reducing the exposed filter area by a factor of 1/10 to 1/20.

5. The Pump Filtration Test is able to measure a critical filtration velocity below which intentionally degraded AMK filters like Jet A, but above which filter plugging occurs. The CFV is a better estimate of the performance of intentionally degraded AMK in full-scale filter experiments than the filtration ratio.

6. Because of the difficulty of determining the average strain rate in complex filter geometries, the critical filtration velocity is a function of filter properties and is generally much lower in paper than in metal filters of equivalent size rating.

7. Increasing temperature above ambient increases the critical filtration velocity while decreasing temperature below ambient decreases the critical filtration velocity. With some AMK samples, the critical filtration velocity decreases with time after degradation.

VIII. REFERENCES

1. San Miguel, A. and Williams, M.D., Report No. FAA-RD-78-50, 1978.

2. Klueg, E., 6th US/UK Technical Committee Meeting on Antimisting Fuel, March 1980.

3. Bueche, F.J., Applied Polymer Sci., 4, 101-106, 1960.

4. Marshall, R.J. and Metzner, A.B., Ind. & Eng. Chem. Fund., 6, 393, 1967.

5. Fiorentino, A., Desaro, R., and Franz, T., NASA CR-16528, PWA 5697-29, 1980.

6. Timby, E.A., "Some Comments on the Present Position Regarding AMK Fuel,: 1980.

7. Billmeyer, F.W. Jr., "Textbook of Polymer Science," 2nd Edition, 55, 1971.

8. Ferrara, A.M., "Laboratory Scale Testing of Modified Fuel," 1980.

9. Mannheimer, R.J., FAA-RD-79-62, 1979.

10. Mannheimer, R.J., FAA-CT-81-153, 1981.

11. Sarohia, V., 6th US/UK Technical Committee Meeting.

12. Bagley, E.B., J. Appl. Phys., 28, 264, 1957.

13. Coomber, R., Faul, I., and Wilford, S.P., RAE Tech. Rept. 77157, 1977.

14. Sherter, C.R. and Metzner, A.B., 4th Intl. Soc. Rheo., 603-618, 1963.

15. Oka, S., "Rheology Theory and Application," 3, 25, 1960.

APPENDIX A

TEST METHOD FOR THE CRITICAL IGNITION
VELOCITY OF AMK (SPINNING DISC)

1.0 Summary of Method:

A spinning disc atomizer is used to produce a fuel mist. Ignition and flame propagation are monitored as a function of disc speed with a radiometer and strip-chart recorder. Special attention is given to the measurement of the lowest disc speed that will form an ignitable fuel mist in the presence of an oxyacetylene flame.

2.0 Apparatus:

2.1 Disc atomizer

2.2 Disc drive assembly

2.3 Powerstat (110V-20 amp)

2.4 Fuel metering unit

2.5 Fuel pump

2.6 Test stand

2.7 Oxyacetylene torch

2.8 Radiometer (silicone photodiode integral amplifier type) with variable low-pass filter)

2.9 Recorder (dual pen)

2.10 Thermocouple

2.11 Test cell

2.12 Exhaust fan

3.0 Preparation of Apparatus:

a) Initial Installation

A permanent test facility is required for the spinning disc experiment, e.g., a 10 x 10 x 10 ft. test cell with concrete walls and floor. Provisions for washing off and collecting the unburned fuel are also desirable. The fuel metering unit (Zennith Model ZM No. 7270); fuel pump (Zenith No. 45098) and fuel reservoir (1.0 liter)

are mounted directly below the disc and motor assembly (Fig. A-1). Note: This fuel metering system and fuel pump is recommended because of the very low pump speed (0-100 RPM) that should produce little or no polymer degradation in a single pass. Heavily insulated 1/2-inch copper tubing is used to conduct fuel to the center of the disc head (Fig. A-2). A thermocouple (iron-constantine, open junction) is located in a tee at the end of the tubing which is affixed to metal crossmembers on the test stand. The tip of the oxyacetylene torch is visible to the left and below the disc in Figure A-2. A piece of sheet metal protects the oxygen and acetylene hoses that lead to the torch. The router motor assembly and fuel metering system are also protected by pieces of sheet metal (Fig. A-3). The radiometer (United Detector Technology Inc. - Model No. UDT-500) is located approximately 137 cm (horizontal distance) and 168 cm (vertical distance) from the top edge of the disc* and on the opposite side from the ignition source.

b) Disc Drive Assembly

The disc atomizer and various components of the drive assembly are shown in Figure A-5. These include:

1. 1-1/2 HP router motor
2. Aluminum mounting plate (7 x 20 x 1/4 inch)
3. Slinger (aluminum disc - 3-1/2 in. with 5/8 in. hole in center)
4. Steel extension shaft (1/2 x 3 in. tapered to 1/4 in. at one end)
5. Aluminum housing with needle bearing and grease fitting
6. Disc atomizer
7. Lock nut
8. Collet nut

Installation of a new router motor proceeds as follows: First, several extraneous parts on the router motor are removed such as the dust bag, chip shields, sub-base,and work light. Next, approximately 1/3 of the mounting base of the router motor is cut away to make room for the magnetic pickup (Fig. A-5).

Caution: Do not cut the side of the mounting base where one of the screw holes is located.

* A cross section of the disc is shown in Figure A-4.

Installation of the slinger (this keeps fuel from draining into the lower motor housing), lock nut, collet nut and extension shaft is illustrated in Figure A-6. The magnetic pickup is located on the underneath side of the aluminum mounting plate (7 x 20 x 1/4 inch) as shown in Figure A-7. The plate is then fixed to the router motor (Fig. A-8). Positioning of the magnetic pickup can be accomplished by first backing off on the knurled ring (Fig. A-7) until the pickup clears the hexagonal collet nut. Slowly rotate the steel extension shaft and turn the knurled ring in until it touches one of the lobes of the collet nut. Then, back-off 1/4 to 1/2 turn on the knurled ring and lock the ring in this position.

> Caution: The correct positioning of the magnetic pickup must be checked by comparing the measured RPM with a strobe light.

Next, assemble extension shaft housing to mounting plate as shown in Figure A-9. Finally, install the disc head to the extension shaft (Fig. A-10). The fully assembled component is now ready to be mounted to the test stand.

4.0 Calibration:

a) The magnetic pickup should be checked against a strobe light.

b) The metering unit and fuel pump should be checked at different settings by collecting a quantity of fuel over a timed interval.

c) Before conducting ignition tests with AMK, a baseline experiment should be conducted with Jet A (see Section 5.0).

5.0 Test Procedure:

Set the fuel metering system to the desired fuel flow rate (this can be varied but is generally held fixed at 2.0 ℓ/m). With the powerstat set to produce a low disc speed (2000 RPM), turn on the pump and purge the fuel lines (1/4-inch copper tubing) and disc head for several seconds. Turn the fuel pump off and refill the fuel reservoir. Light the oxyacetylene torch and check that the tip of the torch (which is positioned vertically upward) is 10 cm from the edge of the disc.

Set the powerstat to produce a disc speed that is below the critical ignition velocity that is expected for the fuel being tested. For example, the critical ignition velocity for Jet A or highly degraded AMK is 10-15 m/s. On the other hand, the critical velocity for undegraded AMK is 60-70 m/s. For the 63 mm diameter disc, 10,000 RPM = 33 m/s. Therefore, the initial disc speed for Jet A or highly degraded AMK samples should be near 3000 RPM, while experiments with undegraded AMK should begin near 15,000 RPM. With partially degraded AMK, the

critical velocity can be quickly bracketed by starting at some intermediate speed (10,000 RPM) and either increasing or decreasing the speed by 5000 RPM, depending on whether or not the radiometer indicates that ignition has occurred.

Just prior to the ignition test, turn on the exhaust fan and recorder. Finally, turn on fuel pump and allow it to remain on for 3.0 seconds. Turn off the fuel pump, powerstat, and chart drive. Record the peak radiometer output and the disc speed from the dual pen recorder. Because of the slight drop in disc speed after the fuel pump is started, an average disc speed is reported. However, this change is generally small. For example, with Jet A the speed typically drops from 4100 to 3600 RPM (reported disc speed 3850 RPM) and with undegraded AMK the speed may drop from 21,700 to 19,500 RPM (reported value 20,600 RPM). This procedure is repeated several times (generally at least 7 to 10 data points per test) with particular attention given to the onset of ignition and flame propagation.

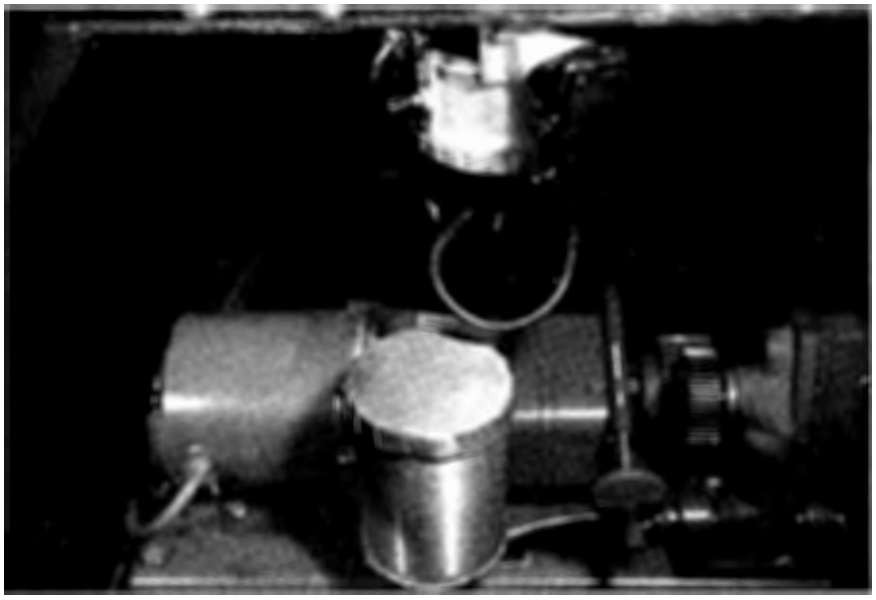

FIGURE A-1. LOCATION OF FUEL METERING UNIT AND FUEL PUMP

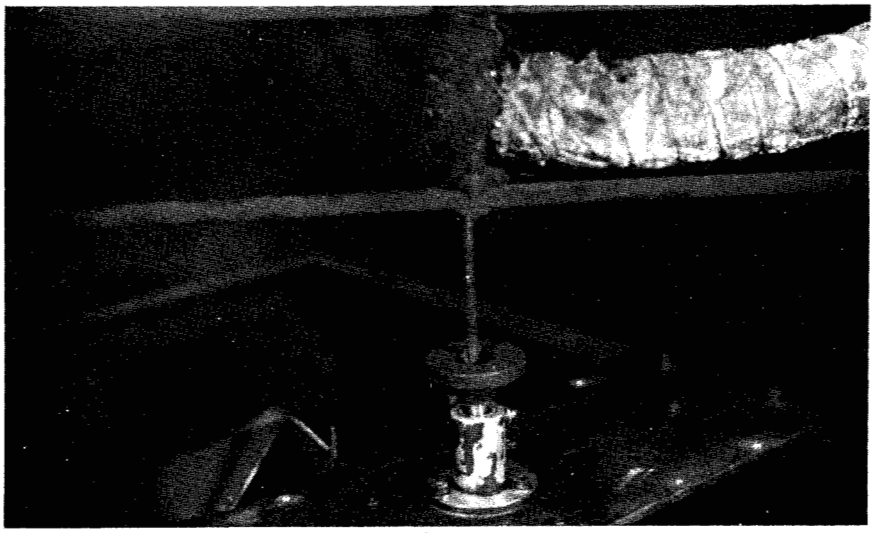

FIGURE A-2. INSULATED (¼in.) FUEL LINES AND DISC

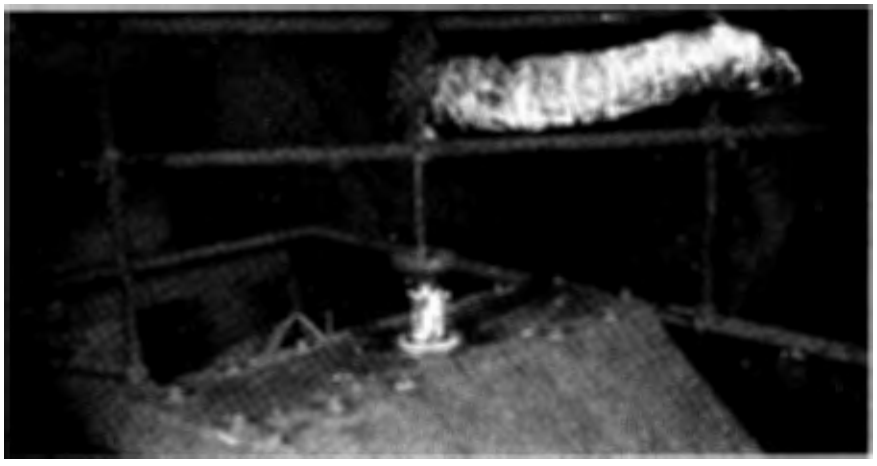

FIGURE A-3. SHEET METAL PROTECTS
ROUTER MOTOR AND FUEL SYSTEM

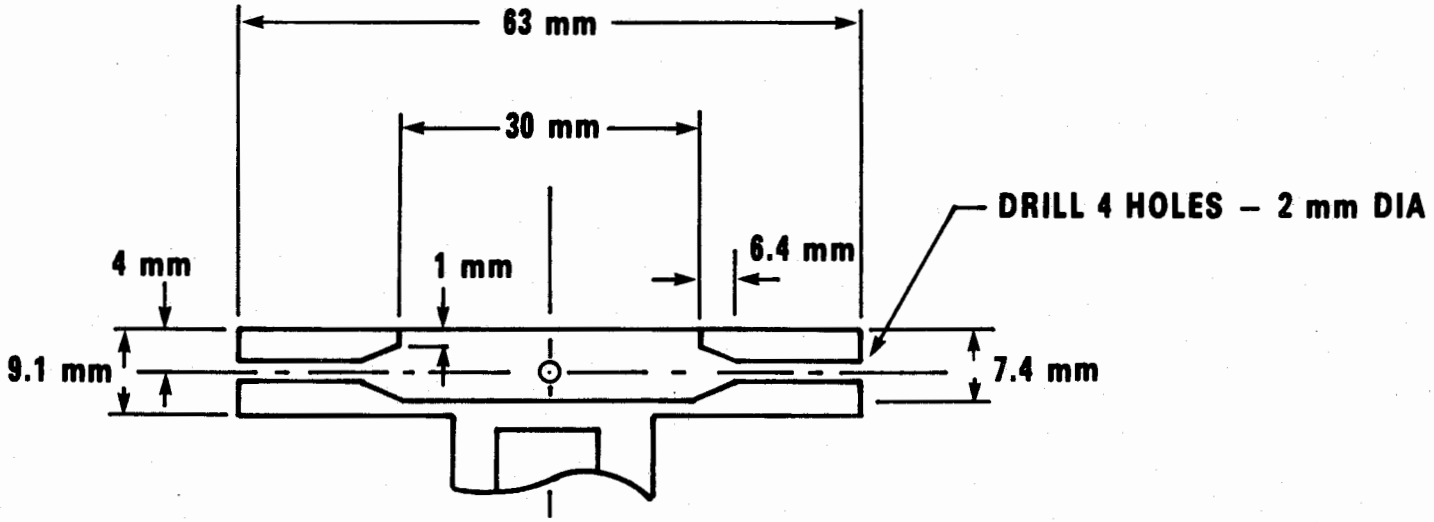

FIGURE A-4. CROSS SECTION OF DISC

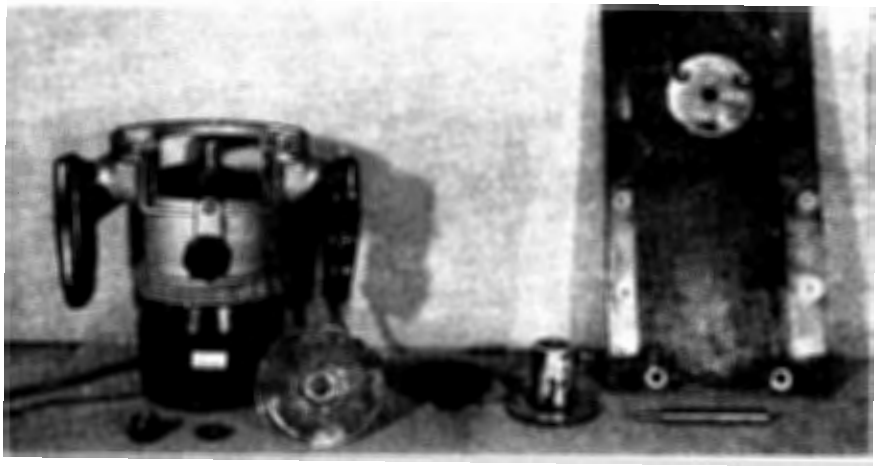

FIGURE A-5. VARIOUS COMPONENTS OF THE DISC DRIVE ASSEMBLY

FIGURE A-6. INSTALLATION OF SLINGER AND EXTENSION SHAFT

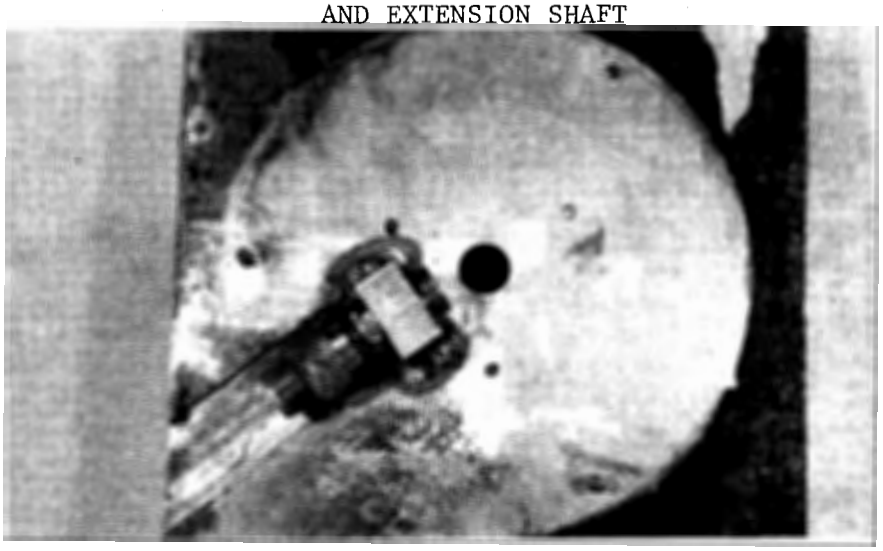

FIGURE A-7. LOCATION OF MAGNETIC PICKUP

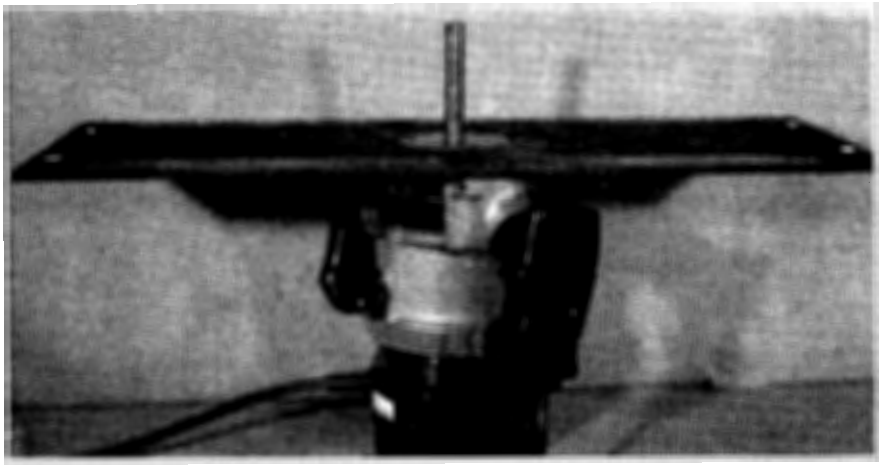

FIGURE A-8. ASSEMBLY OF MOUNTING PLATE

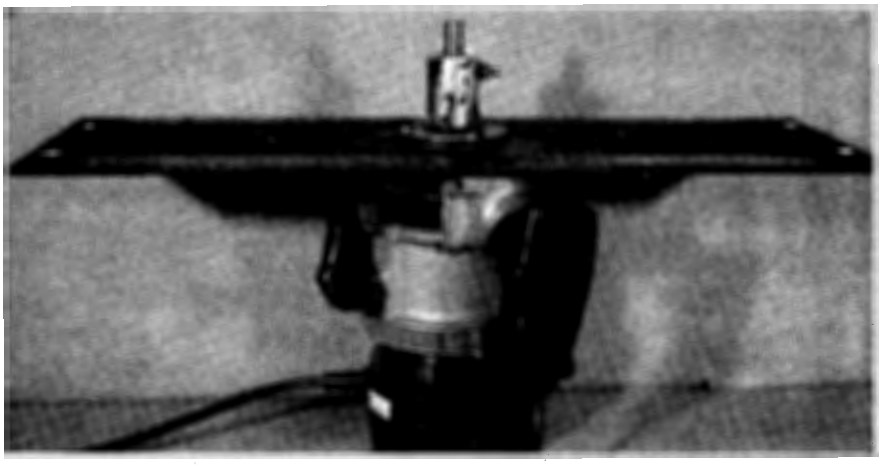

FIGURE A-9. ASSEMBLY OF EXTENSION SHAFT HOUSING

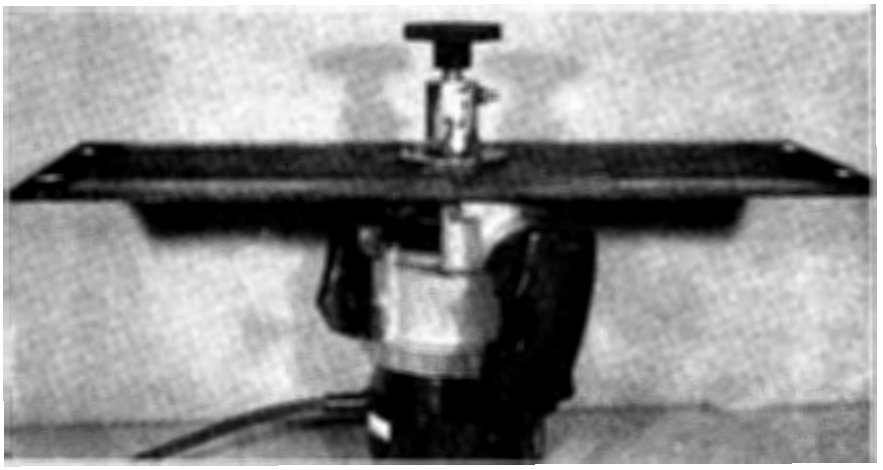

FIGURE A-10. FULLY ASSEMBLED
DISC AND DRIVE ASSEMBLY

APPENDIX B

TEST METHOD FOR THE FILTRATION CHARACTERISTICS OF INTENTIONALLY DEGRADED AMK (PUMP FILTRATION TEST)

1.0 Summary of Method:

Degraded AMK is forced through a small section of a filter with a variable speed (0-100 RPM) gear pump. The pressure, associated with the flow resistance, is measured as a function of flow time and superficial velocity (flow rate/filter area). Below a critical velocity* the pressure with AMK is only slightly greater than with Jet A, and it remains at this low level for at least 2 minutes.

2.0 Apparatus:

2.1 Metering unit, Zenith, Type 1ZM-4890

2.2 Variable speed pumps, Zenith, 0.584 cc/rev, and 2.92 cc/rev

2.3 Pressure transducer, CEC, Type 4-313, 0-10 psid

2.4 Strip-chart recorder, single pen

2.5 Amplifier, Action Pak, Model 4051-203

2.6 1/2-inch stainless steel tubing:

a) 20 cm long with a 90° bend

b) 10 cm long with flat ends. Note the flat end of this piece of tubing must be polished so as to fit flush against the back-up discs.

c) 5 cm long with flat ends

d) 5 cm long with one flared and one flat end (4 each)

2.7 1/2-inch stainless steel union (2 each)

2.8 Stainless steel female branch tees with 1/2-inch tubing and 3/8-inch pipe connections (2 each)

---

* The maximum or average deformation rate would be a better parameter; however, this is not easily determined for filters, consequently the critical velocity is a function of filter geometry.

2.9 Stainless steel reducing unions, 1/2 inch to 1/4 inch (2 each)

2.10 Stainless steel tubing 1/4 inch, 3 cm long with flat ends

2.11 Hose clamps 1/2 inch (3 each)

2.12 Tygon tubing 1/4 inch, 30 cm long

2.14 Back-up discs (D = 1.27 cm L = 0.18 m):

ID = 0.356 cm (2 each)

ID = 0.504 cm (2 each)

ID = 0.714 cm (2 each)

2.15 Iron-constantine type thermocouple shrouded with 1/8-inch tubing

2.16 Digital readout, Omega, Model 199

3.0 Filtering Procedure:

Pour two liters of fuel into a large separatory flask. Place a No. 41 Whatman filter paper in a regular funnel and collect the filtered fuel in a clean container.

4.0 Cleaning Procedure:

After the apparatus has been used with intentionally degraded AMK, flush the pump thoroughly with Jet A. The removable components such as: unions, sections of stainless steel tubing, back-up discs, and transducer adapter are cleaned with trichloroethylene and acetone and then are air dried. The pump should be taken apart after every 5-7 experiments and cleaned with trichloroethylene and acetone.

5.0 Preparation of Apparatus:

The fully assembled apparatus is shown in Figure B-1. While satisfactory assembly of the various components might be achieved by different methods, the following method has been found to minimize the entrapment of the air in the system. Connect one end of the 1/2-inch tygon tubing to the suction side of the pump and place the other end of the tube in a clean container that holds approximately 2 liters of fuel. Fill this container with filtered fuel (see Section 3 for filtering procedure). Raise the baseplate of the pump slightly to help displace air from the lines as they are filled. Connect the 1/2-inch stainless steel tube with the 90° bend to the discharge end of the pump so that the downstream end of the tube is vertical. Fill the lines at a relatively high flow rate (30 mℓ/min). Return the baseplate to its

original position, and then connect the thermocouple, pressure transducer and the piece of 1/2-inch stainless steel tubing with polished end as shown in Figure B-2. Note: The polished end of the tube should be positioned downstream so as to fit against the filter back-up disc. Restart the pump and fill the remainder of the line with fuel.

Place the filter element* between the two back-up discs and insert all three components into a 1/2-inch union. Set the pump at its lowest output (almost zero flow) and continue to fill the system until a convex meniscus is formed at the top of the tube. This procedure helps to prevent air entrapment below the filter.

> Caution: Because of the vertical positioning of the tubing, there is a tendency for fuel to flow back through the pump when it is shut off. Since this may draw air into the system, it is advisable to leave the pump barely running (except for very brief periods) for the remainder of the test.

Next, attach the union that contains the filter and the filter back-up discs to the fuel line and tighten the entire assembly. Also connect the pressure transducer lead to the amplifier and recorder**. To further insure that all the air has been removed, place a rubber stopper in the end of the union and allow the pressure to build up for a few seconds. Quickly release the pressure by removing the stopper and check for the evolution of bubbles.

> Caution: Do not exceed the pressure limit of the transducer (10 psi).

Repeat this procedure two or three times or until no bubbles are observed. Finally, connect the remaining pieces of tubing as shown in Figure B-1.

6.0 Experimental Procedure:

Before conducting experiments with degraded AMK, the system should be checked with Jet A. This will insure that the apparatus has been adequately cleaned (Section 4) and that the filter has been properly installed (Section 5). For example, the pressure with Jet A should not increase over the two minute flow time that is used in this test. If the pressure increases with time, either the fuel is contaminated or the apparatus has not been cleaned adequately. In any event the apparatus should be recleaned, a new filter installed and the system retested with a fresh sample of filtered Jet A. If the pressure remains constant but appears to be higher or lower than normal (this

---

* Almost any type of filter material can be used that has sufficient structural integrity and that can be cut into a disc-shaped element.

**The pressure is measured immediately upstream of the filter. Use of the transducer in the differential mode was found to make it difficult to remove air from the system.

can only be determined by experience), the filter should be changed and the system again checked with Jet A. If the results with Jet A prove to be satisfactory, experiments can then be conducted with degraded AMK. It is unneccessary to reclean the apparatus after the experiments with Jet A. The lines are merely drained and then flushed with degraded AMK. Furthermore, the same filter should be used, however, the 1/2-inch union that holds the filter should be removed and the system refilled with degraded AMK according to Section 5 to insure complete removal of the air from the system.

At least duplicate experiments should be performed with each sample of degraded AMK. Without any prior knowledge of the critical filtration velocity (CFV), it is advisable to start at a low velocity, such as 0.25 cm/s and increase the velocity by 0.25 cm/s until the pressure starts to increase with time. This procedure works well for paper filters and relatively fine metal screens (i.e., 16-18 μm or less); however, for larger metal screen (40 μm or greater) it is suggested that one start at a velocity of 1 to 2 cm/s and increase the velocity by proportionately higher increments.

Generally, the experiment is not terminated after the first point at which the pressure increases with time. Rather, the rate of pressure rise is measured at increasingly higher flow rates until either the maximum pressure of the transducer or the maximum flow rate of the pump is exceeded. These data are then plotted to make a better estimate of the CFV. A second experiment should be conducted to more accurately estimate the CFV. In this second experiment, a new filter must be installed and the lines purged of air as described in Section 5. Measurements are then made near the estimated CFV using smaller increments than were used in the first test.

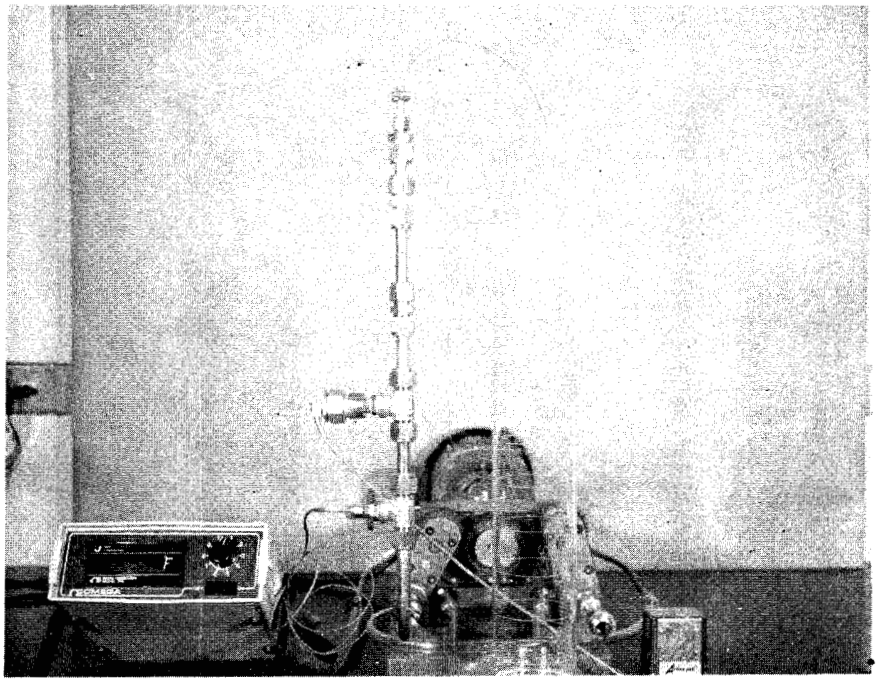

FIGURE B-1. FULLY ASSEMBLED FILTRATION APPARATUS

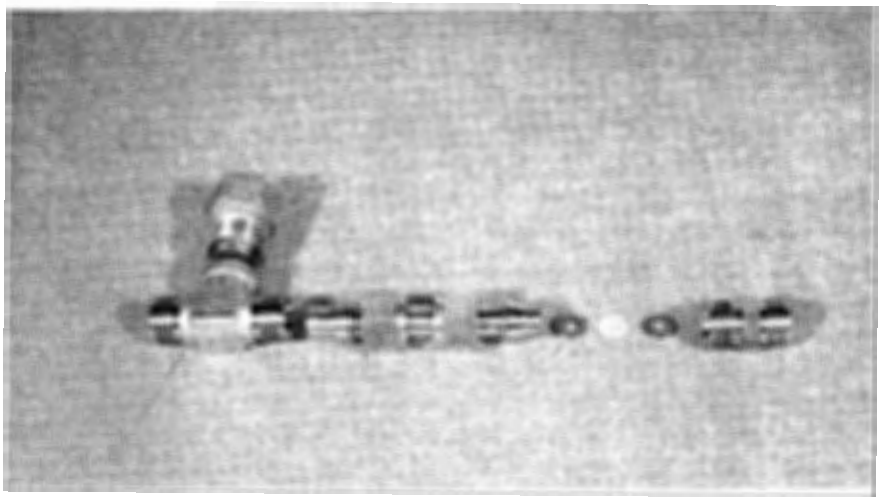

FIGURE B-2. ASSEMBLY OF PRESSURE TRANSDUCER AND FILTER AND FILTER BACKUP DISCS

APPENDIX C

TEST METHOD FOR THE GLYCOL CONTENT OF AMK

1.0 Summary of Method:

An infrared (IR) method has been developed to determine the amount of glycol present in AMK. Infrared absorbance at 3542 cm^{-1} is correlated to weight percent glycol in a sample. Concentrations from 0.35 to 0.70 weight percent glycol show a linear correlation to absorbance. The addition of FM-9 and amine in appropriate concentrations (FM-9 $\sim$0.3 wt% and amine $\sim$150 RPM) does not affect the absorbance factor.

2.0 Apparatus:

2.1 Beckman Microlab 620 XM computing spectrophotometer

2.2 0.7 to 1.0 mm CaF_2 liquid sample cell

2.3 1 cc turberculin syringe

3.0 Reagents:

3.1 Xylene, reagent grade

3.2 Hexadecane, reagent grade

3.3 Hexylene glycol

4.0 Preparation of Apparatus:

For operating instructions of spectrophotometer, refer to the Beckman Microlab 620 MX Operation Manual. The Microlab 620 MX Computing Infrared Spectrophotometer combines double-beam infrared spectrophotometry with microprocessor hardware and associated software to control operations and data processing. Several routines are available in two modes, Scan and Quantitative. Spectra may be scanned and peaks pinpointed using single-step and peak-pick routines. Quantitative measurements may be made at selected wavelengths using a point program routine.

5.0 Calibration:

Standards, prepared in a 25 vol. % xylene, 75 vol. % hexadecane mixture, ranged from 0.35 to 0.70 wt % glycol. Standards were examined in a peak-pick routine to determine the optimum wavelength for measuring absorbance of the glycol. Using a single-step routine, 3542 cm^{-1} was

selected and entered in a point program routine. This routine measures absorbance at the chosen wavelength for a specified number of times, then it averages the readings and gives a percent transmittance (%T) value. Ten readings was the number specified in this routine. The cell was left completely assembled to avoid variation in the pathlength, and was washed with filtered heptane and dried between runs.

> Note 1: Values of %T dropped ∿2% over 10 minutes in the sample cell, so immediate measurement is necessary.
>
> Note 2: Ten runs of a single sample to test for repeatability gave a standard deviation relative to the mean glycol content of 2%.

6.0 Procedure:

Using a 1 cc tuberculin syringe, fill an 0.7 to 1.0 mm CaF_2 liquid sample cell with AMK. Put the cell into the sample chamber of the spectrophotometer and record %T at 3542 cm^{-1} (see Note 1 under calibration).

7.0 Calculations:

The %T values at 3542 cm^{-1} are used to calculate absorbance using the Beer's law equation A = log 1/T. A %T value of 42.38% would be calculated as follows: A = log 1/.4238 = .3728. Absorbance values may be plotted versus wt% glycol to give a standard curve and sample wt% glycol read directly from the curve (Fig. C-1). Absorbance versus concentration data from the standards was entered in an Apple II computer least squares program. A fit with relative standard deviation of 4.77% and average deviation of 0.0162 absorbance was obtained.

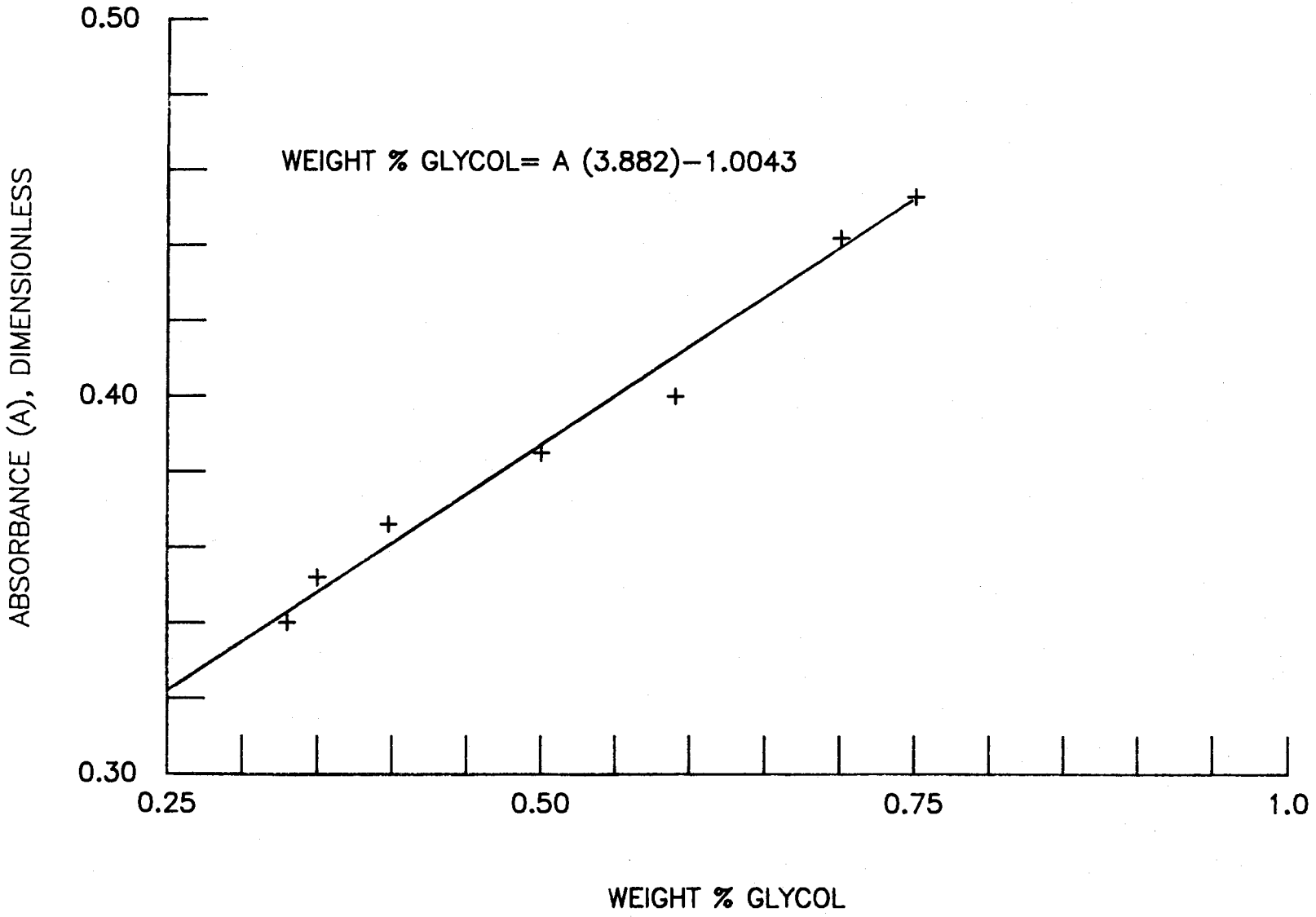

FIGURE C-1. CALIBRATION CURVE FOR WEIGHT % GLYCOL IN AMK

APPENDIX D

TEST METHOD FOR AMINE (PPM) CONTENT OF AMK

1.0 Summary of Method:

AMK samples are prepared by diluting with tetrahydrofuran (THF). The diluted AMK samples are injected into the pyrolysis furnance where the nitrogen compounds are oxidized and then measured as NO_2 by the chemiluminescence detector. The digitally displayed counts for AMK are compared to a standard nitrogen calibration curve.

2.0 Apparatus:

2.1 Antek Model 771 Pyro-reactor

2.2 Antek Model 720 Nitrogen detector

2.3 Microsyringe, 5.0 µℓ with 2" x 26 ga. needle

2.4 Silicone Septa

2.5 Pipettes, Class A, 1 mℓ, 4 mℓ

2.6 Quartz combustion tube, as per instrument manufacturer's design

3.0 Reagents:

3.1 Magnesium perchlorate, 8-20 mesh

3.2 Argon, 99.9% purity

3.3 Oxygen, 99.9% purity

3.4 Tetrahydrofuran, 99% Nitrogen free

3.5 Charcoal, activated 8-20 mesh

4.0 Preparation of Apparatus:

Assemble and adjust the instrument as per the manufacturer's instructions. Set the operating parameters according to Table D-1.

5.0 Calibration:

Nitrogen standards were made by diluting a stock solution of dimethylformamide (DMF) in toluene. An example of the calculation that was

used in establishing the nitrogen content of these samples is as follows:

1. Molecular Weight DMF (C_3H_7NO) = 73.11 g

2. Wt% nitrogen in pure DMF = (14.0/73.11) x 100 = 19.16

3. Wt% nitrogen in 0.1017 wt%/stock solution = 0.001017 x 19.16 = 0.01949 (194.9 ppm)

4. PPM (Nitrogen) in diluted standards:

   2 mℓ of stock solution diluted to 100 mℓ = 3.9 ppm

   4 mℓ of stock solution diluted to 100 mℓ = 7.8 ppm

   6 mℓ of stock solution diluted to 100 mℓ = 11.7 ppm

The counts for nine consecutive (3.0 μℓ) injections of these three standards (utilizing a constant rate syringe drive), are presented in Table D-2. The average counts were used to establish a calibration curve (Fig. D-1) in which the error bars represent two standard deviations. In order to establish a similar calibration curve, it is recommended that at least three consecutive (3.0 μℓ) injections should be made for each standard. Furthermore, at least three dilutions should be used to produce counts in the same range as AMK. For the highest precision, the calibration curve should be checked before and after analysis of AMK samples. However, recalibration should be done at least daily or any time the apparatus has been turned-off.

6.0 Procedure:

Into a tared 10 mℓ vial, dispense 0.8 mℓ of AMK and 3.2 mℓ of tetrahydrofuran (THF). Weigh each component to the nearest 0.1 mg. Seal the vial tightly with a solvent resistant cap and mix thoroughly by shaking. Let the sample stand long enough to dissipate the bubbles. Then inject three consecutive (3.0 μℓ) samples of AMK into the nitrogen analyzer using the same technique as described in Section 5. The average counts from these three injections can be used to calculate the nitrogen content of the AMK sample from a calibration curve such as Figure D-1. Since the density of the diluted AMK samples may be different than the standards, a density correction factor (density of standards/density of diluted AMK solutions) should be applied to average AMK counts. For all practical purposes, the density of the standards is the same as toluene (0.867 g/mℓ) and the density of the AMK samples is essentially that of THF (0.889 g/mℓ). Consequently, a correction factor of 0.975 would account for the slightly larger mass of AMK injected. Finally, in order to convert the nitrogen content of the AMK sample to PPM (n-butylamine) one must account for the dilution of the sample and the weight fraction nitrogen in the amine.

These factors are illustrated in the following calculation:

1. Average counts for diluted AMK (uncorrected for density) = 1000

2. Average counts for diluted AMK (corrected for density) = 1000 x 0.975 = 975

3. PPM nitrogen in diluted AMK (from Fig. D-1) = 5.8

4. PPM nitrogen in undiluted AMK (from dilution factor) = 5.8 (wt fraction AMK in THF) = $\frac{5.8}{0.21}$ = 27.6

5. Molecular weight of amine ($C_4H_{11}N$) = 73.13 g

6. Wt% nitrogen in amine = $\frac{14.0 \times 100}{73.13}$ = 19.14

7. PPM amine in AMK = $\frac{27.6}{0.194}$ = 144

TABLE D-1. INSTRUMENT OPERATING PARAMETERS

Instrument:	Antek Model 771 Pyro-Reactor/Model 720 Digital Nitrogen Detector
Oxygen Flow:	120 mℓ/min. to Ozone Generator 410 mℓ/min. to Pyrolysis Tube
Argon Flow:	30 mℓ/min.
Pyro-Reactor Temperature:	Inlet - 850°C Center - 950°C Outlet - 950°C
Instrument Sensitivity:	I-Low (counts between 300 and 60,000)*
Injection Rate:	1.0 µℓ/second

TABLE D-2. CALIBRATION DATA FOR DMF/TOLUNE STANDARDS

PPM Nitrogen:

	Nitrogen Counts		
	3.9	7.8	1.7
	642	1375	2395
	642	1347	2365
	631	1358	2287
	540	1413	2215
	576	1347	2267
	698	1402	2365
	667	1363	2285
	608	1406	2266
	579	1383	2260
$\bar{X}$:	616	1377	2300
σ:	49	25	60

* It is unadvisable to change sensitivity setting during analysis.

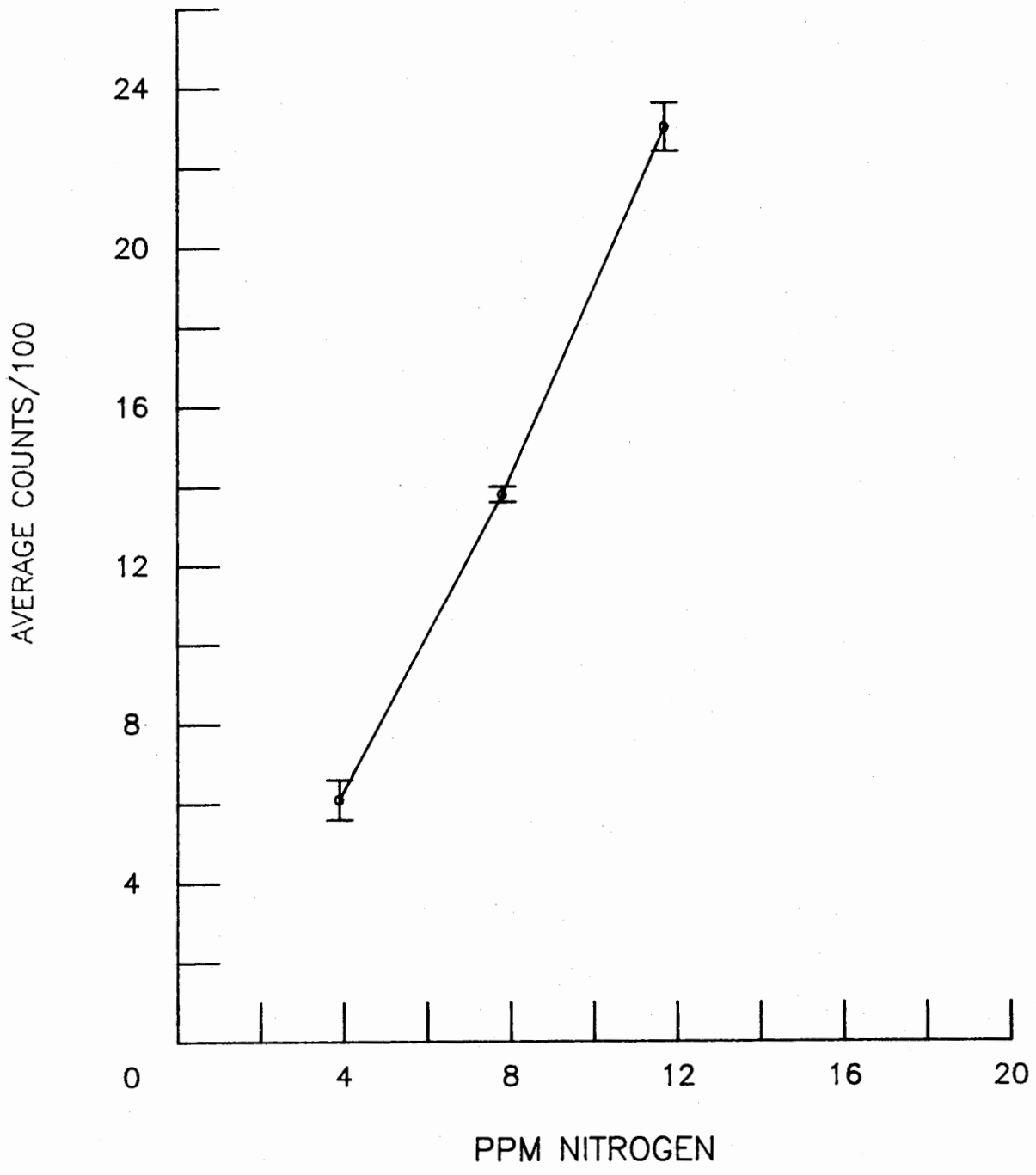

FIGURE D-1. NITROGEN CALIBRATION CURVE DMF/TOLUENE SOLUTIONS